

# **Stock assessment of the outer-shelf species in the Kimberley region of tropical Western Australia.**

**Principal Investigator:** Dr. Stephen J. Newman

**Co-Investigator:** Dr. Michael J. Moran

**Co-Investigator:** Dr. Rodney C.J. Lenanton.



Department of  
**Fisheries**



FISHERIES  
RESEARCH &  
DEVELOPMENT  
CORPORATION



*Fish for the future*

**Project No. 1997/136**

**May, 2001**

**ISBN No. 0 7309 8460 5**

<b>Table of Contents</b>
--------------------------

Non Technical Summary.....	4
Principal Investigator.....	4
Background.....	7
Need.....	8
Objectives.....	9
Methods.....	9
Methods – Age and Growth.....	9
Methods - Reproduction.....	16
Results.....	19
1. Spatial distribution of catch and effort in the Northern Demersal Scalefish Fishery <i>Stephen J. Newman &amp; Richard A. Steckis</i> .....	19
2. Age, growth and mortality of the goldband snapper, <i>Pristipomoides multidens</i> <i>Stephen J. Newman, Iain J. Dunk &amp; Jerry Jenke</i> .....	31
3. Reproductive biology of the goldband snapper, <i>Pristipomoides multidens</i> <i>Stephen J. Newman, Richard A. Steckis &amp; Jerry Jenke</i> .....	46
4. Age, growth and mortality of the red emperor snapper, <i>Lutjanus sebae</i> <i>Stephen J. Newman, Iain J. Dunk &amp; Jerry Jenke</i> .....	58
5. Reproductive biology of the red emperor snapper, <i>Lutjanus sebae</i> <i>Stephen J. Newman, Richard A. Steckis &amp; Jerry Jenke</i> .....	72
6. Yield per recruit and egg per recruit models <i>Stephen J. Newman</i> .....	85
7. Selectivity of fish traps <i>Stephen J. Newman &amp; Peta C. Williamson</i> .....	90

Discussion.....	97
Acknowledgments .....	100
Benefits .....	101
Further Development.....	101
Conclusion.....	102
References.....	104
Publications .....	106
Appendix 1: Intellectual Property .....	107
Appendix 2: Staff .....	107
Appendix 3: Spatial distribution of catches, line and trap effort, and catch rates of key species and species groups in the NDSF .....	108

**1997/136**

Stock assessment of the outer-shelf species in the Kimberley region of tropical Western Australia.

**PRINCIPAL INVESTIGATOR:** Dr. Stephen J. Newman**ADDRESS:** Fisheries Research Division  
Department of Fisheries  
Government of Western Australia  
P.O. Box 20  
North Beach, WA, 6920  
Telephone: 08 92468444  
Fax: 08 94473062  
Email: [snewman@fish.wa.gov.au](mailto:snewman@fish.wa.gov.au)**OBJECTIVES:**

1. Estimate essential population parameters of goldband snapper and other key demersal species.
2. Estimation of yield-per-recruit and egg-per-recruit optimum combinations for the regulation of size-at-first capture and fishing mortality.
3. Examination of the size selectivity of commercial trap gear to investigate methods of altering selectivity to enable targeting of fish of a specific size.
4. Advise fishery managers and industry on the combinations of gear and effort controls to produce optimal sustainable yields.

**NON TECHNICAL SUMMARY:****OUTCOMES ACHIEVED**

The results obtained from this project will be incorporated into age-structured stock assessment models for red emperor and goldband snapper in the Northern Demersal Scalefish Fishery (NDSF) of Western Australia. The NDSF is managed under individual transferable effort quotas and this data will provide the basis for assessing the validity of the current target total allowable catch (TAC) and provide advice on appropriate future levels of TAC required to meet future sustainability objectives.

Given the low production potential of stocks of goldband snapper and red emperor, cautious management arrangements are required for the ongoing sustainable utilisation of these demersal fish resources. These results are of relevance to all tropical demersal finfish fisheries in northern Australia.

The direct benefit to fishermen will be the sustainability of their fishery, while the community will benefit from the preservation of inter-generational equity and the sustainable exploitation of tropical fish resources.

Goldband snapper, *Pristipomoides multidens*, collected from commercial trap and line fishers in the Northern Demersal Scalefish Fishery (NDSF) off the Kimberley coast of North-western Australia were aged by the examination of thin sections of otoliths (ear stones). A total of 3833 goldband snapper, 9.8-80.5 cm total length (TL) were examined from commercial catches from 1995-1999. The oldest fish collected was estimated to be at least 30 years of age. The length at maturity of goldband snapper was estimated to be 55.2 cm TL for females and 54.9 cm TL for males, corresponding to an age at maturity, of 8.2 years for females and 8.0 years for males.

Age estimates from thin sections of ear stones were validated using marginal increment analysis with opaque and translucent zones each formed once per year. The von Bertalanffy growth curve was used to describe growth. No significant differences were found in the growth curves between sexes. Growth parameters are  $L_{\infty} = 598$  mm,  $K = 0.187 \text{ yr}^{-1}$ ,  $t_0 = -0.173$  ( $r^2 = 0.76$ ), indicating moderately slow growth. Total mortality estimates generated from catch-at-age data of goldband snapper from the NDSF were 0.65 for 1995/96, 0.87 for 1996/97 and 0.76 for 1997/1998, representing an annual percentage removal of approximately 38%, 49% and 43% respectively for each year. Estimates of natural mortality were in the range 0.104-0.139, these instantaneous rates indicate that 9.9-13.0% of the annual removal of fish was due to natural causes. When compared to accepted international reference points, these results indicate that the NDSF population of goldband snapper is currently exploited above optimum levels. The protracted longevity, moderately slow growth, large size and age at maturity and low natural mortality rates of goldband snapper imply that this species is particularly vulnerable to overfishing.

A total of 2386 red emperor *Lutjanus sebae*, were examined from the commercial catches of fishers in the NDSF from 1997 to 1999. Specimens ranged from 18.3 to 72.8 cm fork length (FL); males had a mean FL of 50.9 cm and were significantly larger than females that had a mean FL of 45.1 cm. The length at maturity, for red emperor was 46.1 cm TL for females and 49.1 cm TL for males, corresponding to an age at maturity, of 8.2 years for females and 8.0 years for males.

Ages were estimated from thin sections of ear stones, which showed a single annual minimum during September and October and indicated that one annual growth ring is formed each year. Male red emperor (21.1-72.8 cm FL) ranged from age 2 to 30 and females (18.3-58.4 cm FL) ranged from age 1 to 34. There was significant

differential growth between sexes. Slow growth in length was evident for each sex. The slow growth, long life span and large size and age at maturity of red emperor indicates that they have a low production potential and are vulnerable to over-exploitation. The natural mortality rate was estimated to be in the range 0.104-0.122, these instantaneous rates indicate that 9.9-11.5% of the annual removal of fish was due to natural causes. The rate of total mortality estimated from catch at age data for fully recruited ages, was 0.321 in 1997/98 and 0.275 in 1998/99, representing an annual percentage removal of approximately 28% and 24% in each year.

Yield and egg per recruit models indicate that yield to fishers can be increased if age at first capture can be delayed several years. However, gear controls do not appear to be effective in regulating the size/age at first capture of the key demersal fish species in the NDSF. In addition, the capture of goldband snapper from depths of 60 metres or greater results in a high mortality of fish from swim bladder over-expansion injuries and hence there is a low probability of survival of any fish returned to the sea.

Given the low production potential of *P. multidentis* and *L. sebae*, harvest strategies of low frequency or low intensity are suggested for the sustainable exploitation of these fish stocks in the Indo-Pacific region. The demersal fish resource in the NDSF is currently being managed with an innovative total allowable effort / individually transferable effort unit system, however the highly mobile, efficient and wide ranging capacity of the NDSF fleet may require more complex management arrangements to maintain future breeding stock levels. Furthermore, as a consequence of the apparent low survival rate for released (tagged) fish in the fishing depths of the NDSF fleet, the traditional use of legal minimum sizes to increase survival to spawning sizes is not a practical option. Inclusion of targeted spatial or temporal closures within the effort management framework is however likely to be a useful mechanism to maintain spawning stock biomass and protect against recruitment overfishing.

**KEYWORDS:** Goldband snapper, *Pristipomoides multidentis*, Red emperor, *Lutjanus sebae*, Age, Growth, Mortality, Otoliths, Reproduction, Gear selectivity, Yield-per-recruit, Egg-per-recruit, Reference points, Fisheries management.

## Background

The demersal fish resources of the Kimberley region of Western Australia were first explored and fished by the Japanese in the late 1950s and were intensively fished by Taiwanese pair trawlers in the 1970s. The ratification of Australia's Exclusive Economic Zone (EEZ) in November 1979 allowed further foreign fishing in these waters under a licence agreement with the Commonwealth of Australia. Fishing continued in the Kimberley by Taiwanese pair trawlers until 1990. Chinese pair trawlers also fished Kimberley waters in 1989.

The Kimberley region extends along the continental shelf from approximately 120°E to 129°E longitude. Foreign trawling effort in the Kimberley was low compared to the Pilbara region of Western Australia (114°E to 120°E longitude). The history of foreign fishing in the Kimberley, and the possible implications for the stock assessment of currently exploited resources was assessed in FRDC Project 94/26 (Nowara and Newman 1996). The foreign fishing fleets departed in 1990, and a domestic trap fishery operating out of Broome and Darwin and, more recently, a line fishery, have subsequently developed in this region. The demersal trap and line fishery in the Kimberley region of Western Australia is now known as the Northern Demersal Scalefish Fishery (NDSF).

The NDSF came under formal management on 1 January 1998. The fishery is now managed on the basis of time gear units in combination with a nominal total allowable catch (TAC), which is assumed to be sustainable. The NDSF forms a major component of Western Australia's commercial finfish production, contributing over 570 tonnes in 1999 for a catch value of approximately \$ 2.98 million. The catch consists primarily of species of the Lutjanidae (snappers), Lethrinidae (emperors) and Serranidae (cods/groupers). Goldband snapper (*Pristipomoides multidens*) and red emperor (*Lutjanus sebae*) dominate landings in the NDSF. Trap fishing is the dominant fishing method in the NDSF. Further expansion and development of fishing in deeper outer-shelf waters using trap and lines are likely to occur in the future.

Outer shelf fishes may be particularly sensitive to exploitation pressure because they are likely to be long-lived, have slow growth rates, a late onset of maturity and low rates of natural mortality (Polovina and Ralston 1987). Little is known of the biology of the commercial outer-shelf fishes from the Kimberley or the

habitats upon which they are dependent. If these species are overfished, the recovery rates of their populations are likely to be very slow.

Preliminary estimates of maximum sustainable yield (MSY) for demersal fishes in this region although useful, are insufficient to enable the development of sustainable management arrangements for these fish stocks. There is also little information available on the population parameters of the major species of commercial and recreational importance in the Kimberley region. Within Western Australian waters key stock assessment information on species such as the red emperor is being produced from the Pilbara fishery (FRDC Project 93/25), but to date no studies have examined the king snappers or other commercial outer-shelf species

### **Need**

The Kimberley Fishery developed rapidly and is now a complex fishery producing a high quality product. The small amount of information available at present causes concern at the state of exploitation of the stocks. Information is required to enable effective management of the fishery. The tools available are controls on size at first capture and overall fishing mortality. It is more practical in the first instance to obtain information, which will enable control of size at first capture, and to follow this with the information needed to control fishing mortality.

The size selectivity of traps and lines needs to be examined to explore the possibility of using hook sizes and escape gaps in traps to reduce catches of smaller fish and hence increase long-term yields. Initial management controls can then be based on the outcome from size-at-first capture models. The size-at-first capture may be able to be controlled through the use of a mixture of fishing gear types (eg. fish traps in combination with lines and hooks of a specified size). The size-at-first capture of these fishes may also possibly be regulated through area controls, provided the distribution of adults and juveniles is known. Direct controls on fishing mortality by area can be applied by zoning of fishing effort, monitored through the use of Vessel Monitoring Systems.

## Objectives

1. Estimate essential population parameters of goldband snapper and other key demersal species.
2. Estimation of yield-per-recruit and egg-per-recruit optimum combinations for the regulation of size-at-first capture and fishing mortality.
3. Examination of the size selectivity of commercial trap gear to investigate methods of altering selectivity to enable targeting of fish of a specific size.
4. Advise fishery managers and industry on the combinations of gear and effort controls to produce optimal sustainable yields.

This study has focused on the red emperor snapper, *Lutjanus sebae* in addition to the goldband snapper, *Pristipomoides multidens*.

## Methods – Age and Growth

Commercial landings of *P. multidens* from fishers of the Northern Demersal Scalefish Fishery (NDSF) off the Kimberley coast of Western Australia were sampled from 1995 to 1999. Samples were obtained opportunistically from July 1995 to December 1996, while samples obtained from January 1997 to December 1999 were collected on a monthly basis across all vessels in the fleet. All the specimens collected were captured with using either lines or fish traps (predominantly fish traps) in depths of 80 to 200 metres from 12°-20°S latitude (see Fig. 1.1). Additional catch samples were obtained from research vessel cruises. Monthly samples consisted of at least 60 fish sampled randomly from fish processors. The locations of samples from the commercial catches were randomly distributed throughout the extent of the fishery for both species. Comparison of line and trap selectivity could not be undertaken in this study and requires further investigation.

Commercial landings of *L. sebae* from fishers in the NDSF were sampled opportunistically from July 1995 to November 1996, and subsequently on a monthly basis across all vessels from May 1997 to December 1999. All fish sampled were caught with fish traps in waters from 60 to 150 metres depth, from 12°-20°S latitude (see Fig. 1.1). Small specimens under the minimum legal size of 410 mm total length

were obtained directly from commercial catches with additional specimens sourced from both commercial fishermen and research vessel cruises.

All fish were measured to the nearest mm total length (TL), fork length (FL) and standard length (SL), weighed to the nearest g total weight (TW) and cleaned weight (CW), and where possible, sex was determined by macroscopic examination of the gonads. Cleaned weight is defined as the total weight after removal of the gills and viscera. Measurements of fish length (TL, FL, SL) were used to derive length conversion equations using the following generalised linear regression models:  $TL = a + b (FL)$ ,  $FL = a + b (TL)$ ,  $FL = a + b (SL)$  and  $SL = a + b (FL)$ .

### **Length-weight models**

The relationship between length and weight was described by the power relationship;  $W = aL^b$ , where W is weight (g) and L is length (mm). The relationship between length and weight was fitted to a log-transformed set of data, and the parameters were back-transformed (with correction for bias) to the above form.

Analysis of covariance ( $\alpha = 0.05$ ) was used to determine if there were significant differences in the weight-at-length (FL) relationship between sexes. Length and weight data were transformed to a natural logarithm function ( $\log_e x$ ) to satisfy assumptions of normality and homogeneity. Multiple comparisons were performed using Tukey's honestly significant difference (HSD) test. One-way analysis of variance ( $\alpha = 0.05$ ) was used to compare mean age, length and weight between sexes. Trends in the mean age, otolith weight, length and weight of fish over time were also assessed using analysis of variance ( $\alpha = 0.05$ ).

### **Otolith preparation and analysis**

The sagittal otoliths were removed by opening the otic bulla from under the operculum. Otoliths were then washed in freshwater and stored dry in envelopes prior to processing. Left and right sagittae were weighed (to 0.01 mg) and measured along three axes (total length, breadth and height (thickness) through the central core of the otolith) to the nearest 0.01 millimetre using digital callipers. Only intact otoliths were weighed and measured.

All age estimates were based on the analysis of transverse sections of otoliths. Initially, ten sagittal otolith pairs were examined to determine the number of opaque bands in each. The counts in each otolith pair were identical in all cases. Therefore, one sagitta per fish was randomly selected and embedded in epoxy resin. Thin transverse sections (250 - 300  $\mu\text{m}$ ) were made through the core of the otolith from the dorsal apex to the ventral apex using low-speed jewellery saw with a diamond-wafering blade. Three thin sections were taken from each otolith, washed by agitating in 2% HCl for up to 10 seconds, rinsed twice in  $\text{H}_2\text{O}$ , dried and mounted on microscope slides with casting resin. These sections were then examined under a dissecting microscope at 10-30 $\times$  magnification with reflected light on a black background.

The otoliths from 8 juvenile *P. multidentis* (80-140 mm FL) were examined for daily bands using a different technique. One sagitta per fish was embedded in epoxy resin and a thick transverse section (> 500  $\mu\text{m}$ ) was cut. The section was then ground and polished from each side to a level near the core, perpendicular to the long axis of the otolith. This was done by hand using ebony paper (1000 grade) and lapping film (9 and 3  $\mu\text{m}$ ). A polished, thin transverse section approximately 100  $\mu\text{m}$  thick was produced. The section was then examined using a compound microscope.

### **Age validation**

Marginal increment analysis (MIA) is normally used to validate age. MIA relies on the assumption that if a translucent zone is laid down once per year, there should be a clear pattern of periodic growth on the edge of the otolith during the year. MIA is appropriate only if all the fish in the population lay down the translucent zone at the same time. An annulus would then consist of a single opaque zone and a single translucent zone. The opaque zone is believed to form during periods of slow growth.

MIA usually implies measurement of marginal growth and hence many researchers have measured the width of the edge of the otolith section over an annual cycle. This measurement approach has an advantage in that it should be possible to plot growth of the edge over time to validate that only a single translucent mark is laid down each year. However, in *P. multidentis*, it can be difficult to determine a consistent location to measure on the otolith because of the inherent variability of the otoliths, hence this technique was not used.

Edge type analysis was adopted for the marginal increment analysis of *P. multidentis* with edge types classified according to Pearson (1996) as either translucent, narrow opaque (opaque area less than half of the previous opaque zone) or wide opaque (opaque area greater than half of the previous opaque zone). Sectioned otoliths of fish of all ages were examined under a dissecting microscope using reflected light on a black background. An annulus consists of a single opaque and a single translucent cycle within a 12-month period.

The marginal increment of each otolith for *L. sebae* was determined by the proportional method where the amount of otolith growth from the outermost growth increment to the otolith edge is expressed as a fraction of the total growth in the preceding whole increment cycle (opaque and translucent zone). Measurements for MIA were undertaken in the ventral lobe of the otolith with an ocular micrometer and a compound microscope at 100× magnification. Measurements were made as close as was practicable to the margin of the sulcus acousticus. Otolith sections were excluded from the analysis if the discrimination between the end of a translucent zone and the beginning of the subsequent opaque zone was unclear. The margin of each otolith was recorded as being either translucent or opaque, and the frequency of opaque margins plotted over the course of the sampling period. Mean marginal increments were plotted across all age classes in each month from April 1997 through to November 1998 to ascertain if they follow a consistent annual trend. If a single growth zone is laid down in each otolith at a consistent time within each year, then these growth zones can be considered to be valid annuli.

Direct validation of annulus formation was attempted through the use of calcein marking. From April 1997 to September 1999, 1,291 *L. sebae* were caught in fish traps off the Kimberley coast of north-western Australia in depths ranging from 40-115 metres, tagged with large dart tags and injected with calcein (10 mg ml<sup>-1</sup>) before being released. Injection was carried out with a syringe and 26 gauge needle which was inserted under the scales and through the skin into the coelomic cavity in close proximity to the pelvic fin region. A minimum dosage of 15 mg of calcein per kg of fish was given. The otoliths of any recaptured fish were sectioned and viewed under ultra-violet light.

### Age determination

By convention all fish were assigned a birth date to assure proper year-class identification. A birth date of 1 April was chosen for *P. multidentis* as peak spawning occurs in late March. A birth date of 1 January was chosen for *L. sebae*. Ages were assigned based on counts of annuli (alternating opaque and translucent bands) from sectioned otoliths. Annuli were counted without reference to fish length or date of capture. Each otolith section was examined on either 3 or 4 separate occasions depending on the species. All counts were made by one reader (SJN) to ensure consistency. When the counts differed, otolith sections were re-examined. In most cases requiring resolution, the final count was used for analysis of age and growth, since by this time considerable experience had been gained in the interpretation of the otolith structure. Otoliths with structural irregularities such as unusual calcification, deterioration of the ventral lobe, or poorly defined annuli were considered indecipherable, and were excluded from analysis of fish age.

Counts were compared and the precision of age estimates calculated using the Index Average Percent Error (IAPE) of Beamish and Fournier (1981). Greater precision is achieved as the IAPE is minimised. The relationship between age and otolith weight is often significantly correlated and linear in form. The relationship between fish length and age and otolith dimensions was assessed using generalised linear regression techniques.

Timing of translucent zone formation in *P. multidentis* and mean sea surface temperatures (SST; assumed to reflect the temperature at depth) were compared by standardising values. The standardisation process allows direct comparison of each series and any time lags of one in relation to the other. Standardised score =  $1 - ((\text{maximum value} - x) \div \text{range})$ , e.g. in November, standardised SST =  $1 - ((29.7 - 29) \div 3.7) = 0.81$ ; standardised % Frequency Translucent =  $1 - ((67 - 20) \div 67) = 0.30$ .

### Growth and mortality models

The von Bertalanffy growth function (VBGF) was fitted to estimates of fork length-at-age using nonlinear least squares estimation procedures. The VBGF is defined by the equation:  $L_t = L_\infty \{1 - \exp[-K(t - t_0)]\}$ ; where  $L_t$  = mean length at age  $t$ ;  $L_\infty$  = asymptotic mean length;  $K$  = Brody growth coefficient and defines the growth

rate towards  $L_{\infty}$ ;  $t$  = age of the fish; and  $t_0$  = the hypothetical age at which fish would have zero length if it had always grown in a manner described by the equation. The von Bertalanffy growth curves between sexes were compared using the likelihood ratio test of Cerrato (1990) in order to determine if there was a single underlying growth curve for both sexes.

Estimates of the instantaneous rate of total mortality ( $Z$ ) were obtained from catch-at-age data for each species from the NDSF. Annual catch in weight was converted to annual catch in numbers-at-age by the use of age frequency data standardised by fishing effort to obtain catch rate per age class. Catch in weight was converted to catch in numbers based on the mean weight of each species observed in the sampled catch each year. Mortality estimates were then derived between successive years by obtaining the natural logarithm of the catch rate per age class (e.g. age 4) in year  $t$  and subtracting the natural logarithm of the catch rate per age class (e.g. age 5) in year  $t + 1$  for all fully recruited age classes. Mean total  $Z$  was then calculated across all fully recruited age classes. Estimates of the survival rate of each species ( $S$ ) were then calculated by  $S = e^{-Z}$  (Ricker 1975).

Estimates of the instantaneous natural mortality rates ( $M$ ) were derived using the general regression equation of Hoenig (1983) for fish, where:  $\log_e Z = 1.46 - 1.01 \log_e t_{\max}$  ( $t_{\max}$  is the maximum age in years). The Hoenig (1983) equation has provided similar estimates of  $M$  to those derived from age-based catch curves for unfished populations (Newman et al. 1996, 2000b, Hart and Russ 1996).

Estimates of  $F$  were derived by subtraction, since  $F = Z - M$ . The annual harvest rate or percentage removal by the fishery was estimated by: harvest rate =  $[F/Z (1 - e^{-Z})] \times 100\%$ . Exploitation rates ( $E$ ) were derived from the estimates of  $Z$  and  $F$  as defined by the equation  $E = F/Z$ .

### **Estimation of optimum fishing mortality rates ( $F_{\text{opt}}$ )**

Until the 1990's fishing mortality objectives such as  $F = M$  were often prescribed for sustainability (e.g. Gulland 1970). Adoption of harvest strategies such as setting  $F = F_{0.1}$  (which ignore stock-recruitment effects) were thought to be quite conservative, and usually resulted in  $F = M$  harvest strategies (Walters in press). Recently, the meta-analysis of Myers et al. (1999) synthesized information about

stock-recruitment curve slopes expressed as maximum reproductive rates per spawner at low spawner biomass. When their results were substituted into age-structured population models and optimum equilibrium fishing rates ( $F_{opt}$ ) calculated, the results implied that  $F_{opt}$  was substantially lower than  $M$  for most species and stocks (Walters in press, pers. comm.). The main exceptions were cases where regulation or natural phenomena resulted in age selectivity patterns where most fish have at least one chance to spawn before becoming vulnerable to high harvest rates (Walters in press, but see also Myers and Mertz 1998).

The harvest strategy of  $F_{opt} = 0.5 M$  (Walters in press) is proposed as an optimum fishing mortality rate for the sustainable exploitation of the demersal fish resources of the NDSF. This harvest strategy seeks to ensure adequate egg production and hence the maintenance of recruitment such that the current set of fishers in the NDSF should not compromise the ability of future generations to harvest the resource. Walters (in press) reported that any fishery assessment that results in levels of  $F_{opt}$  above  $0.5 M$  needs to be very carefully justified, either by clear demonstration that higher fishing mortality rates have been sustained for several fish generations or that the age-selectivity schedule permits virtually full replacement of recruits (by the fish that survive to spawn) prior to the age at first capture. The  $0.5 M$  harvest strategy is a conservative harvest strategy that seeks to account for the uncertainty of the parameters derived from stock assessment analyses. Therefore these reference points are proposed in order to account for uncertainty in parameter estimates.

Furthermore, Patterson (1992) reported that fishing mortality rates above  $2/3 M$  are often associated with stock declines, whereas fishing mortality rates below this level have resulted in stock recovery. Therefore, we consider that fishing mortality rates above  $2/3 M$  to represent an undesirable state for the resource, and a situation which management action should avoid. In essence, a limit reference point ( $F_{limit}$ ) for fishery managers. Calculation of  $F_{opt}$  and  $F_{limit}$  requires an estimate of the natural mortality ( $M$ ), since  $F_{opt} = 0.5 M$  and  $F_{limit} = 2/3 M$  (Walters in press, Patterson 1992).

### Methods - Reproduction

Samples of *Pristipomoides multidens* and *Lutjanus sebae* were randomly collected from commercial catches of trap and line vessels operating in the Northern

Demersal Scalefish Fishery (NDSF) off the Kimberley coast of north-western Australia (Fig. 1). These fish were obtained fresh on ice from either local or regional processors (gonads were not frozen). Sampling was undertaken at monthly intervals between July 1997 and June 1999. Each month 30 female and 30 male fish were dissected and fork length (FL, mm), total weight (g), clean weight (weight after removal of gills, gonads and viscera in g) and sex of each fish recorded.

Gonads were removed when they could be identified macroscopically as either an ovary or a testis and subsequently weighed to the nearest 0.01 g. Each gonad was macroscopically assigned one of the following eight stages, similar to those used by Laevastu (1965): I = virgin; II = maturing virgin; III = developing; IV = maturing; V = mature; VI = spawning; VII = spent and VIII = resting. Generally, there was little difficulty in assigning a stage to a gonad.

A sample of gonad material was excised from the centre of one of the gonad lobes in 25 females and 5 males each month and placed in 10% formalin buffered with 0.03 M  $\text{NaH}_2\text{PO}_4 \cdot 2\text{H}_2\text{O}$  and 0.12 M  $\text{Na}_2\text{HPO}_4$ . Each gonad tissue sample was embedded in a paraffin wax block. The gonad tissue was then cut into 7-8  $\mu\text{m}$  transverse sections and placed on a microscope slide. The slides were then stained with haematoxylin and eosin. The stained and mounted slides were examined under transmitted light.

The stages of the oocytes in sectioned samples were examined to ensure that they were assigned to appropriate macroscopic stages. Gonad stages are described as; stage I – chromatin nucleolar; stage II – perinucleolar stage; stage III – cortical alveoli stage; stage IV – early and late yolk vesicle oocytes; stage V – migratory nucleus stage; stage VI – hydrated oocyte stage (modified from West (1990) and Davis and West (1993)). Stages I to III represent the pre-vitellogenic stage. A detailed description of the histological staging is given in Table 3.1. Oocyte diameters were determined using image analysis software. The diameters of 30 oocytes per ovarian section were determined by measuring the circumference of the oocyte to the nearest 5  $\mu\text{m}$ , then calculating the diameter by dividing the circumference by pi ( $\pi$ ). All histological sections were examined for the presence of post-ovulatory follicles (POFs).

Gonadosomatic indices (GSIs) were determined for all mature (gonad stages IV-VIII) female and male fish using the following equation:  $GSI = (W_g + W_{cw}) \times 100$ , where GSI = gonadosomatic index expressed as a %;  $W_g$  = gonad weight in g, and  $W_{cw}$  = clean weight (weight after removal of gills, gonads and viscera) of the fish in g. GSI was calculated using the cleaned fish weight in order to reduce variation due to the weight of the gonad and contents of the viscera. A  $\chi^2$  analysis was used to determine whether the number of males and females of each species differed (from an expected ratio of 1:1) throughout the year or over increasing length classes.

To examine the proportion of immature and mature fish in the landed commercial catch, a population maturity index (PMI) was created. The PMI is estimated as:  $PMI = [(total\ number\ of\ mature\ fish\ in\ each\ sample) \div (total\ number\ of\ fish\ in\ each\ sample)] \times 100$ , with stages IV-VIII classified as mature fish. Variation in the PMI was examined seasonally throughout a yearly cycle and temporally over the duration of the sampling period.

The length at which 50% of individuals attain sexual maturity ( $L_{50}$ ) is considered to best represent a mean population value. The length at maturity ( $L_{50}$ ) for both species was estimated from the length and maturity data of all individuals obtained from commercial catches.  $L_{50}$  was estimated by fitting a logistic model to the proportion of female and male fish in each 10 mm length interval, which possessed gonads from Stage IV to VIII during the spawning season. Fish with gonad stages from IV-VIII were considered to be capable of spawning in the year of capture. The logistic expression was used to fit the proportion of mature fish in each length interval by maximising the log-likelihood of the distribution function. The logistic equation is  $P_{(L)} = 1 \div [1 + \exp(-r\{L-L_m\})]$ , where  $P_{(L)}$  is the proportion of fish with mature gonads at length interval  $L$ ,  $r$  is the slope of the curve and  $L_m$  is the mean length at sexual maturity (the length which corresponds to a proportion of 50% in reproductive condition).

The age at which 50% of female and male fish become sexually mature ( $A_{50}$ ) was determined from the inverse von Bertalanffy growth function described by Stergiou (1999) where  $A_{50} = t_0 - (1+k) \times (1 - (L_{50} + L_{\infty}))$ . This calculation uses the  $L_{50}$

derived from the logistic equation above and the von Bertalanffy growth parameters  $(t_0, k, L_\infty)$  derived from the concurrent age and growth study.

## Results

### 1. Spatial distribution of catch and effort in the Northern Demersal Scalefish Fishery.

*Stephen J. Newman and Richard A. Steckis*

The waters of the NDSF are defined as all Western Australian waters off the north coast of Western Australia east of longitude 120°E. The western boundary borders the waters of the Northern Territory. The waters of the NDSF extend out to the edge of the Australian Fishing Zone (200 nautical mile) limit under the Offshore Constitutional Settlement arrangements (Fig. 1.1). The fishery is further divided into two fishing zones, an inshore zone (Zone 1) and an offshore zone (Zone 2) (see Fig. 1.1). The demersal fish resources of the deeper waters of the offshore zone (greater than 200 m depth) are currently under investigation; these waters are shown on Figure 1.1 as the research fishing zone. The inshore waters in the vicinity of Broome are closed to commercial fishing. The closed area extends from Cape Bossut to Cape Coulomb, inside a line, which approximates as closely as possible the 30 metre bathymetric contour.

Catches of commercial fishers are widely distributed throughout the NDSF, but are concentrated along the edge of the continental shelf in the vicinity of the 100 metre depth contour from 12°S to 19°S latitude (Fig. A1, Appendix 1). Catches are highest in the areas closest to Broome in all years. A declining catch trend is evident in most areas from 1995-1999. Line fishing effort in the NDSF is concentrated in the northern part of the fishery from 12°S to 14°S latitude (Fig. A2). Line fishing effort has declined markedly in the period from 1995 to 1999, with very little line effort in 1998 and 1999. The spatial distribution of the trap fishing effort clearly indicates that fishing activities are concentrated in the southern part of the fishery in the vicinity of Broome (Fig. A3). In 1999, trap fishing effort increased in the northern part of the NDSF in close proximity to the border with Indonesia.

The line catch of *P. multidentis* is concentrated in the northern part of the fishery (Fig. A4). The line catch for *P. multidentis* has declined substantially since 1995, reflecting the reduced line effort over this time. Line catch per unit effort

(CPUE) over the same period has been variable dependent on location, with some areas showing either a decrease or an increase in line CPUE (Fig. A5). The trend of increasing CPUE in the presence of declining line effort indicates that fishers are attempting to increase their efficiency. However, these data must be interpreted with caution, as there is an element of hyperstability in the line CPUE data, with line CPUE maintained at high levels by targeting of schools. Although, no data is available, anecdotal information obtained from line fishers indicates that the search time in the fishery is increasing as schools are becoming increasingly harder to locate. The trap catch of *P. multidentis* is concentrated in the vicinity of Broome (Fig. A6). Trap catches of *P. multidentis* have increased in recent years, with trap CPUE increasing (Fig. A7). The increasing trap CPUE for *P. multidentis* is a reflection of the targeting capacity of fishers in the NDSF. Since the implementation of effort controls in 1998, trap fishers have begun targeting *P. multidentis* in order to maximise their return from each day fished.

The line catch of *L. sebae* is very small when compared with the trap catch. The line catch of *L. sebae* is highest in the northern sector of the fishery and reflects the concentration of line effort in this region (Fig. A8). The line CPUE for *L. sebae* is small with declining trends present in many areas (Fig. A9). The low line CPUE for *L. sebae* indicates that they are not amenable to this method of harvest and hence they are not the primary target species of line fishers. Trap catches of *L. sebae* have declined in the most heavily fished areas from 1995 to 1999 (Fig. A10). Trap CPUE for *L. sebae* is declining in the highest catching areas in the vicinity of Broome (Fig. A11). The trap CPUE in the northern part of the fishery, are somewhat stable (Fig. A11).

The line catch of other lutjanids (defined as all lutjanid species excluding *P. multidentis* and *L. sebae*) are concentrated in the northern and inshore zones of the NDSF (Fig. A12). Catches of other lutjanids were very low and did not exceed 6 tonnes in any year in any one block. This very low catch indicates that the line fishers are very selective in their targeting practices and not all species are amenable to line fishing. The other lutjanid CPUE is low and variable, with trends obscured by a very high CPUE evident in one fishing block in 1995 (Fig. A13). The overall line CPUE of other lutjanids is somewhat evenly distributed throughout the fishery, with some

higher CPUE values in the inshore zone of the fishery (Fig. A13). The trap catch of other lutjanids is concentrated in the south of the fishery in line with trap effort (Fig. A14). Catch of other lutjanids does not exceed 16 tonnes in any one fishing block. The trap CPUE for other lutjanids is somewhat consistent from 1995 to 1999 (Fig. A15).

The line catch of cods (Serranidae, Epinephelinae) was higher in the northern sector of the NDSF (Fig. A16). The line catch of cods is nearly an order of magnitude lower than the trap catch of cods. The line catch of cods declined in the period from 1995 to 1999 corresponding to the decrease in line fishing effort. The line CPUE for cods is variable (Fig. A17) and substantially lower than the corresponding trap CPUE. The catch of cods by trap fishers is highest in those fishing blocks around Broome in the southern part of the NDSF (Fig. A18). In general the trap catch of cods has declined in the period from 1995 to 1999. The trap catch of cods is insignificant in the northern sector of the NDSF. The trap CPUE for cods is highest in the southern sector of the fishery, particularly in the vicinity of Broome (Fig. A19). The trap CPUE for cods is relatively stable in many areas, however in some blocks declining trends are evident over the five-year period from 1995 to 1999.

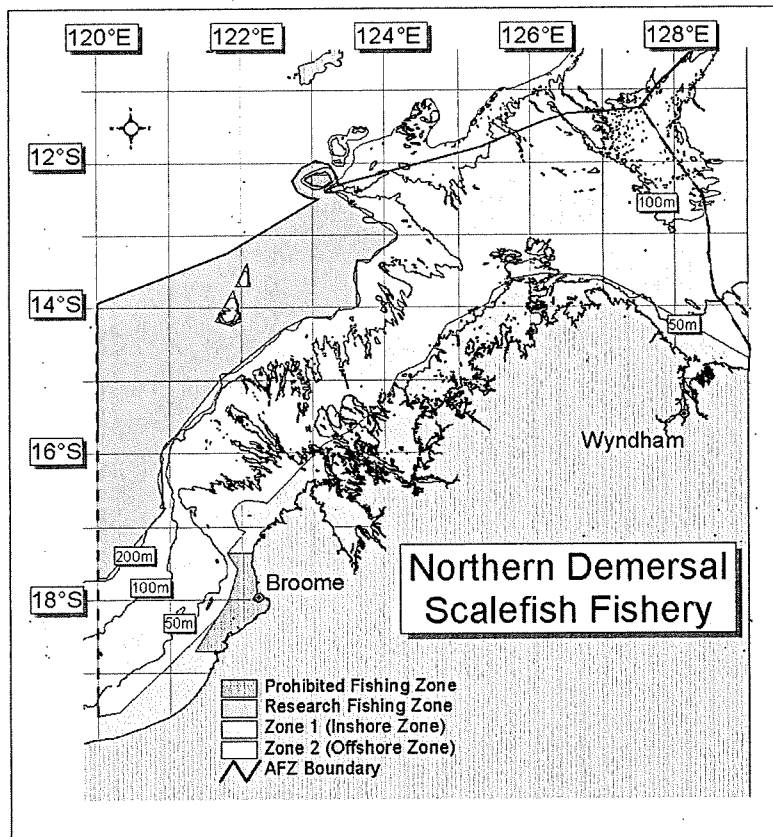


Figure 1.1: Location, boundaries and zones within the Northern Demersal Scalefish Fishery in the Kimberley region of north-western Australia.

### **1.1 Summary of catch and effort data collected to date from the logbook program.**

Despite consistent encouragement, urging and promotion, only two fishers, one trap fisher and one line fisher in the NDSF have contributed to the logbook program. Trap fishing logbook data were received for each trip undertaken between January 1999 and February 2000. No trap logbook data has been received since February 2000. Line fishing logbook data were received for each trip undertaken between October 1999 and April 2000. Given the poor response to the logbook program and the limited amount of data available only summary data is presented in order to preserve confidentiality of fishers catch data.

Catch rates by the trap vessel over all months from which data is available have varied between approximately 394-797 kg per day. Similarly catch rates by the line vessel over all months from which data is available have varied between ca. 418-837 kg per day. Catch rates by species have also varied considerably with each trip depending on the area fished by each fisher. Catch rates of goldband snapper have varied between ca. 72-632 kg per day from trap fishing and between ca. 307-733 kg per day from line fishing. Catch rates of red emperor have varied between ca. 51-289 kg per day from trap fishing and between ca. 4-93 kg per day from line fishing. Trap and line catch rates are highly variable between fishing trips. It is worth noting that line fishing fails to yield the same high catch rates of red emperor that are achieved using traps.

A typical fishing trip undertaken by a trap fisher is described. The vessel leaves port and steams to retrieve traps from the area where the traps were left. The vessel then continues to steam to their nominated fishing ground. Fishers can travel quite long distances to reach their nominated fishing ground. For example, if the nominated fishing ground is in the vicinity of Browse Island (central Kimberley), then the travel distance is ca. 240 nautical miles from Broome to Browse Island. Once the nominated fishing grounds have been reached, they will be fished for the next 7-10 days on average, depending on trip length. Fishers will move around the area fishing the gear with between 60 and 100 trap pulls per day recorded (this is dependent upon the number of traps which vessels nominate to fish, the minimum is 20). Typical catch

rates are between 400-800 kg of fish per day. The fleet is quite mobile and has the capacity to move long distances if fish are not being caught in the immediate vicinity. The key target species are goldband snapper and red emperor. The area over which fishing occurs in any one trip is ca. 30 square nautical miles. When fishing activity ceases the vessel usually steams back to Broome, offloading the traps close to Broome to make unloading the catch easier. Arrival in Broome is generally timed to coincide with the refrigerated truck departures for Perth. Vessels usually spend no more than 12 days at sea, due to the limited storage capacity, shelf life of fish and timing to coincide with freezer truck departures, which occur only three days per week (Monday, Wednesday and Friday).

A line-fishing trip is somewhat similar, however, they will pull between 20 and 75 line sets per day. Goldband snapper is by far the major component of the line catch. Typical line boat catch rates are between 420-840 kg per day (from logbooks) when fishing. Line fishers have reported that in recent years these catch rates have not always been met and that line fishing operations are no longer economically viable.

The logbook program to date has had very limited success. There has been a general reluctance from fishers to actively participate in the program. Given the limited success of the logbook program to date, the data generated is limited in value and is presently not useful as an aid for stock assessment purposes. For detailed spatial analyses of fishing effort to be undertaken, fishers across the fleet would have to embrace the program and provide detailed logbook over time. In the absence of logbook data to provide detailed spatial information of fishing catch and effort and its effect on fish stocks, management strategies need to be conservative.

## 1.2 Surveys aboard fishing industry vessels.

A total of fifty-nine species of fish were sampled from surveys aboard industry vessels (see Table 1.2.1, 1.2.2). The two most important and dominant species in the landed catch were *Lutjanus sebae* (36.75%) and *Pristipomoides multidens* (23.02%), which together represent ca. 60% of the total catch (Table 1.2.2). The next most abundant commercially important group is the cods (Serranidae: Epinephelinae) representing ca. 19% of the catch. Of the cods the two most important species are *Epinephelus areolatus* (7.32%) and *Epinephelus bleekeri* (6.63%). A number of other lutjanids and lethrinids comprise the remainder of the commercial catch (Table 1.2.1). Species, which were discarded and hence are considered by-catch are listed in Table 1.2.2. There is an extremely small by-catch from the trap fishery in the NDSF. The observed by-catch was less than 4% of the landed catch. Triggerfish of the genus *Abalistes* were the most common by-catch species comprising 1.1% of the landed catch.

Catch rates of all species combined were  $0.651 \text{ kg trap-hour}^{-1}$ . Soak times (i.e. the time calculated from when a trap entered the water to the time a trap was hauled to the surface) varied depending on whether traps were set during the day or overnight. The average number of trap sets during the day was 3.4, with only one set overnight. Traps set during the day had soak times on average of 3.30 hours ranging from 0.92 to 8.55 hours. Traps set overnight had soak times on average of 11.99 hours ranging from 5.70 to 14.90 hours. Catch rates of traps set during the day ( $0.77 \text{ kg trap-hour}^{-1}$ ) were higher than those recorded for traps set overnight ( $0.16 \text{ kg trap-hour}^{-1}$ ). It is not logistically possible for many boats to fish through the night thus mimicking the fishing activities undertaken throughout the day. However, the overnight catch is significant and forms an important component of the catch. Hence, there are diel differences in catch rates among species. For example, catch rates of *P. multidens* in day set traps ( $0.183 \text{ kg trap-hour}^{-1}$ ) are much higher on average than overnight trap sets ( $0.017 \text{ kg trap-hour}^{-1}$ ). Similarly, the catch rates of *Lutjanus sebae* in day set traps ( $0.294 \text{ kg trap-hour}^{-1}$ ) are much higher on average than traps set overnight ( $0.084 \text{ kg trap-hour}^{-1}$ ).

The length frequency of *P. multidens* sampled aboard industry vessels indicates that a large proportion of small fish (< 500 mm FL) are present in the landed

catch (Fig. 1.2.1). Surveys aboard industry vessels consisted of sampling trap vessels only, due to the low amount of line fishing effort it was not logistically possible to survey any line fishing vessels during the project. The modal peak in the length frequency distribution occurs in the 520 mm length class, the number of fish present in the larger size classes declines rapidly to ca. the 600 mm length class (Fig. 1.2.1). Fish over 600 mm FL are not very abundant in the catch. The length frequency distribution of *L. sebae* sampled aboard industry vessels is somewhat bimodal (Fig. 1.2.2). There is a rapid increase in frequency of length classes from 300 mm FL to an initial peak in the 450 mm length class. The second and smaller mode occurs in the 520–550 mm length classes. Fish over 600 mm FL are not very abundant in the catch.

A wide size range of *Epinephelus areolatus* were sampled aboard industry vessels (Fig. 1.2.3), indicating that the trap fishery is capable of harvesting this species throughout most of its life history. Little is known about the biology of *E. areolatus*, yet it comprises about 7.3% of the catch sampled aboard industry vessels and is one of the dominant small spotted cods landed in the fishery (Table 1.2.1). The second most abundant cod species landed in surveys aboard industry vessels was *Epinephelus bleekeri* (6.6% of the landed catch, Table 1.2.1). The majority of the fish caught are in the length classes between 420 and 490 mm FL (Fig. 1.2.4). Fish above 490 mm FL decline rapidly in the catch and few fish above 530 mm are landed (*E. bleekeri* can attain lengths in excess of 700 mm FL). Furthermore, few fish less than 400 mm FL were present in the landed catch. Juvenile *E. bleekeri* have been recorded from shallow nearshore waters. The absence of smaller fish in traps may reflect ontogenetic movement of this species offshore.

Scientific Name	Common Name	% Frequency
<i>Lutjanus sebae</i>	Emperor, Red	36.75
<i>Pristipomoides multidens</i>	Snapper, Gold-Band	23.02
<i>Epinephelus areolatus</i>	Rockcod, Yellow-spotted	7.32
<i>Epinephelus bleekeri</i>	Cod, Duskytail/Grouper, Bleeker's	6.63
<i>Lutjanus malabaricus</i>	Seaperch, Saddle-tailed (Scarlet)	4.21
<i>Epinephelus stictus</i>	Grouper, Black-dotted	2.14
<i>Lutjanus bitaeniatus</i>	Seaperch, Indonesian	2.12
<i>Pristipomoides typus</i>	Jobfish, Sharptooth	1.67
<i>Lutjanus russelli</i>	Perch, Moses	1.63
<i>Lethrinus atkinsoni</i>	Emperor, Yellow-tail	1.27
<i>Lutjanus bohar</i>	Bass, Red	1.08
<i>Lethrinus lentjan</i>	Emperor, Purple-headed	1.01
<i>Lutjanus lemniscatus</i>	Seaperch, Dark-Tailed	0.84
<i>Epinephelus amblycephalus</i>	Rockcod, Blunt-headed	0.76
<i>Lethrinus hutchinsi</i>	Emperor, Lesser Spangled/Emperor, Blue-Spotted	0.67
<i>Epinephelus multinotatus</i>	Rockcod, Rankin's	0.65
<i>Lethrinus olivaceus</i>	Emperor, Longnose/Emperor Longface	0.48
<i>Gymnocranius grandoculis</i>	Seabream, Robinson's	0.43
<i>Epinephelus bilobatus</i>	Cod, Frostback	0.37
<i>Lutjanus erythropterus</i>	Seaperch, Crimson	0.36
<i>Lutjanus vitta</i>	Seaperch, Striped	0.33
<i>Cephalopholis sonnerati</i>	Rockcod, Tomato	0.31
<i>Epinephelus malabaricus</i>	Cod, Greasy/Cod, Slimy/Grouper, Malabar	0.23
<i>Epinephelus morrhua</i>	Grouper, Comet	0.19
<i>Epinephelus polyphemadion</i>	Cod, Camouflage	0.14
<i>Lutjanus argentimaculatus</i>	Mangrove Jack	0.14
<i>Carangoides orthogrammus</i>	Trevally, Thicklip	0.11
<i>Plectropomus maculatus</i>	Trout, Bar-cheeked Coral	0.09
<i>Gnathanodon speciosus</i>	Trevally, Golden	0.08
<i>Hapalogenys kishinouyei</i>	Javelinfinch, Lined	0.08
<i>Choerodon zamboangae</i>	Tuskfish, Zamboanga	0.06
<i>Epinephelus coioides</i>	Cod, Estuary	0.06
<i>Wattsia mossambica</i>	Mozambique Large Eye Bream	0.06
<i>Carangoides fulvoguttatus</i>	Trevally, Gold Spotted	0.05
<i>Diagramma labiosum</i>	Sweetlips, Painted	0.05
<i>Lethrinus xanthochilus</i>	Emperor, Yellowlip	0.05
<i>Seriola dumerili</i>	Amberjack	0.05
<i>Argyrops spinifer</i>	Snapper, Long-Spined	0.03
<i>Bodianus perditio</i>	Pigfish, Goldspot	0.03
<i>Glaucosoma buergeri</i>	Pearl Perch	0.03
<i>Lethrinus rubrioperculatus</i>	Emperor, Spotcheek	0.03
<i>Epinephelus chlorostigma</i>	Grouper, Brown-spotted	0.02
<i>Epinephelus cyanopodus</i>	Cod, Maori/Grouper, Speckled Blue/Rockcod, Purple	0.02
<i>Epinephelus fuscoguttatus</i>	Cod, Flowery	0.02
<i>Gymnocranius griseus</i>	Seabream, Naked-Headed	0.02
<i>Lethrinus sp. 2</i>	Emperor, Variegated	0.02
<i>Lutjanus bouton</i>	Seaperch, Moluccan	0.02
<i>Lutjanus gibbus</i>	Snapper, Paddletail/Snapper, Humpback Red	0.02
<i>Lutjanus rivulatus</i>	Seaperch, Maori	0.02
<i>Pristipomoides flavipinnis</i>	Jobfish, Yellow/Jobfish, Golden-eye	0.02
<i>Symphorus nematophorus</i>	Chinaman Fish	0.02

Table 1.2.1: Species composition of the landed commercial catch sampled during surveys aboard NDSF industry vessels and their relative contribution (% frequency) to the total catch.

Scientific Name	Common Name	% Frequency
<i>Abalistes stellaris</i>	Triggerfish, Starry	1.07
<i>Sufflamen fraenatus</i>	Triggerfish, Brown	0.08
<i>Abalistes sp.</i>	Triggerfish, Long-finned Starry	0.03
<i>Heniochus acuminatus</i>	Bannerfish, Longfin	0.02
<i>Myripristis murdjan</i>	Squirrelfish, Crimson	0.02
<i>Pterois volitans</i>	Lionfish/ Firefish, Red	0.02
<i>Sargocentron rubrum</i>	Squirrelfish, Red	0.02

Table 1.2.2: Species composition of the by-catch or discard component of the landed commercial catch sampled during surveys aboard NDSF industry vessels and their relative contribution (% frequency) to the total catch.

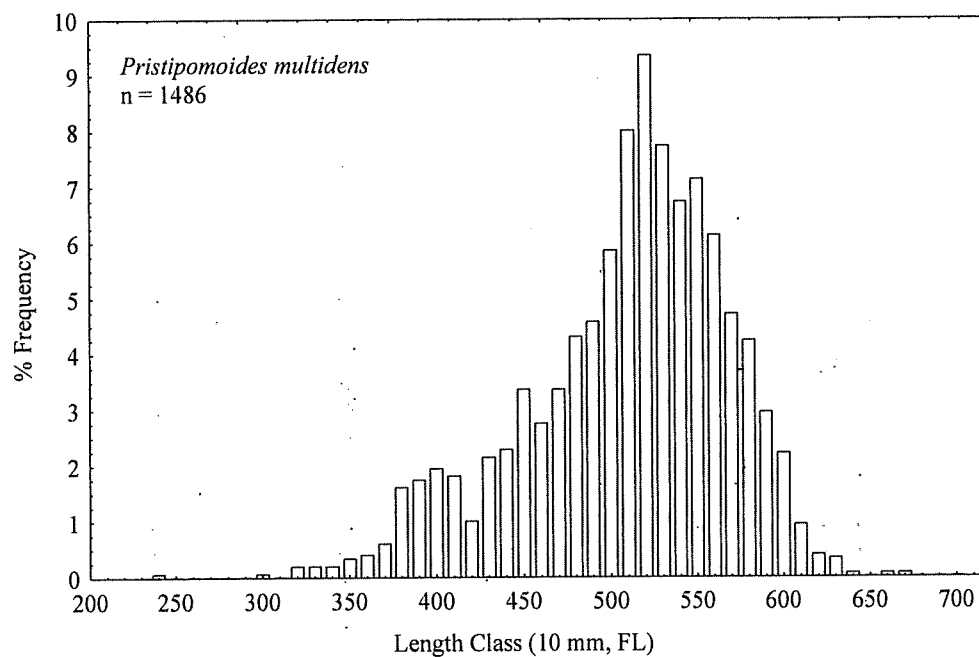


Fig. 1.2.1: Length frequency distribution of *Pristipomoides multidens* sampled aboard fishing industry vessels.

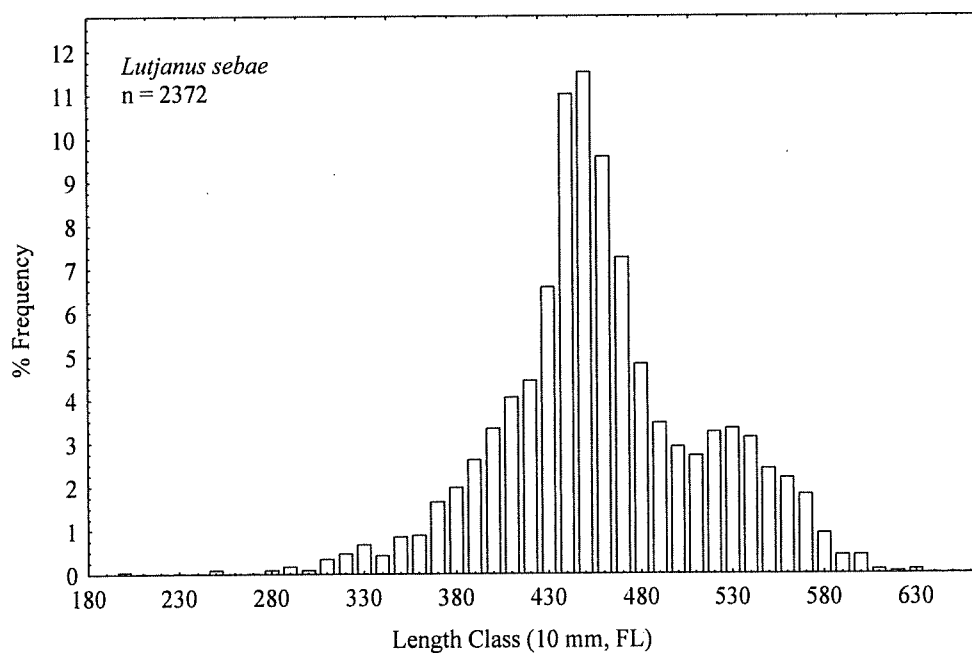


Fig. 1.2.2: Length frequency distribution of *Lutjanus sebae* sampled aboard fishing industry vessels.

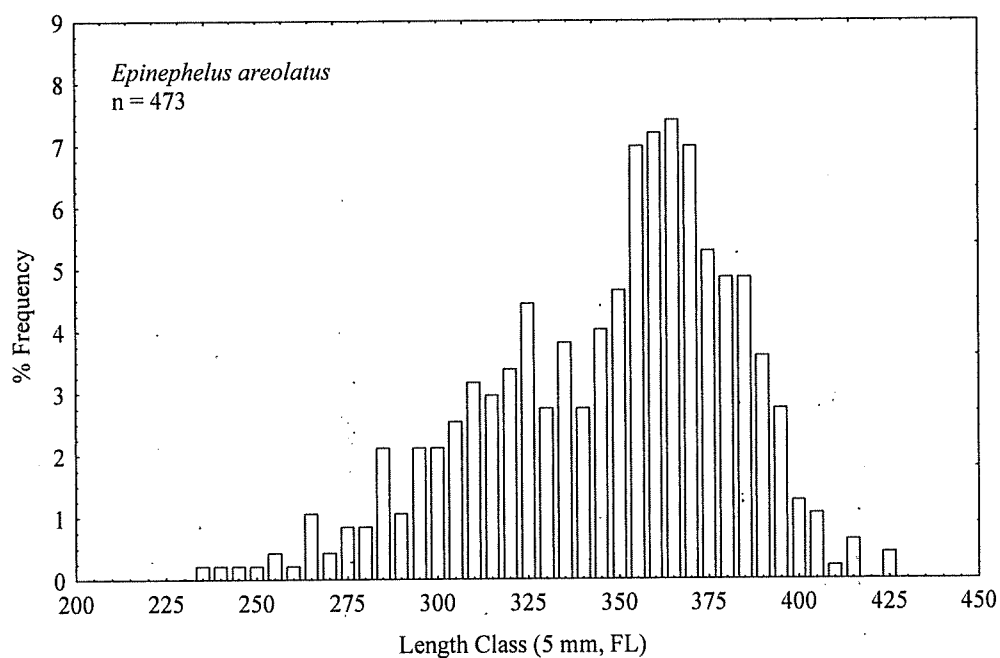


Fig. 1.2.3: Length frequency distribution of *Epinephelus areolatus* sampled aboard fishing industry vessels.

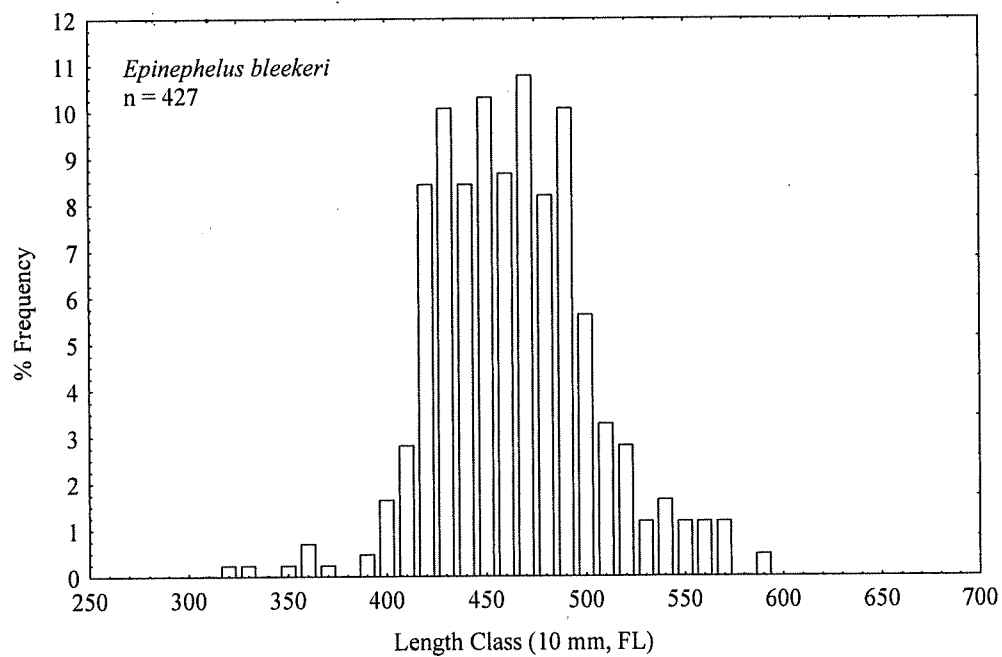


Fig. 1.2.4: Length frequency distribution of *Epinephelus bleekeri* sampled aboard fishing industry vessels.

## 2. Age, growth and mortality of the goldband snapper, *Pristipomoides multidens*.

Stephen J. Newman, Iain J. Dunk and Jerry Jenke

### 2.1 Results

A total of 3833 *P. multidens* were examined for age analysis from the NDSF ranging in size from 80-701 mm FL (10.6-5770 g TW). Of the fish collected, 2063 were identified as males ranging from 245-671 mm FL and 296-5195 g TW, while 1751 were female ranging from 284-701 mm FL and 450-5770 g TW. Length conversion equations were derived for total length, fork length and standard length (Table 2.1).

#### 2.1.1 Length-weight models

Length-weight relationships were calculated separately for males, females and for both sexes combined (Table 2.2). The relationship between TW and FL is presented in Figure 2.2. ANCOVA of total weight-at-length and clean weight-at-length were both significantly different between sexes for *P. multidens* (TW:  $F = 33.65$ ;  $df: 1, 3615$ ;  $p < 0.001$ ; CW:  $F = 87.76$ ;  $df: 1, 3031$ ;  $p < 0.001$ ), with males larger than females. ANOVA of mean weights (TW:  $F = 22.61$ ;  $df: 1, 3236$ ), mean lengths (FL:  $F = 17.03$ ;  $df: 1, 33812$ ) and mean ages ( $F = 28.07$ ;  $df: 1, 3467$ ) of *P. multidens* between sexes were all significantly different ( $p < 0.001$ ), with males larger than females.

Temporal trends were evident in the mean age, length and weight of the samples of *P. multidens* over time. Mean FL was significantly different among years from 1995 to 1999 (ANOVA:  $F = 31.29$ ;  $df: 1, 4193$ ,  $p < 0.001$ ; Fig. 2.3), with (1995 = 1996 = 1997) > (1998 = 1999). Mean TW was also significantly different among years from 1995 to 1999 (ANOVA:  $F = 89.33$ ;  $df: 1, 3295$ ,  $p < 0.001$ ; Fig. 2.4), with 1995 > 1996 > 1997 > (1998 = 1999). Mean ages were also significantly different among years from 1995 to 1999 (ANOVA:  $F = 16.99$ ;  $df: 1, 3825$ ,  $p < 0.001$ ; Fig. 2.5), with 1997 > all other years; (1996 = 1998 = 1999); (1995 = 1998 = 1999) and (1996 > 1995).

The length frequency distribution of each sex indicates that a large proportion of the harvested population is below the size-at-50%-maturity determined from Chapter 3 (Figs. 2.6, 2.7). For males 23% of fish sampled were below the size at

maturity (Fig. 2.6), while for females 41% of fish sampled were below the size at maturity (Fig. 2.7).

### 2.1.2 Age validation

Otoliths displayed alternating opaque and translucent zones. A consistent annual trend was evident with the translucent zone laid down from January to May and the opaque zone formed from June to December. The trend in thin opaque zone formation in June and July was replicated in both 1997 and 1998. Figure 2.8 clearly demonstrates that the opaque and translucent zones are laid down once per year and represent valid annuli. As the marginal increment analysis involved random sampling across all age classes in the catch (or sampled population), the validation of annuli can be expected to hold across all age classes. The formation of the translucent zone in the sagittal otoliths of *P. multidentis* was found to be closely related to the annual cycle of sea surface temperatures in the Kimberley region of north-western Australia (Fig. 2.9).

### 2.1.3 Otolith morphology, analysis and functionality

The sagittae of *P. multidentis* are somewhat laterally compressed, elliptical structures. The distal surface is concave and the rostrum and postrostrum are somewhat pointed. The sagittae are characterised by variable growth reticulations along the dorsal edge from the postrostrum to the antirostrum and along the ventral edge from the postrostrum to the rostrum. A curved sulcus crosses the proximal surface longitudinally, with the depth of the sulcal groove increasing with fish age. Annuli were counted in the ventral lobe of the otolith from the primordium to the proximal surface as close as was practicable to the ventral margin of the sulcus acousticus.

The precision of otolith readings of *P. multidentis* was relatively high, with the Index Average Percent Error (IAPE), 10.4%. Given the variability encountered among otoliths this IAPE reflects a relatively high level of precision among otolith readings and indicates that the ageing protocol adopted is relatively robust.

Otolith length and breadth were useful predictors of fish length in *P. multidentis*, accounting for more than 77% of the variability (Table 2.3). In contrast, otolith weight and in particular height were poor predictors of fish length (Table 2.3). Otolith weight was the best predictor of fish age for *P. multidentis*, accounting for

94.4% of the variability in age (Table 2.3, Fig. 2.10). Otolith height was also a useful predictor of fish age, accounting for 88% of the variability in age. In contrast, otolith length and breadth were poor predictors of age for *P. multidentis* (Table 2.3).

#### 2.1.4 Growth and mortality models

The von Bertalanffy growth curve was fitted to lengths-at-age for all *P. multidentis* (Fig. 2.11), and separately for each sex (Table 2.4). Growth of *P. multidentis* is slow to age 9, with growth in length much reduced beyond the 9+ age cohorts. Parameters of the VBGF are listed in Table 2.4. Length-at-age of *P. multidentis* was not significantly different between sexes (Log-likelihood = 0.9836, Test Statistic = 1.001,  $p > 0.05$ ; see also Fig. 2.11). Generalised VBGFs of *P. multidentis* from previous studies are compared to that derived from this study in Figure 2.12.

The maximum observed age of *P. multidentis* in the Kimberley region was 30+ years. Given that the *P. multidentis* resource in the Kimberley region of north-western Australia has been exploited for over 20 years, it is possible that the longevity of *P. multidentis* is closer to 40 years. These two estimates of maximum age in *P. multidentis* were applied to the Hoenig (1983) equation for fish in order to derive an estimate of  $M$ . Consequently,  $M$  is considered to be in the range of 0.1038-0.1387, representing an annual survivorship of 87-90% for an unfished population. This range of  $M$  estimates for *P. multidentis* is similar to that observed for other long-lived lutjanid species in the Indo-Pacific region (e.g. Newman et al. 1996, 2000a).

The sampled age structures of *P. multidentis* differed among years. The 1995 sample had a peak in year class 5 and relatively strong age classes 6, 8 and 10, with abundance per age class declining rapidly to age 18 (Fig. 2.13). Few fish older than 20 years were represented in the catch in 1995 (Fig. 2.13). The 1996 and 1997 samples were somewhat similar. In 1996 relatively strong year classes were present from age 5 through to age 11, with abundance per age class declining rapidly to age 20 (Fig. 2.14), similar to 1995. The 1997 sample had relatively strong year classes present from age 6 through to age 12 (Fig. 2.15), one year distant from the 1996 sample providing further evidence of the annual formation of growth increments.

The 1998 sample had relatively strong 6, 7 and 8 age classes, with abundance per age class declining rapidly to age 20 (Fig. 2.16). The 1999 sample was similar to the 1998 sample with relatively strong 6, 7 and 8 age classes, with abundance per age

class declining rapidly to age 20 (Fig. 2.17). Age classes 9 through 12 were somewhat eroded in the 1998 and 1999 samples in comparison to the 1996 and 1997 samples. In all years abundance per age class declined rapidly to age 20, with fish older than 20 years not well represented in the catch over the five years of catch sampling. In all years there was a strong mode of age 5 or age 6 individuals present and this may reflect the age at full recruitment to the sampling gear (fish traps).

*Pristipomoides multidentis* less than age 5 or age 6 (depending on the year) were in general not fully recruited to the sampled population and were excluded from the mortality estimates derived from catch-at-age data. The year-specific total annual rate of mortality,  $Z$ , of *P. multidentis* in the NDSF, was 0.65 for 1995/1996 (fish aged 6-21 years), 0.87 for 1996/1997 (fish aged 6-21 years) and 0.76 for 1997/1998 (fish aged 6-21 years), representing an annual percentage removal of approximately 38%, 49% and 43% respectively for each year (Table 2.5). In addition, exploitation rates were 0.79, 0.84 and 0.82 respectively.

In 1999 fishers increasingly targeted goldband snapper and this is likely to have affected their catchability, and hence influenced the mortality estimates derived from catch-at-age information. This result is not reported here and requires further investigation.

### 2.1.5 Estimation of optimum fishing mortality rates ( $F_{opt}$ )

The optimum fishing mortality rate,  $F_{opt}$  for *P. multidentis* is estimated to be 0.0519-0.069, while the limit reference point,  $F_{limit}$  was estimated to 0.069-0.093 (see Table 2.5). These results indicate that only approximately 5-6% of the available stock of *P. multidentis* can be harvested on an annual basis in a sustainable manner, and that in order to prevent stock declines annual harvest rates should not exceed 7-9% of the stock size.

**Table 2.1**

Length conversion equations for *P. multidens* off the Kimberley coast of north-western Australia. Estimates were obtained of the parameters  $a$  and  $b$  of the length-length relationships, sample size ( $n$ ) and regression  $r^2$  value (all lengths are in mm).

Length-length relationship	$n$	$r^2$
$TL = (1.1215 \times FL) + 21.8381$	2137	0.9946
$FL = (0.8868 \times TL) - 16.6058$	2137	0.9946
$FL = (1.1157 \times SL) + 6.4368$	2148	0.9920
$SL = (0.8892 \times FL) - 2.1369$	2148	0.9920

**Table 2.2**

Length-weight relationships for *P. multidens* off the Kimberley coast of north-western Australia. Estimates were obtained of the parameters  $a$  and  $b$  of the relationship  $W = aL^b$ , the sample size ( $n$ ) and the regression  $r^2$  value (lengths used are FL in mm and the weight is TW or CW in g). Parameters have been corrected for the bias associated with the log-transform.

Group	$a$	$b$	$n$	$r^2$
<i>P. multidens</i> (all fish - TW)	$2.483 \times 10^{-5}$	2.9501	3680	0.9832
<i>P. multidens</i> (all fish - CW)	$2.356 \times 10^{-5}$	2.9425	3073	0.9834
<i>P. multidens</i> (male - TW)	$2.156 \times 10^{-5}$	2.9737	1963	0.9847
<i>P. multidens</i> (female - TW)	$2.825 \times 10^{-5}$	2.9281	1671	0.9868

**Table 2.3**

Comparisons among otolith dimensions and length and age of *P. multidentis*. The predictive equations are of the simple linear regression form  $y = a + bx$  (codes for the independent variables are described in the text). For regression analyses fish length (FL) and age were used as the dependent variables (all regressions were significant at  $p < 0.001$ ). The standard error (SE) of the estimate is a measure of the dispersion of the observed values about the regression line. OW, OL, OB and OH are otolith (sagitta) weight, length, breadth and height, respectively.

Dep. Var.	Ind. Var.	Sample Size	Equation	$r^2$	SE of Estimate
FL	OW	2590	$FL = (315.370 \times OW) + 339.458$	0.683	37.572
FL	OL	2493	$FL = (33.466 \times OL) - 111.434$	0.773	32.077
FL	OB	3745	$FL = (50.429 \times OB) - 124.357$	0.832	28.476
FL	OH	3988	$FL = (118.389 \times OH) + 175.141$	0.529	48.355
Age	OW	2408	$Age = (21.864 \times OW) - 0.683$	0.944	0.9389
Age	OL	2305	$Age = (1.767 \times OL) - 21.683$	0.582	2.6289
Age	OB	3469	$Age = (2.397 \times OB) - 19.135$	0.595	2.4872
Age	OH	3652	$Age = (8.523 \times OH) - 12.811$	0.880	1.3603

**Table 2.4**

Growth parameters derived from the von Bertalanffy growth function (VBGF) and population characteristics of *P. multidentis* off the Kimberley coast of north-western Australia ( $n$  = sample size, FL is in mm, and age (t) is in years).

Parameters	Male	Female	Total
$n$	1879	1600	3479
$L_{\infty}$	594.49	603.23	598.08
K	0.1868	0.1867	0.1873
$t_0$	-0.3601	0.0018	-0.1730
$r^2$	0.7394	0.7875	0.7630
$n$	2281	1916	4573
FL <sub>mean</sub>	501.5	493.5	495.1
FL <sub>min</sub>	245	284	80
FL <sub>max</sub>	671	701	701
$n$	1872	1597	3833
$t_{mean}$	10.24	9.54	9.73
$t_{min}$	3	4	0.35
$t_{max}$	30	27	30

**Table 2.5**

Summary of total mortality ( $Z$ ) estimates for *P. multidentis* derived from catch-at-age data based on ages determined from sectioned otoliths. Estimates of fishing mortality ( $F$ ) are derived by subtraction since  $Z = F + M$  and are compared to estimates of optimum fishing mortality rates.

Year	$Z$	$F$	$F_{opt}$	$F_{limit}$
1995/6	0.649	0.510-0.545	0.052-0.069	0.069-0.092
1996/7	0.869	0.730-0.765	0.052-0.069	0.069-0.092
1997/8	0.764	0.625-0.660	0.052-0.069	0.069-0.092

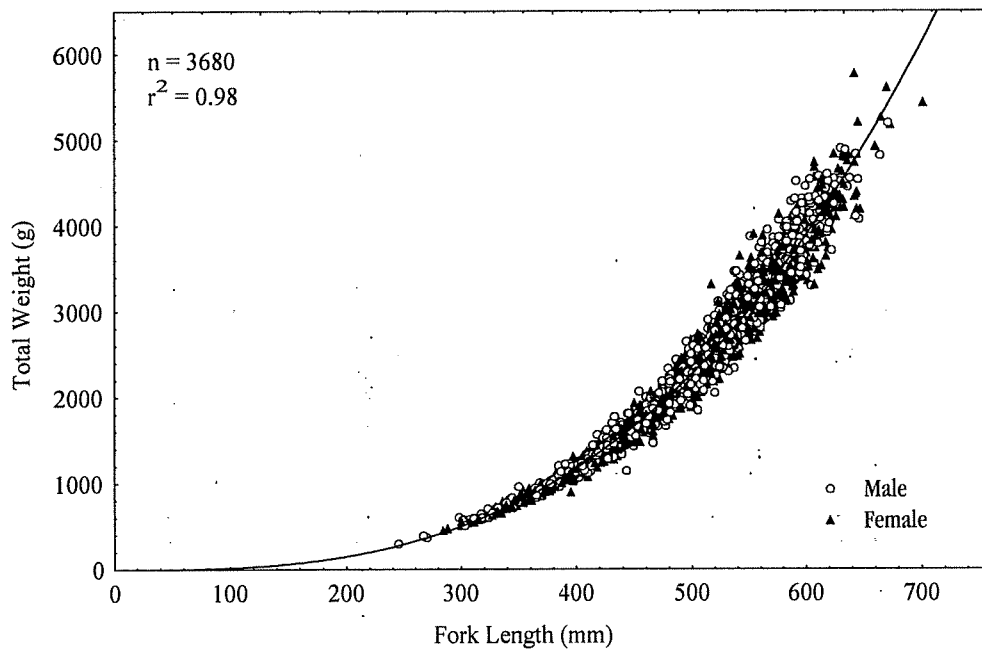


Figure 2.2: Relationship between fork length and total weight for *P. multidentis* off the Kimberley coast of north-western Australia.

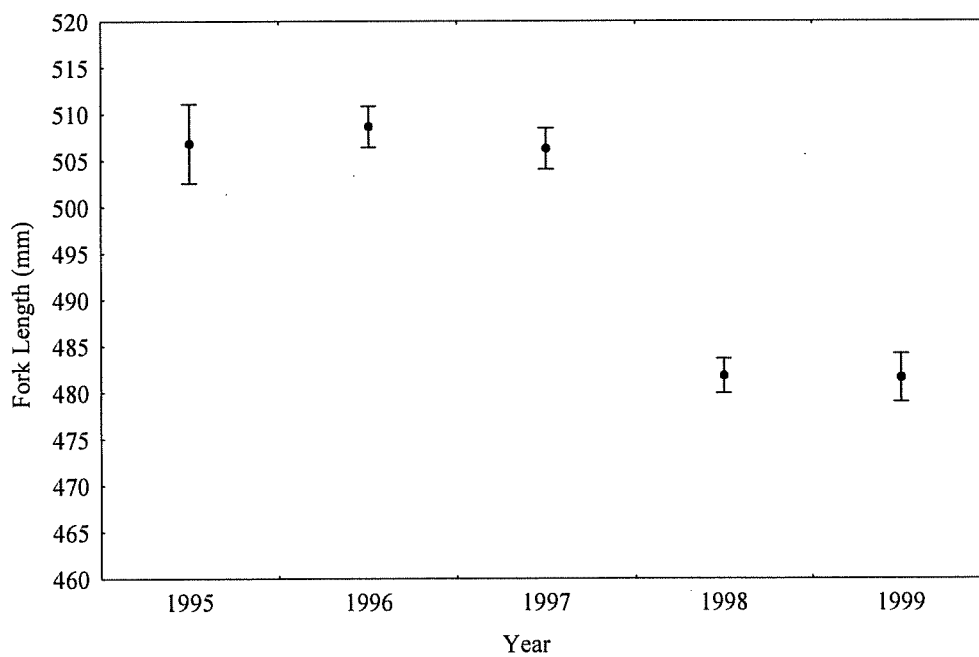


Figure 2.3: Temporal change in mean length ( $\pm$  SE) of *P. multidentis* off the Kimberley coast of north-western Australia from 1995 to 1999.

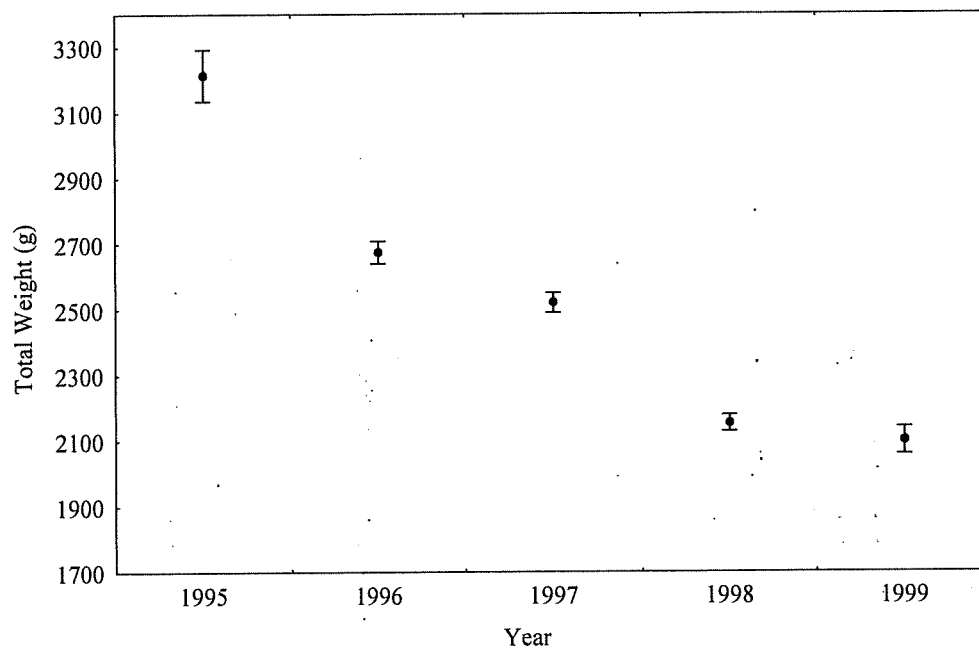


Figure 2.4: Temporal change in mean weight ( $\pm$  SE) of *P. multidentis* off the Kimberley coast of north-western Australia from 1995 to 1999.

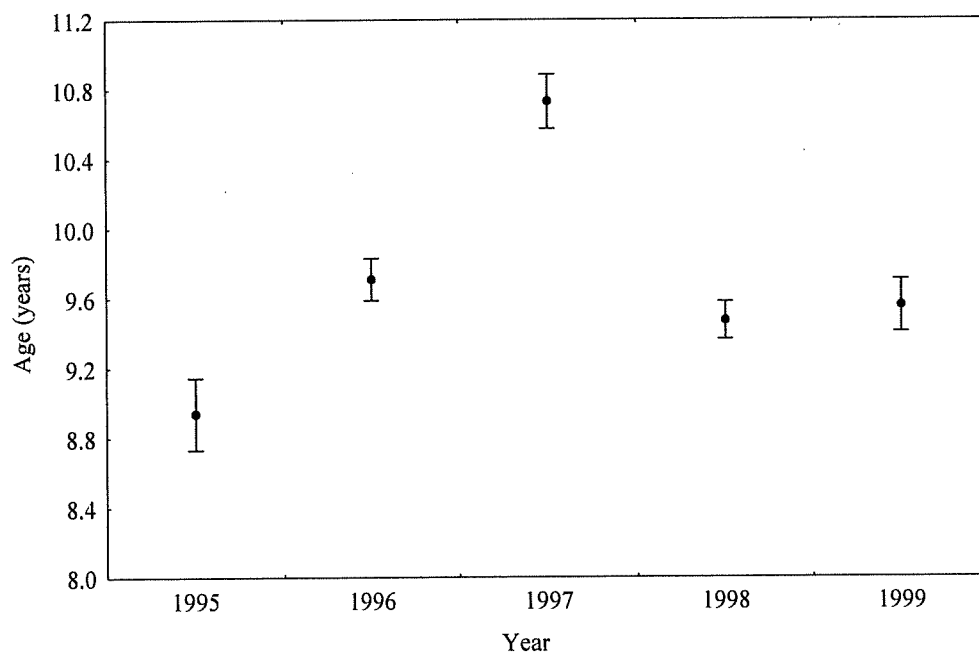


Figure 2.5: Temporal change in mean age ( $\pm$  SE) of *P. multidentis* off the Kimberley coast of north-western Australia from 1995 to 1999.

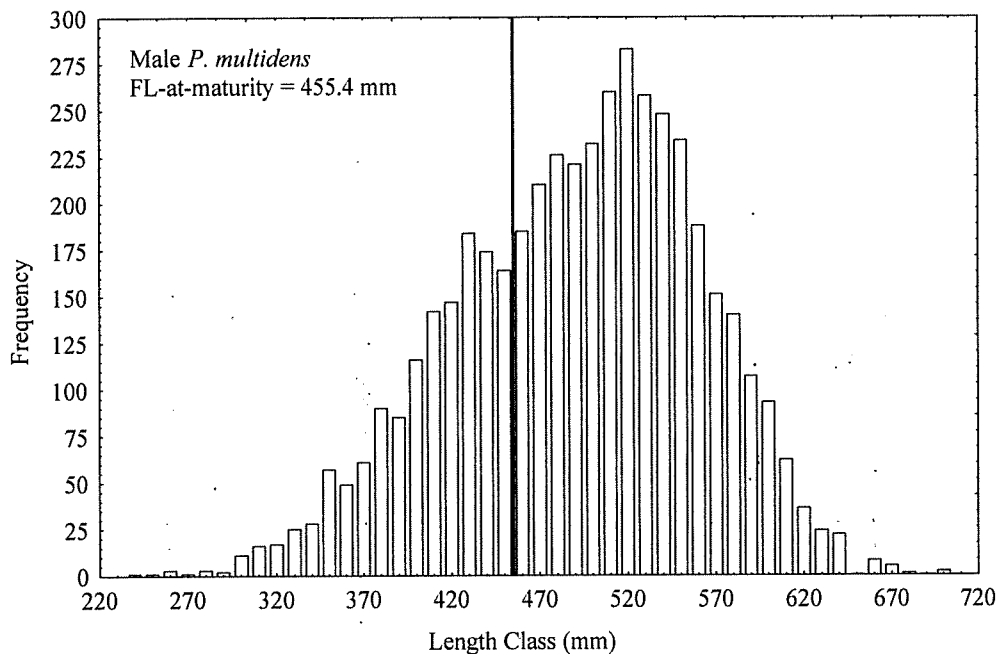


Figure 2.6: Length frequency distribution (10 mm length classes) of male *P. multidentis* sampled for age determination in association with the size-at-maturity for male *P. multidentis*.

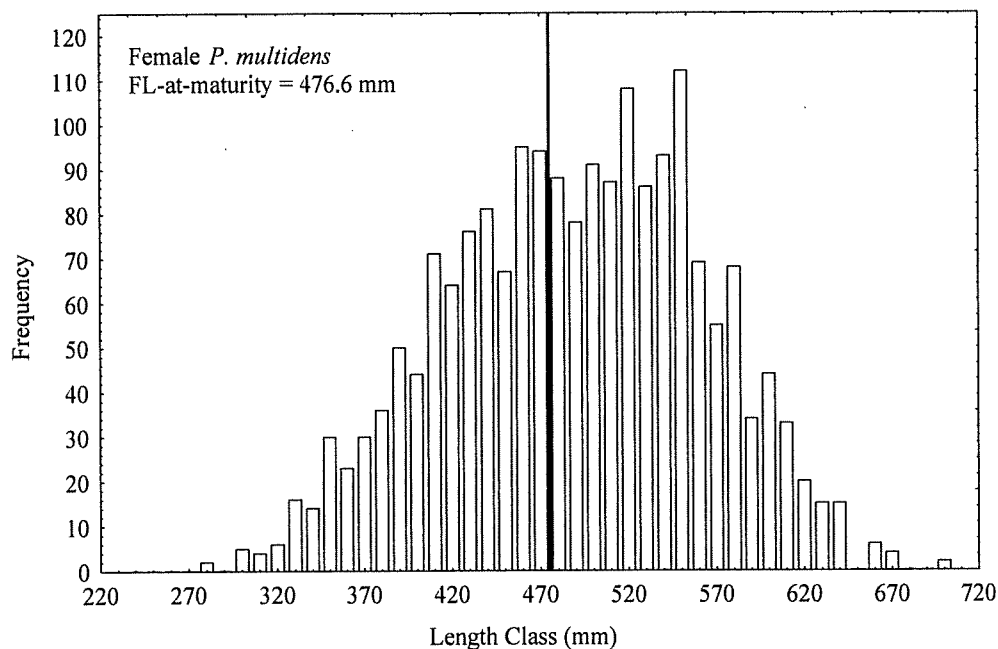


Figure 2.7: Length frequency distribution (10 mm length classes) of female *P. multidentis* sampled for age determination in association with the size-at-maturity for female *P. multidentis*.

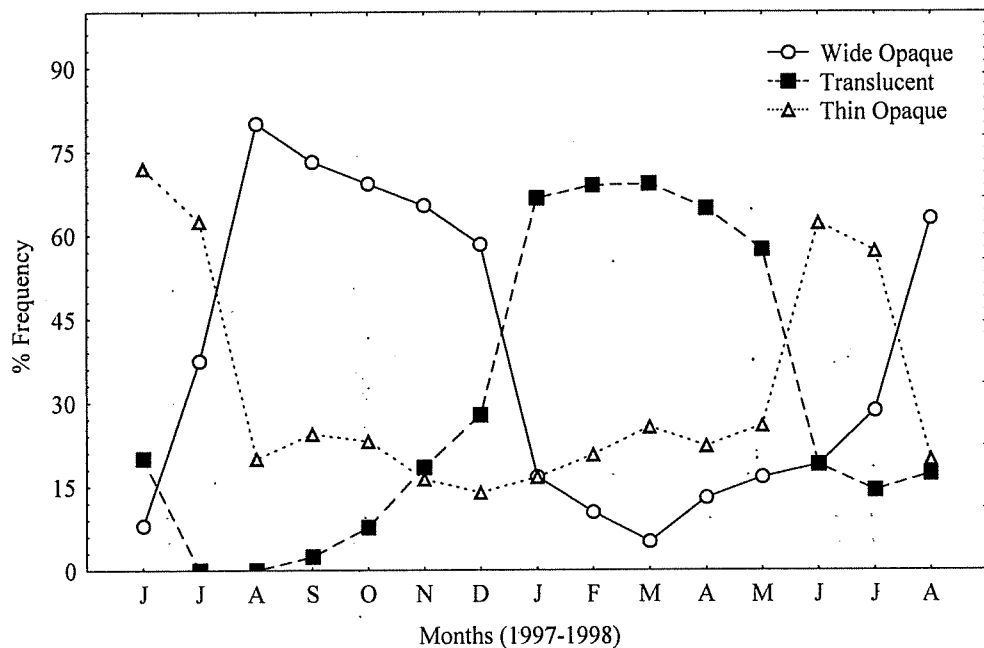


Figure 2.8: Marginal increment analysis of *P. multidens* sagittal otoliths using an edge type classification system (edge types: wide opaque, thin opaque and translucent).

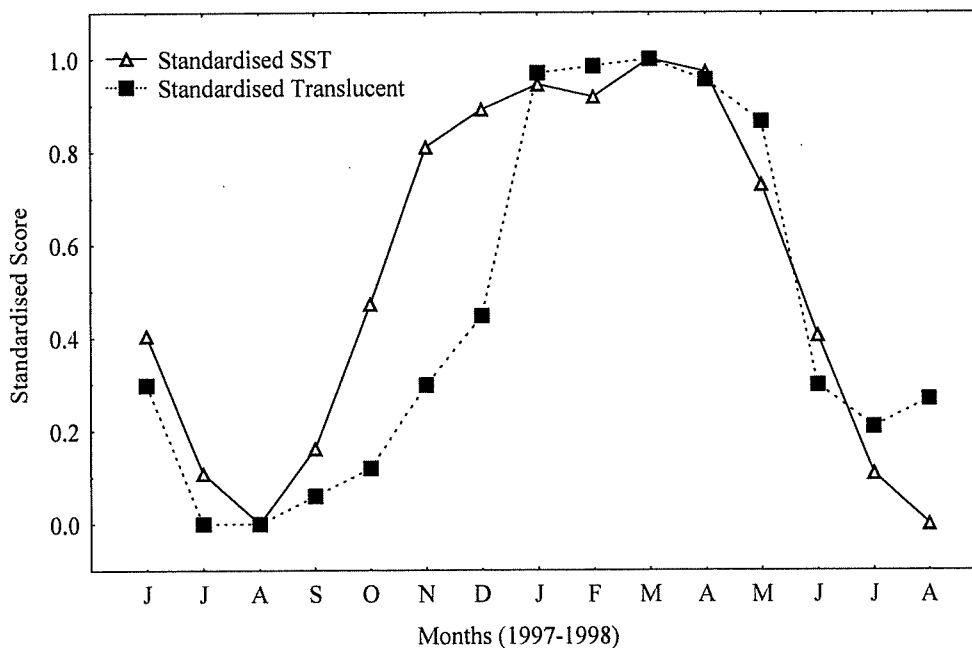


Figure 2.9: Comparison of translucent zone formation with sea surface temperature. Values are standardised to take into account any time lags and to allow comparison of each time series.

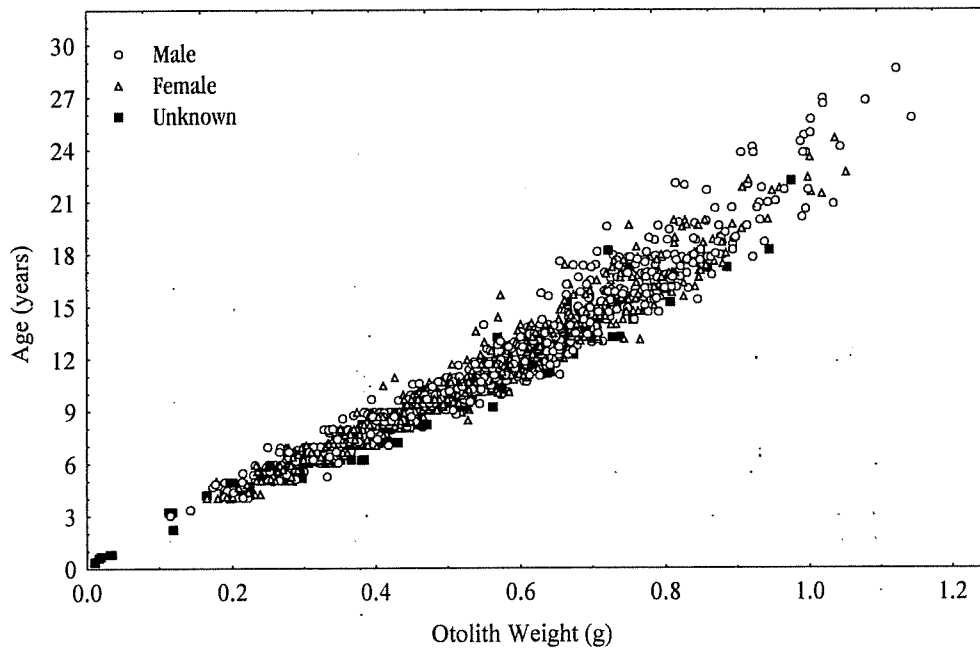


Figure 2.10: Relationship between otolith weight and age of *P. multidentis* estimated from sectioned otoliths.

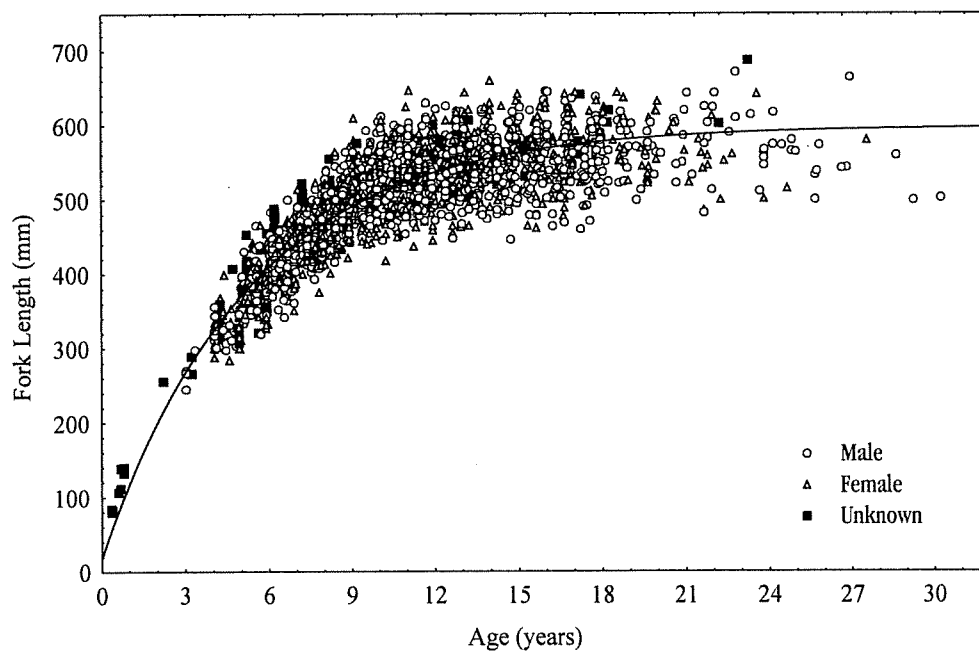


Figure 2.11: Length-at-age and von Bertalanffy growth curve for *P. multidentis* off the Kimberley coast of north-western Australia.

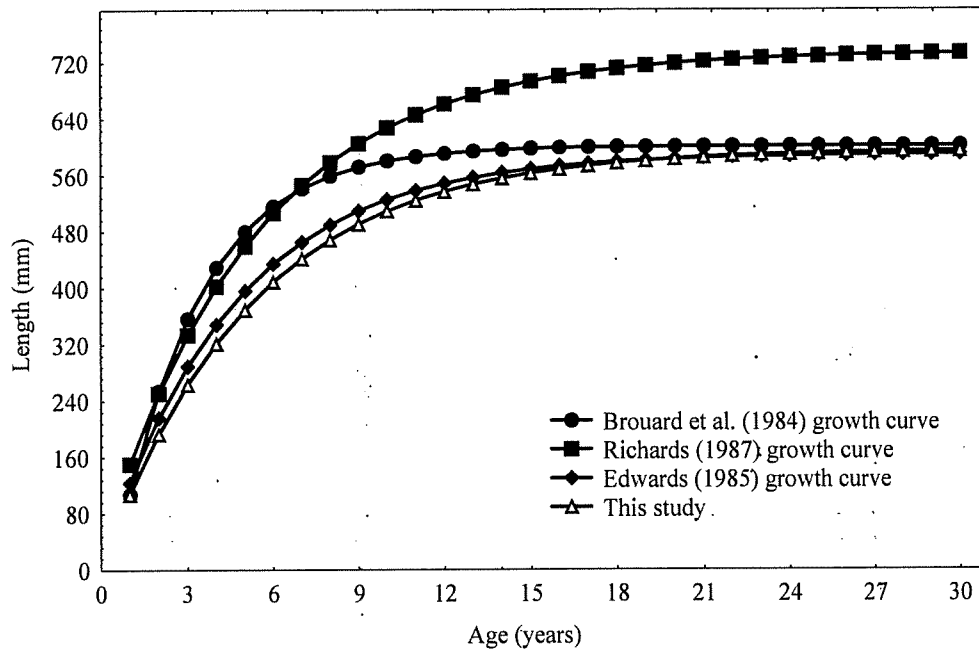


Figure 2.12: Comparison of generalised von Bertalanffy growth curves from previous studies with that derived from this study.

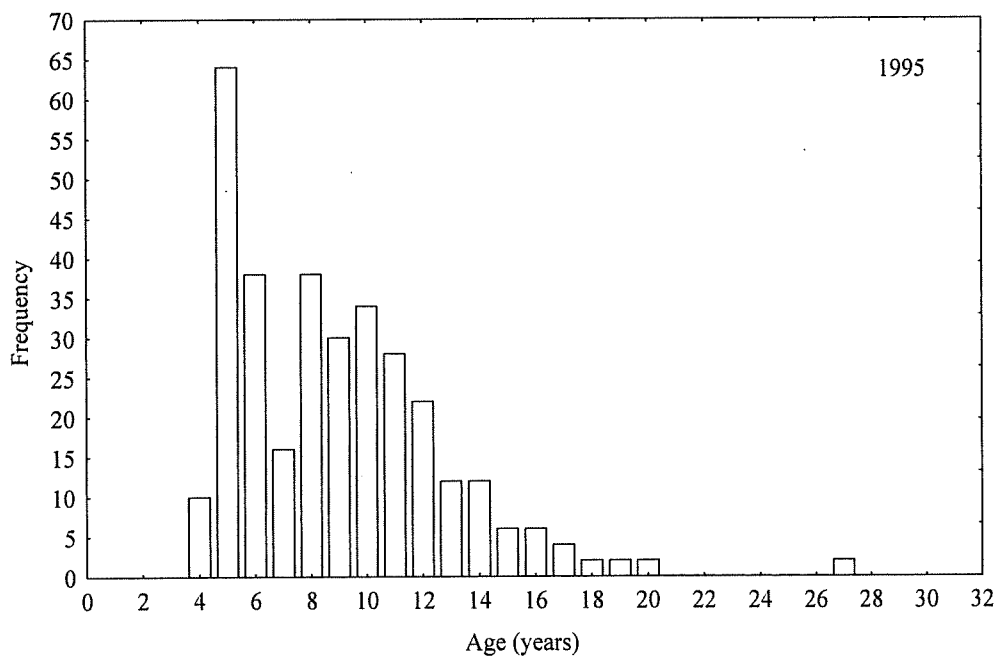


Figure 2.13: Age frequency distribution of *P. multidentis* from the NDSF in 1995.

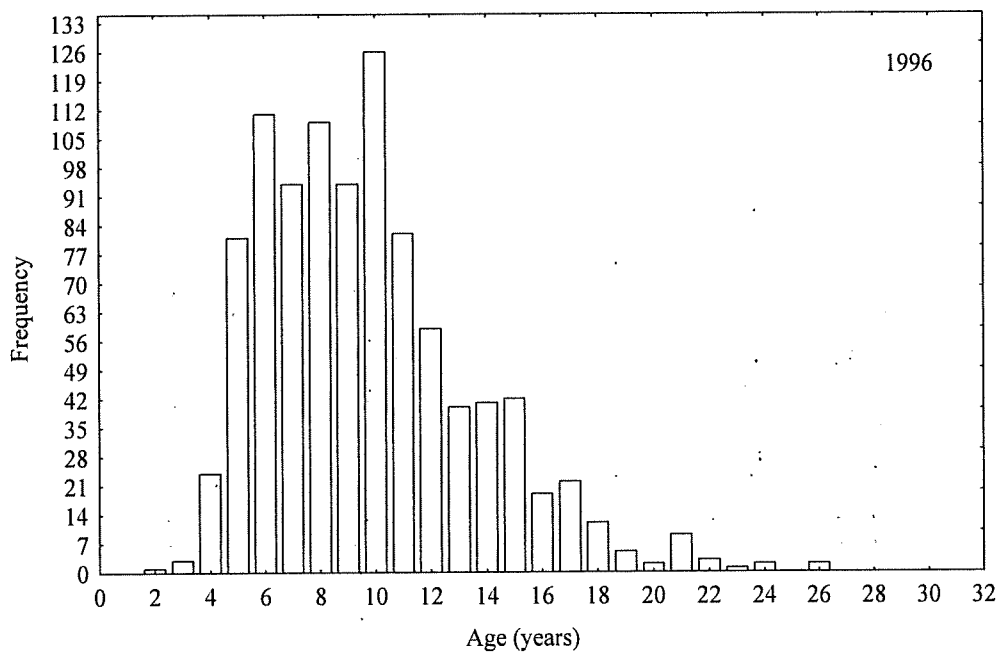


Figure 2.14: Age frequency distribution of *P. multidentis* from the NDSF in 1996.

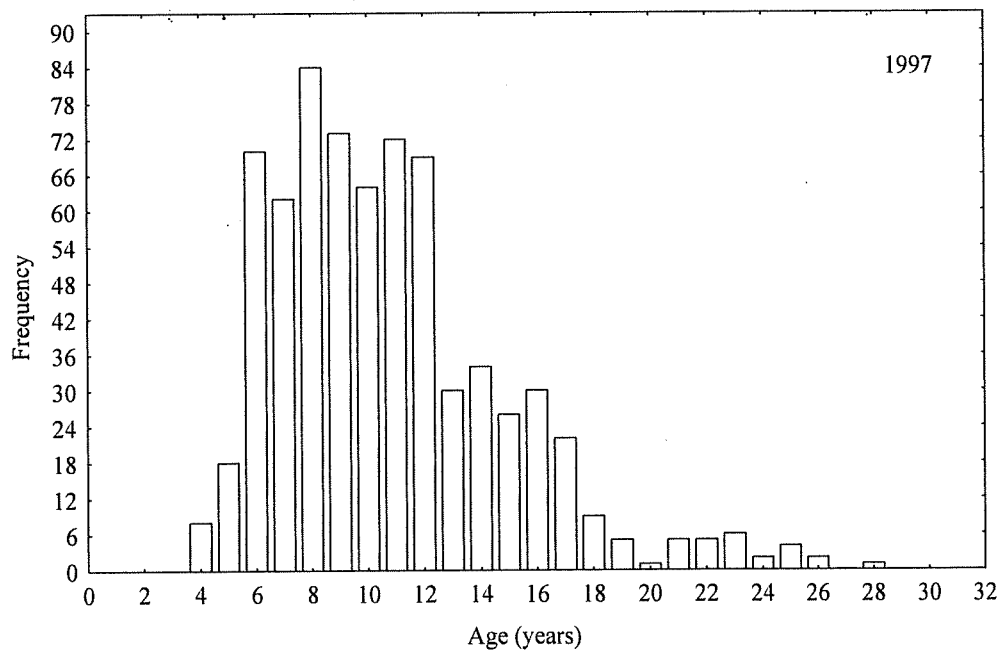


Figure 2.15: Age frequency distribution of *P. multidentis* from the NDSF in 1997.

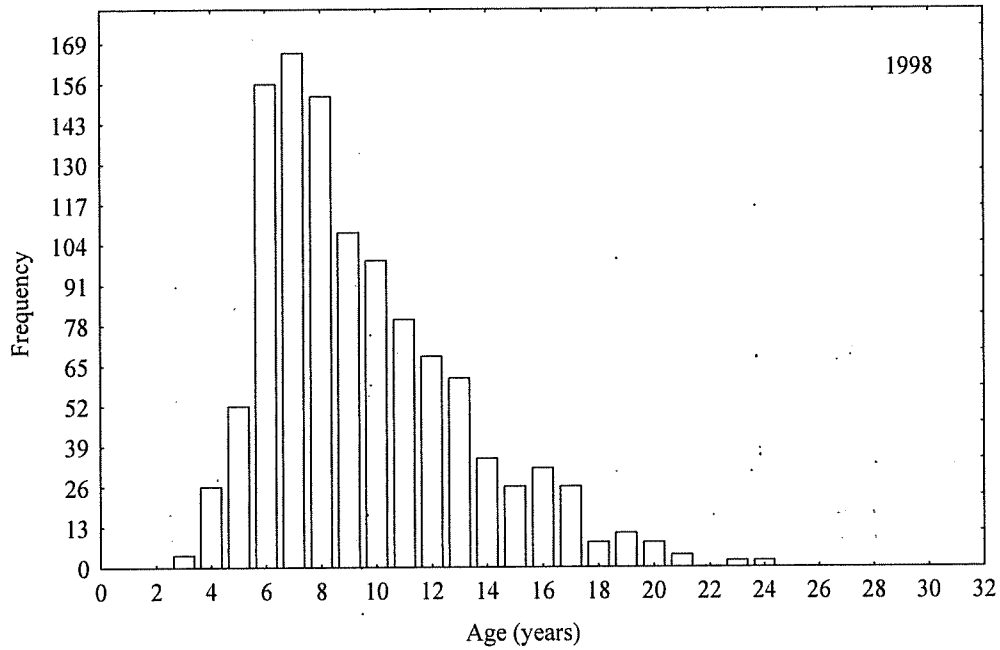


Figure 2.16: Age frequency distribution of *P. multidentis* from the NDSF in 1998.

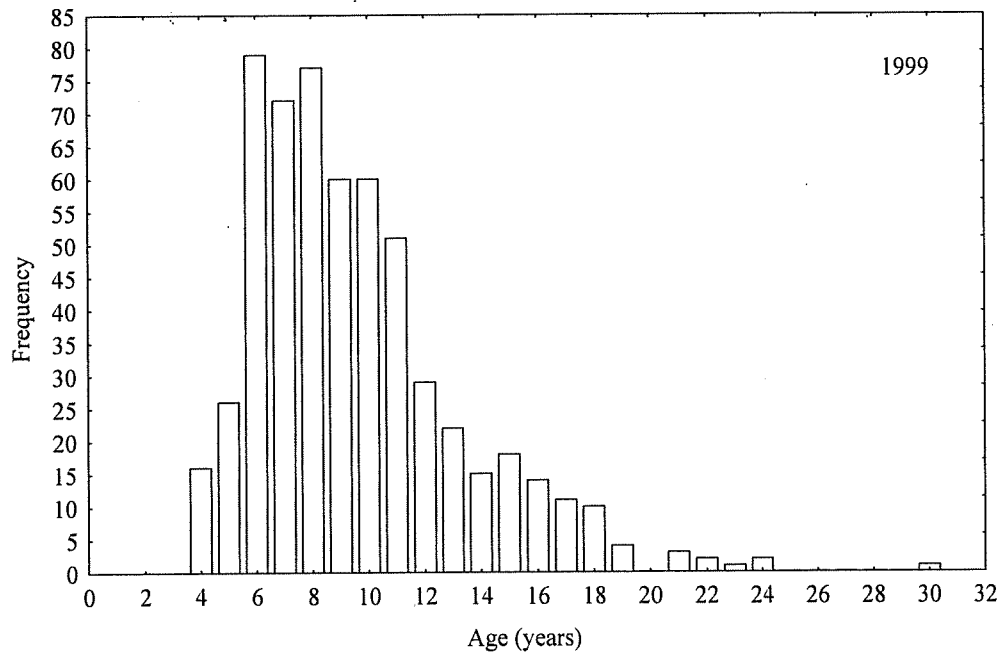


Figure 2.17: Age frequency distribution of *P. multidentis* from the NDSF in 1999.

### 3. Reproductive biology of the goldband snapper, *Pristipomoides multidens*.

*Stephen J. Newman, Richard A. Steckis and Jerry Jenke*

In the Kimberley region, the mean monthly GSIs for mature females rose sharply from ca. < 1.1 in the period from July to September to ca. 3.0 in January, with a peak at 3.4 in March, before declining to ca. 1.1 in June (Fig. 3.1). The mean monthly GSIs for mature males displayed trends similar to those exhibited by female fish (although values were much lower). The peak in GSI for male fish occurred in January, earlier than that recorded for female fish. However, the GSI values for male fish were somewhat constant from January through April. The male GSI recorded in April was proportionally higher to that exhibited by female fish at this time. The similarity in the variation in gonadosomatic indices indicates that the significant reproductive period for *P. multidens* was January to April inclusive, with the peak in March (Fig. 3.1).

Females with ovary Stages II and III were present throughout the year. Stage IV ovaries are present in the landed catch from December with the proportion increasing to a peak in March and declining in April and May, with few present in June and they are absent from July to November (Fig. 3.2). Stage V ovaries were present in similar proportions from February to April. Stage VI ovaries were only recorded in February and no Stage VII ovaries were recorded. The proportion of Stage VIII ovaries was lowest in March in comparison to other months and indicates that the developmental activity within the ovary is at a maximum at this time (Fig. 3.2). March is also the month, which represents the peak in female GSI (Fig. 3.1). The increasing number of females with Stage VIII ovaries in May and the decline in the prevalence of Stage IV ovaries indicates that the spawning season was complete at this time.

The progressive changes exhibited by the developmental stages of the testes throughout the year were analogous to those of the ovaries (Fig. 3.2). However, Stage VII testes (spent condition) were present in April and May. The prevalence of Stage III ovaries and testes throughout the year and the absence of Stage IV ovaries and testes from July to November indicate that fish possessing Stage III gonads during the spawning period do not progress through to maturity in that spawning season. Therefore, fish were only considered mature if gonad stages IV through VIII were present.

Oocytes from ovaries of *P. multidentis* < 150  $\mu\text{m}$  in diameter were present in all months of the year, with well defined modes at ca. 70.  $\mu\text{m}$  in diameter in the frequency distributions of oocytes for each month (Fig. 3.3). These oocytes represent an early stage in development, either chromatin nucleolar or perinucleolar oocytes. Oocytes > 100  $\mu\text{m}$  in diameter were not present in ovaries from July to October. Although no spawning individuals were found in the landed catch, the distribution of larger oocytes (> 150  $\mu\text{m}$  in diameter) increased from November through to a peak in March before declining in April, May and June (Fig. 3.3). The maximum diameter of oocytes was recorded in February and March, with the progression of oocytes through to the yolk vesicle stage and some to the yolk granule stage. Oocytes larger than 300  $\mu\text{m}$  in diameter present in ovaries between April and June contained declining numbers of viable yolk vesicle and yolk granule stages, with most oocytes in the process of undergoing atresia. By July, all oocytes present in the ovaries are pre-vitellogenic and remain so until November. February and March are visibly the key months for oocyte progression (Fig. 3.3). The increased number of modes of large oocytes (> 300  $\mu\text{m}$  in diameter) present in March in comparison to all other months is identical to the peak recorded in the GSI for females (Fig. 3.1). In addition to the distribution of development stages (Fig. 3.2) described above, it becomes apparent that March is the most significant month for spawning in *P. multidentis* in the Kimberley region of north-western Australia.

The overall sex ratio of *P. multidentis* was determined to be 1:1.22, female to male. This sex ratio was significantly different from 1:1 ( $\chi^2$  test,  $p < 0.01$ ). The proportion of each sex in the landed catch in each month over the study period was somewhat similar (Fig. 3.4). However, males were significantly more abundant (50% or greater) in the period from November through to June ( $\chi^2$  test,  $p < 0.01$ ). Similar ratios of females to males were recorded only in the period from July to October (Fig. 3.4). The distribution of sexes by length interval (Fig. 3.5) revealed that the proportion of females increased significantly with increasing length ( $\chi^2$  test,  $p < 0.01$ ). Females and males were present in somewhat similar proportions up to 600 mm FL. From the 600 mm length class onwards the preponderance of females in the landed catch increased, with all fish greater than 680 mm FL recorded as females (Fig. 3.5).

The seasonal PMI indicated that the number of mature fish in samples decreased at the end of April (< 40%) and remained low until July (Fig. 3.6), with the PMI increasing from November to March. We interpret these results to indicate that mature fish are more prevalent in catches around the spawning period. The temporal trend in PMI indicated a decreasing number of mature fish over the study period and a corresponding increase in the number of immature fish in the landed catch (Fig. 3.7). At the end of the study period, in May and June 1999, over 90% of the *P. multidentis* sampled, were immature compared with only 28% and 36% immature recorded in May and June 1998 (Fig. 3.7).

The relationship between length and gonad weight was examined for females and males (Fig. 3.8). Gonad weight increased exponentially with increasing length of fish. However, there was a large amount of variation in gonad weight in relation to length as fish mature. The point at which the variation in gonad weight begins to show marked variability reflects the transitional period associated with the onset of maturity. For *P. multidentis* this occurs at approx. 475 mm FL for females and approx. 450 mm FL for males (Fig. 3.8). The length at maturity,  $L_{50}$  for *P. multidentis* derived from the logistic model was 473 mm FL (552 mm TL) for females and 470 mm FL (549 mm TL) for males (Fig. 3.9). These data are in close agreement to that estimated visually from the relationship between length and gonad weight. Furthermore, the high level of agreement between the observed data and the logistic model (Fig. 3.9) for *P. multidentis*, in particular for female fish, is an indication of relative accuracy of the macroscopic staging methodology. The estimated age at maturity ( $A_{50}$ ) for females was 8.2 years, while the  $A_{50}$  for males was 8.0 years.

Table 3.1: Development stages of ovaries and testes of *Pristipomoides multidens* based on macroscopic and histological examination of gonads (modified from West (1990) and Davis and West (1993)).

Stage	Macroscopic description	Histological description
I – Immature (Virgin)	Small thread-like gonads, ovaries brownish-grey to translucent, testes small flat and threadlike, occupy one-third of the length of body cavity	Chromatin nucleolar stage: very small oocytes, nucleus surrounded by a thin layer of dark-blue stained cytoplasm
II – Early developing (Maturing virgin)	Ovary translucent, grey-red, small capillaries present, ovary taught and round, occupies 1/3 length of body cavity, oocytes not visible. Testes still threadlike but thicker in cross section, no milt present	Perinuclear stage: oocyte size increases slightly as dark blue-stained cytoplasm thickens, nucleoli appear at the periphery of nucleus
III – Developing	Ovary opaque-reddish with increased capillary development, occupies 1/2 the length of body cavity, small granular oocytes becoming visible. Testes lobed in formation, flattened edges, milt sometimes present	Cortical alveoli stage: appearance of cortical alveoli in pale-blue-stained cytoplasm, pink stained zona radiata distinguishable, oil vesicles appearing, lampbrush chromosomes often visible In the nucleus
IV – Late developing (Maturing yolked)	Gonads occupy well over 1/2 the length of body cavity, ovaries have small granular oocytes visible, ovary taught and round, ovary wall thin and transparent, many small capillary vessels evident. Testes large with some folding and flattened edges to lobes, milt present	Yolk stage: marked increase in oocyte size, cytoplasm filled with pink-stained yolk granules, cortical alveoli and oil vesicles increase in size and number, degenerating postovulatory follicles visible if spawning has started
V – Ripe (Pre-spawning)	Gonads occupy well over 1/2 the length of body cavity, ovaries with many blood vessels present, large transparent (hydrating) oocytes visible among smaller opaque oocytes. Testes large with extensive folding and flattened edges to lobes, milt flows when pressure is applied	Nuclear migration stage: migration of nucleus to periphery of oocyte, fusion of yolk granules into yolk plates, fusion of oil vesicles into the oil droplet, degenerating postovulatory follicles visible if spawning has started
VI – Running ripe (Spawning)	Ovaries large distending the body cavity, many large hydrated oocytes visible, oocytes easily expressed from ovaries with slight pressure. Testes large with free flowing milt	Hydration stage: further increase in size of oocytes, all yolk granules fused into a few plates
VII – Spent	Ovary reduced in size and flaccid, ovary wall thickened, greyish colour, some hydrated oocytes still present, no opaque eggs left in ovary, often purple-red in colour through haemorrhage. Testes contracted, flaccid, with extensive folding and flattened edges, brownish and rubbery in appearance, milt sometimes present	Postovulatory follicles clearly visible, no yolked oocytes remain, some atretic oocytes present, structure of oocytes generally loose, hydrated oocytes may be present in lumen
VIII – Resting	Ovary reduced in size and empty. Ovary not taught or round. Testes with flattened edges, brownish in appearance, milt not present	Stage II & III oocytes dominate, no trace of postovulatory follicles left, advanced atresia of remaining yolked oocytes

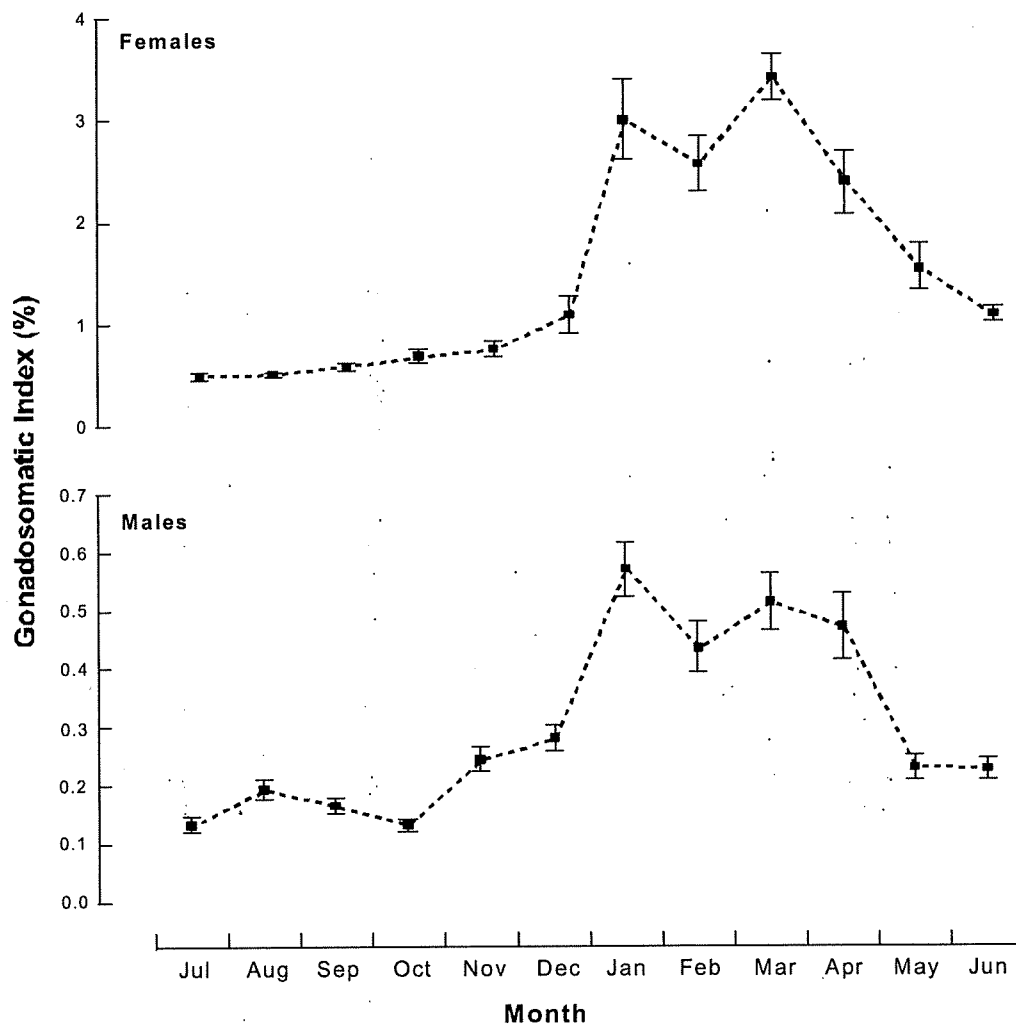


Figure 3.1: Seasonal changes in mean monthly gonadosomatic indices ( $\pm$  SE) for female and male *Pristipomoides multidens* in the Kimberley region of north-western Australia, for gonad stages IV–VIII (all years pooled).

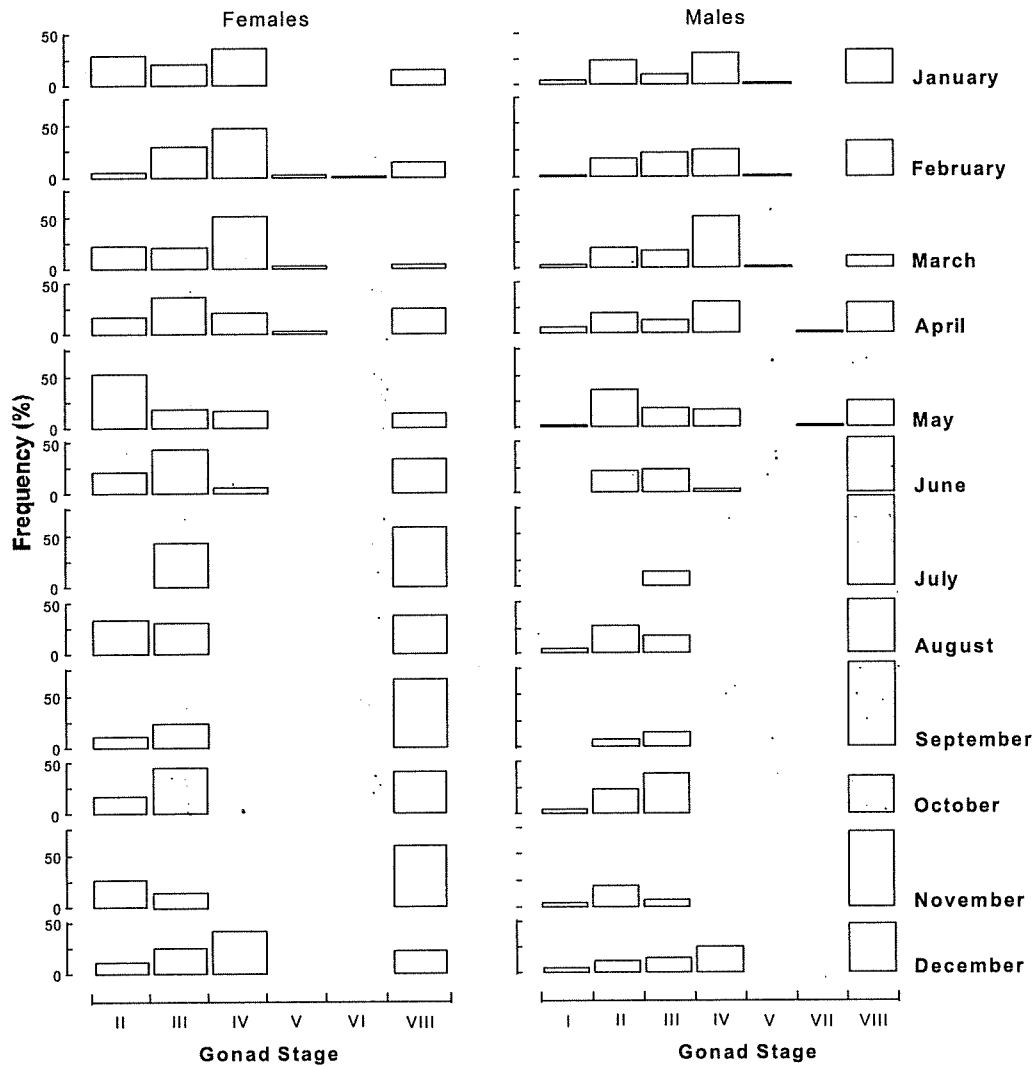


Figure 3.2: Monthly percentage contributions of different stages in gonadal development in female and male *Pristipomoides multidentis* in the Kimberley region of north-western Australia.

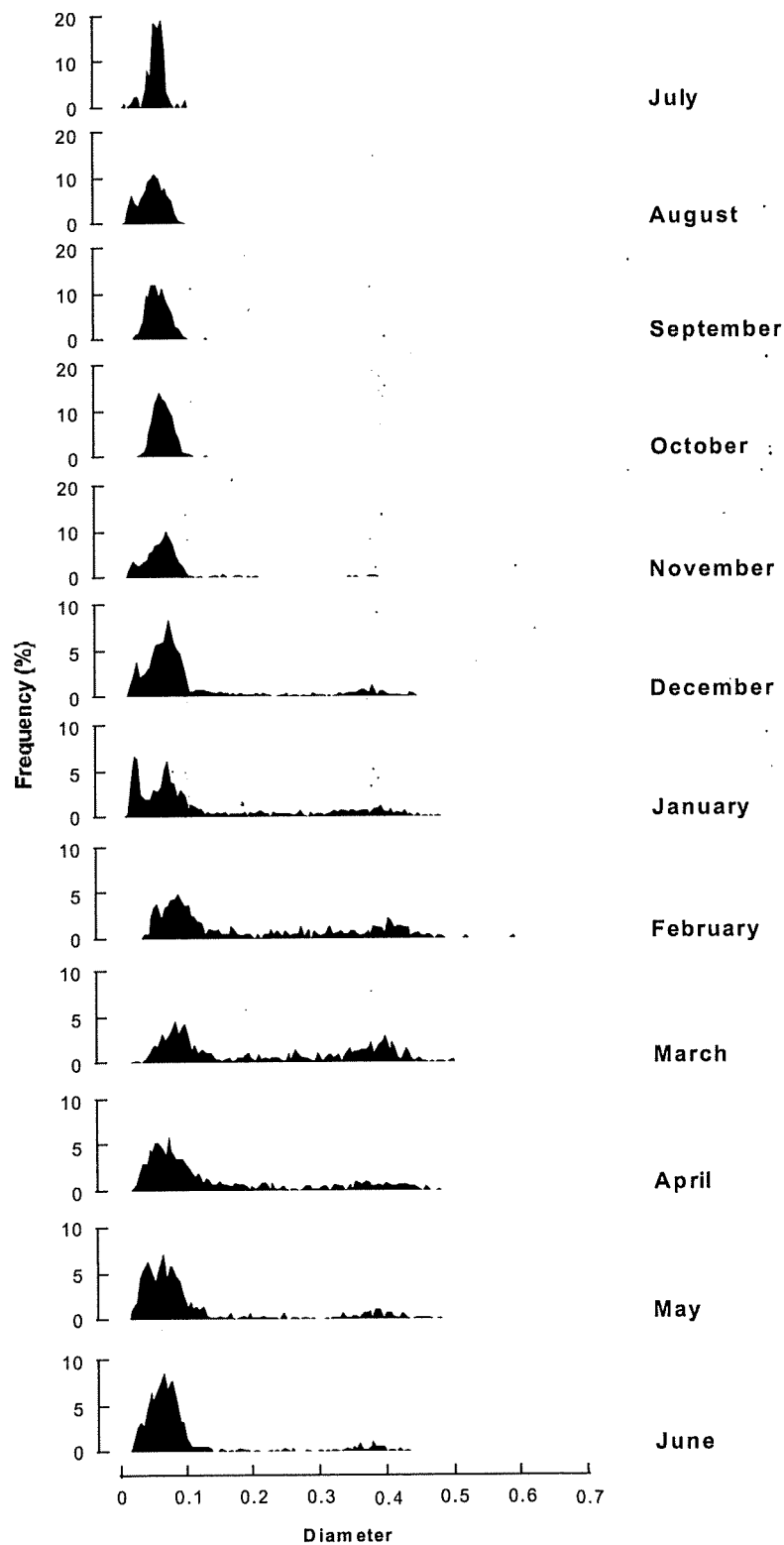


Figure 3.3. Monthly size frequency distributions of oocyte diameters of *Pristipomoides multidentis*, measured from histological sections of ovaries.

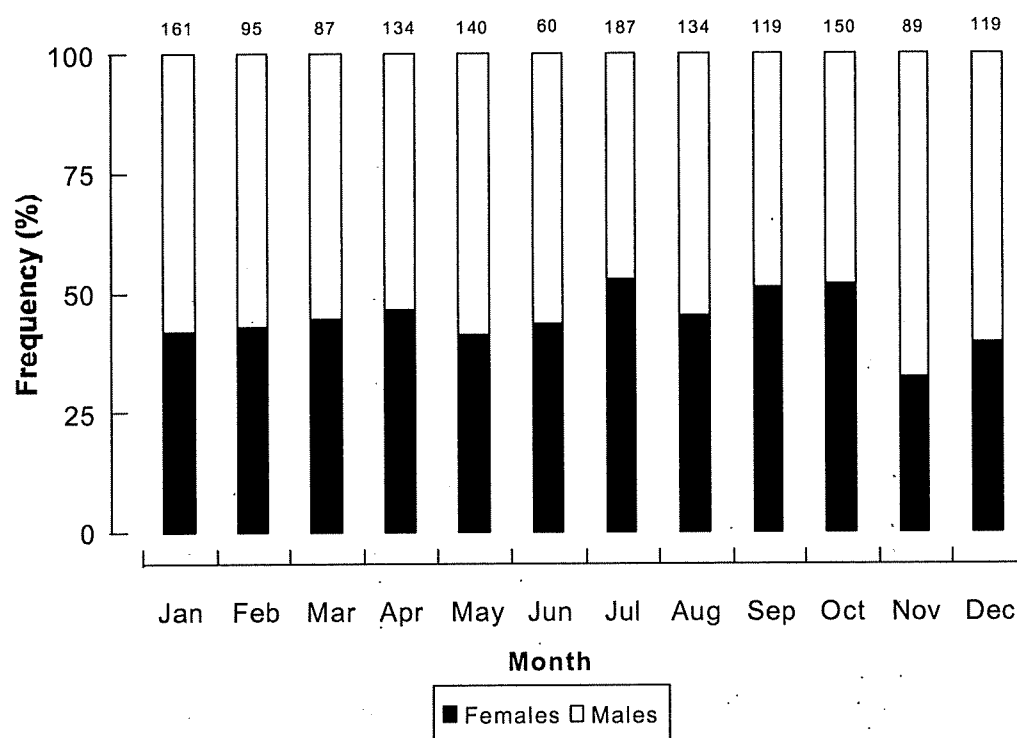


Figure 3.4. Sex ratio of female and male *Pristipomoides multidentis* in each month in the Kimberley region of north-western Australia (sample sizes are shown above each bar).

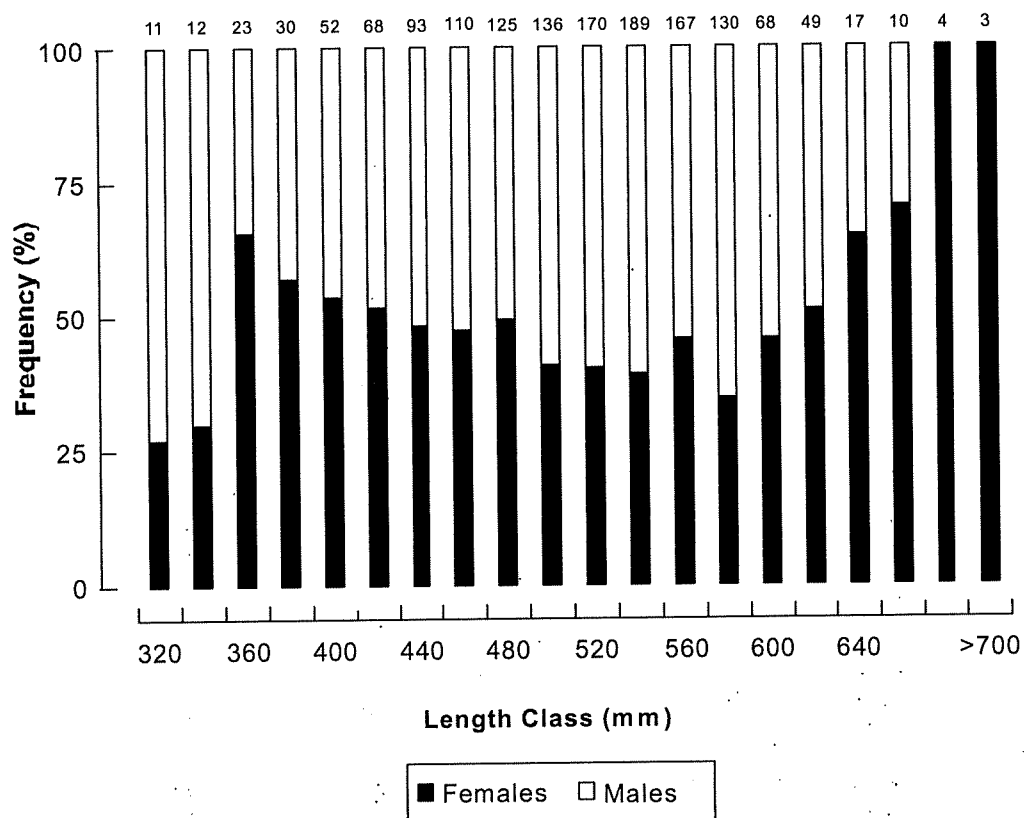


Figure 3.5. Sex ratio of female and male *Pristipomoides multidentis* in the Kimberley region of north-western Australia by 20 mm length classes (sample sizes are shown above each bar).

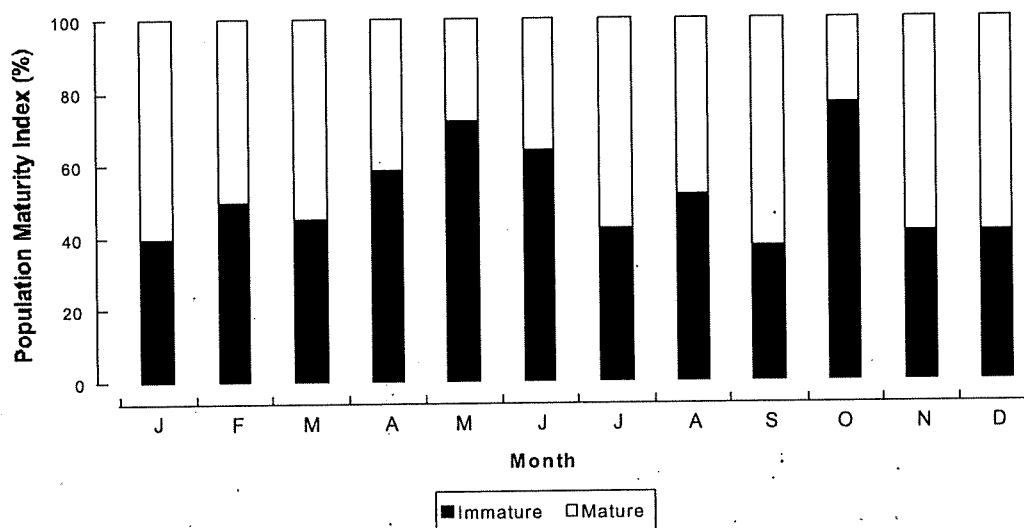


Figure 3.6. Seasonal change in the monthly population maturity index for *Pristipomoides multidentis* in the Kimberley region of north-western Australia.

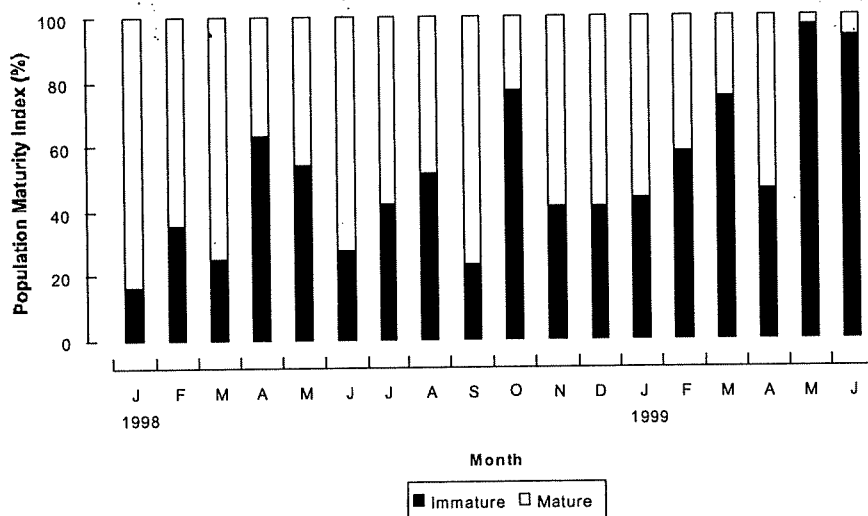


Figure 3.7. Temporal change in the monthly population maturity index for *Pristipomoides multidentis* in the Kimberley region of north-western Australia over the duration of the study period.

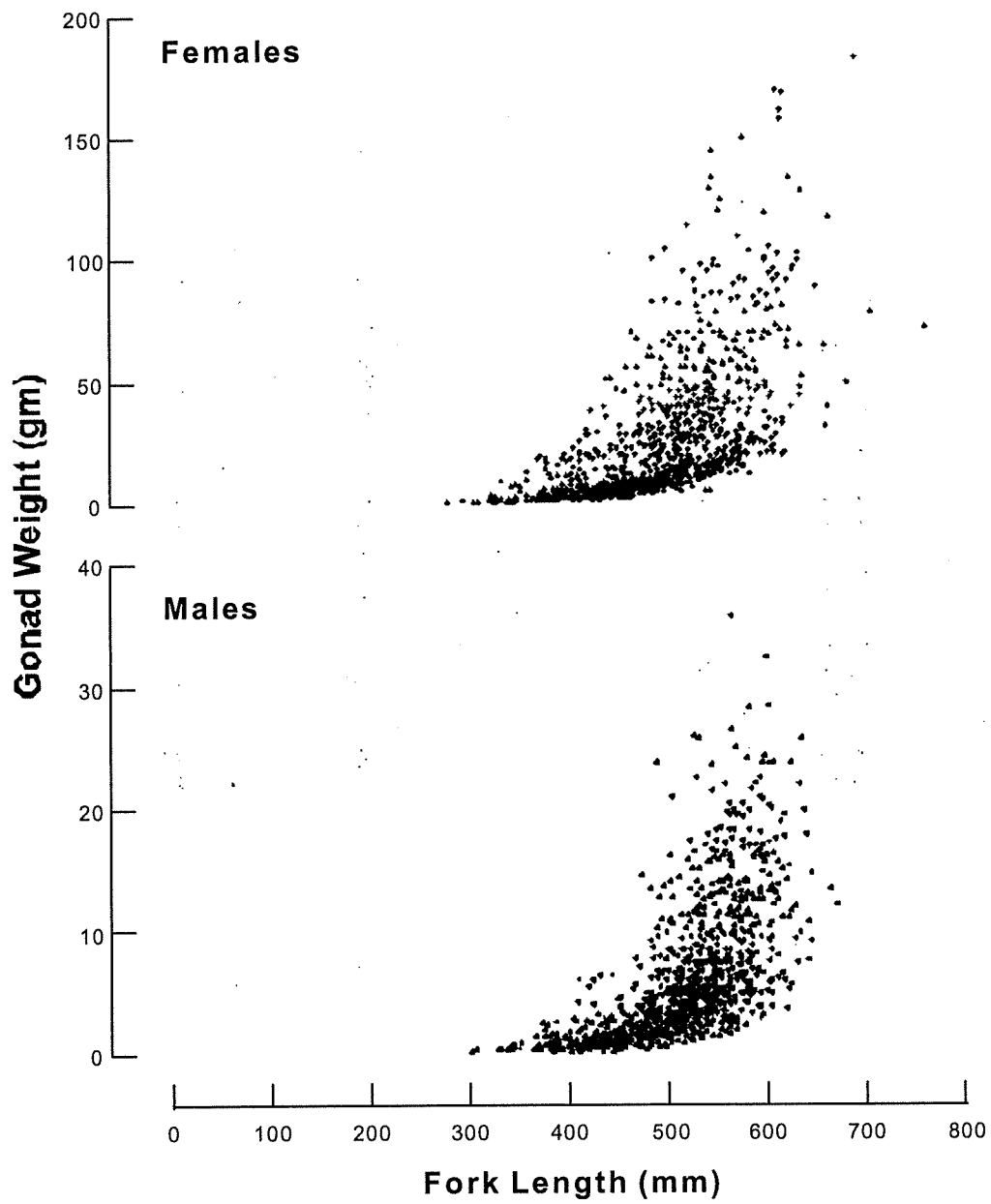


Figure 3.8. The relationship between fork length and gonad weight for female and male *Pristipomoides multidens* in the Kimberley region of north-western Australia.

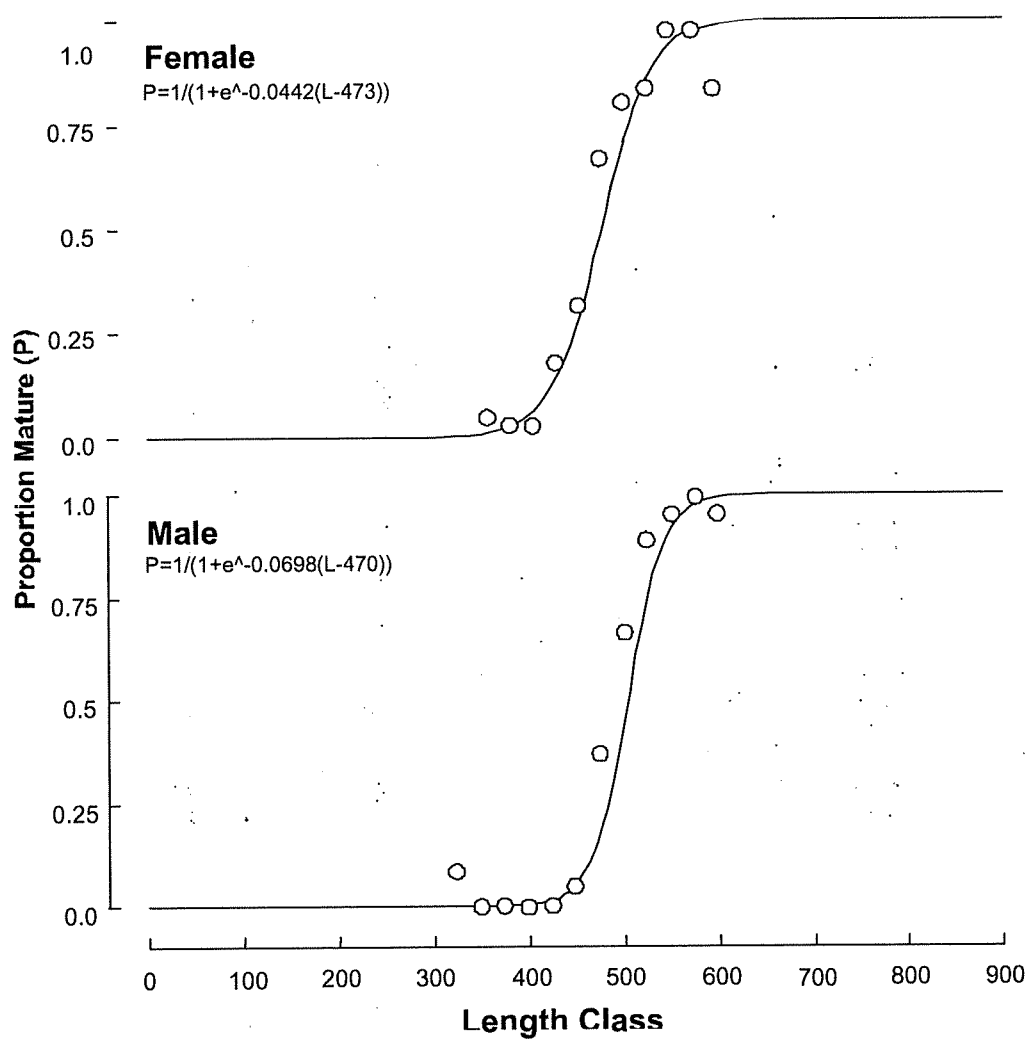


Figure 3.9. Length at maturity relationship showing the proportion of mature female and male *Pristipomoides multidens* from the Kimberley region of north-western Australia. A logistic curve is fitted to the data for each sex. Size classes are in 20 mm intervals.

#### 4. Age, growth and mortality of the red emperor snapper, *Lutjanus sebae*.

Stephen J. Newman, Iain J. Dunk and Jerry Jenke

##### 4.1 Results

A total of 2386 *L. sebae* were examined for age analysis from the NDSF ranging in size from 183-728 mm FL (189-7204 g TW). Of the fish collected, 977 were identified as males ranging from 211-728 mm FL and 274-7204 g TW, while 1384 were female ranging from 183-584 mm FL and 205-3938 g TW. Length conversion equations were derived for total length, fork length and standard length (Table 4.1).

##### 4.1.1 Length-weight models

Length-weight relationships were calculated separately for males, females and for both sexes combined (Table 4.2). The relationship between TW and FL is presented in Figure 4.2. ANCOVA of total weight-at-length and clean weight-at-length were both significantly different between sexes for *L. sebae* (TW:  $F = 22.16$ ;  $df: 1, 2213$ ;  $p < 0.001$ ; CW:  $F = 32.75$ ;  $df: 1, 2204$ ;  $p < 0.001$ ), with males larger than females. ANOVA of mean weights (TW:  $F = 579.96$ ;  $df: 1, 2215$ ,  $p < 0.001$ ) and mean lengths (FL:  $F = 566.48$ ;  $df: 1, 2595$ ,  $p < 0.001$ ) of *L. sebae* between sexes were both significantly different, with males larger than females. Mean ages ( $F = 23.78$ ;  $df: 1, 2359$ ,  $p < 0.001$ ) of *L. sebae* was significantly different between sexes, however, females were older than males.

Temporal trends were evident in the mean age, length and weight of the samples of *L. sebae* over the duration of the study. Mean FL was significantly different among years from 1997 to 1999 (ANOVA:  $F = 6.24$ ;  $df: 1, 2226$ ,  $p < 0.01$ ; Fig. 4.3), with 1997 = 1998, 1998 = 1999, 1997 > 1999. Mean TW was also significantly different among years from 1997 to 1999 (ANOVA:  $F = 10.37$ ;  $df: 1, 1930$ ,  $p < 0.001$ ; Fig. 4.4), with 1997 = 1998, 1997 = 1999, 1998 > 1999. Mean ages were also significantly different among years from 1997 to 1999 (ANOVA:  $F = 9.51$ ;  $df: 1, 2149$ ,  $p < 0.001$ ; Fig. 4.5), with 1997 > (1998 = 1999).

The length frequency distribution of each sex indicates that a substantial proportion of the harvested population is below the size-at-50%-maturity determined

from Chapter 5 (Figs. 4.6, 4.7). Furthermore, numerous fish below the current legal minimum length (LML) of 410 mm TL were obtained from processing outlets (Figs. 4.6, 4.7), and the LML is well below the size at 50% maturity.

#### 4.1.2 Age validation

Otoliths displayed alternating opaque and translucent zones. The mean monthly marginal increment was lowest in September-October and highest in July-August in each of two consecutive years (Fig. 4.8). A transition in the predominance of opaque zones to translucent zones at the otolith margin occurs during the period of May-June to August inclusively, with the opaque zone being deposited at the otolith margin for the greater part of the cycle. The month of September is characterised by a high frequency of opaque margins and a corresponding low marginal increment ratio (MIR). As the MIR increases from September the frequency of opaque otolith margins also increases. The annulus is completed by the end of August in each year, with the new increment beginning to form in September-October. The consistent annual cycle of the mean marginal increment indicates that one annulus is formed each year (Fig. 4.8). As the marginal increment analysis involved random sampling across all age classes in the sampled population, the validation of annuli is expected to persist across all age classes.

Two *L. sebae* were recaptured, with both fish at liberty for 314 days. Both recaptured fish were female with one fish growing 12 mm in length and the other 0 mm. These two calcein injected and tagged fish provide direct evidence of August being the time of transition from translucent to opaque zone formation at the otolith margin. Between the time of capture and recapture all otolith growth was opaque (314 days). Although this does not demonstrate any annual cyclical pattern in deposition as only opaque material was deposited during the intervening period, the dominance of opaque deposition throughout the year is reinforced and indicates that a maximum of one opaque zone is deposited per year.

#### 4.1.3 Otolith morphology, analysis and functionality

The sagittae of *L. sebae* are large elliptical structures that are somewhat laterally compressed with a slightly concave distal surface. A curved sulcus crosses the proximal surface longitudinally, with the depth of the sulcal groove increasing with fish age. Annuli in sectioned otoliths consist of alternating opaque and translucent zones. Annuli were counted in the ventral lobe of the otolith from the primordium to the proximal surface as close as was practicable to the ventral margin of the sulcus acousticus.

The precision of otolith readings of *L. sebae* was high, with the Index Average Percent Error (IAPE), 4.7%. The low IAPE of *L. sebae* indicates a high level of precision among otolith readings and indicates that otoliths were interpreted in a similar manner on each occasion they were examined.

Otolith length and breadth were useful predictors of fish length in *L. sebae*, accounting for more than 77% of the variability (Table 4.3). In contrast, otolith weight and in particular otolith height were both poor predictors of fish length (Table 4.3). Conversely, otolith weight and otolith height were both useful predictors of fish age in *L. sebae*, whereas, otolith length and breadth were not (Table 4.3). When all fish were combined otolith height was a more robust predictor of fish age than otolith weight, accounting for 86% of the variability in age (Table 4.3). However, significant differential growth was evident between sexes (see below). Otolith weight and otolith height were both powerful predictors of fish age for *L. sebae* when sex was known (Table 4.3).

#### 4.1.4 Growth and mortality models

The von Bertalanffy growth curve was fitted to lengths-at-age for all *L. sebae*, and separately for each sex (Fig. 4.10, Table 4.4). Growth of *L. sebae* is slow to age 8, with growth in length much reduced beyond the 8+ age cohorts. Parameters of the VBGF are listed in Table 4.4. Length-at-age of *L. sebae* was significantly different between sexes (Log-likelihood = 1.783, Test Statistic = 1.002,  $p < 0.01$ ; see also Fig. 4.10). The estimated  $L_{\infty}$  and  $K$  values of *L. sebae* were also significantly different between sexes (Log-likelihood = 1.178, Test Statistic = 1.002,  $p < 0.05$  and Log-likelihood = 1.008, Test Statistic = 1.002,  $p < 0.05$ , respectively, Table 4.4).

The maximum observed age of *L. sebae* in the Kimberley region was 34+ years. The *L. sebae* resource in the Kimberley region of north-western Australia has been exploited for over 20 years, therefore, it is possible that the longevity of *L. sebae* is in excess of 40 years. These two estimates of maximum age in *L. sebae* were applied to the Hoenig (1983) equation for fish in order to derive an estimate of  $M$ . Consequently,  $M$  is considered to be in the range of 0.1038-0.1223, representing an annual survivorship of 88-90% for an unfished population. This range of  $M$  estimates for *L. sebae* is similar to that observed for other long-lived lutjanid species in the Indo-Pacific region (e.g. Newman et al. 1996, 2000a).

The age structures of *L. sebae* sampled, differed among years. The 1997 sample had a peak in year class 9 and a relatively strong 8+ year class, with abundance per age class declining rapidly to age 22 (Fig. 4.11). Fish older than 20 years are not well represented in the catch (Fig. 4.11). The 1998 and 1999 samples were somewhat similar. In 1998 relatively strong year classes were present from age 8 through to age 10, with abundance per age class declining rapidly to age 22 (Fig. 4.12). The strong 9+ year class present in 1997, was present as a strong 10+ year class in 1998 (Fig. 4.12) and persisted as a strong 11+ year class in 1999 (Fig. 4.13). The progression of this strong year class provides further evidence of the annual formation of growth increments.

Relatively strong year classes were present from age 9 through to age 11 in the 1999 sample, with abundance per age class declining rapidly to age 22 (Fig. 4.13). The strong 9+ year class present in 1998, was present as a strong 10+ year class in 1999 (Fig. 4.13). In all years abundance per age class declined rapidly to age 22, with fish older than 20 years not well represented in the catch. In all years fish less than 8 years of age were not well represented in the catch, inferring that these fish either do not enter traps or are present in areas not currently fished by operators in the NDSF.

*Lutjanus sebae* less than age 8 were in general not fully recruited to the sampled population and were excluded from the mortality estimates derived from catch-at-age data. The year-specific total annual rate of mortality,  $Z$ , of *L. sebae* in the NDSF, was 0.32 for 1997/1998 (fish aged 8-25 years) and 0.28 for 1998/1999 (fish aged 8-25 years). Estimates of the rate of fishing mortality,  $F$ , were 0.20-0.22 for 1997/98 and 0.15-0.17 for 1998/99, representing an annual harvest rate of approximately 17-19% and 13-15%

by the fishery in each year (Table 4.5). In addition, exploitation rates were in the range 0.62-0.68 for 1997/98 and 0.56-0.62 for 1998/99.

#### **4.1.5 Estimation of optimum fishing mortality rates ( $F_{opt}$ )**

The optimum fishing mortality rate,  $F_{opt}$  for *L. sebae* is estimated to be 0.0519-0.0611, while the limit reference point,  $F_{limit}$  was estimated to 0.069-0.082 (see Table 4.5). These results indicate that only approximately 5-6% of the available stock of *L. sebae* can be harvested on an annual basis in a sustainable manner, and that in order to prevent stock declines annual harvest rates should not exceed 7-8% of the stock size.

**Table 4.1**

Length conversion equations for *L. sebae* off the Kimberley coast of north-western Australia. Estimates were obtained of the parameters  $a$  and  $b$  of the length-length relationships, sample size ( $n$ ) and regression  $r^2$  value (all lengths are in mm).

Length-length relationship	$n$	$r^2$
TL = (1.0654 × FL) + 3.5947	1658	0.9984
FL = (0.9371 × TL) - 2.6297	1658	0.9984
FL = (1.1521 × SL) + 11.8230	1577	0.9890
SL = (0.8584 × FL) - 5.7307	1577	0.9890

**Table 4.2**

Length-weight relationships for *L. sebae* off the Kimberley coast of north-western Australia. Estimates were obtained of the parameters  $a$  and  $b$  of the relationship  $W = aL^b$ , the sample size ( $n$ ) and the regression  $r^2$  value (lengths used are FL in mm and the weight is TW or CW in g). Parameters have been corrected for the bias associated with the log-transform.

Group	$a$	$b$	$n$	$r^2$
<i>L. sebae</i> (all fish - TW)	$2.051 \times 10^{-5}$	3.0147	2242	0.9811
<i>L. sebae</i> (all fish - CW)	$1.553 \times 10^{-5}$	3.0379	2233	0.9849
<i>L. sebae</i> (male - TW)	$1.524 \times 10^{-5}$	3.0614	899	0.9831
<i>L. sebae</i> (female - TW)	$2.227 \times 10^{-5}$	3.0020	1317	0.9594

**Table 4.3**

Comparisons among otolith dimensions and length and age of *L. sebae*. The predictive equations are of the simple linear regression form  $y = a + bx$  (codes for the independent variables are described in the text). For regression analyses fish length (FL) and age were used as the dependent variables (all regressions were significant at  $p < 0.001$ ). The standard error (SE) of the estimate is a measure of the dispersion of the observed values about the regression line.

Dep. Var.	Ind. Var.	Sample Size	Equation	$r^2$	SE of Estimate
FL	OW	2442	$FL = (135.609 \times OW) + 318.077$	0.640	42.160
FL	OL	2268	$FL = (29.102 \times OL) - 108.684$	0.870	24.211
FL	OB	2422	$FL = (44.572 \times OB) - 131.607$	0.774	32.148
FL	OH	2429	$FL = (64.161 \times OH) + 234.735$	0.387	53.174
Age	OW	2210	$Age = (11.118 \times OW) - 0.642$	0.786	2.3720
Age <sub>male</sub>	OW	902	$Age = (9.097 \times OW) + 0.495$	0.883	1.4218
Age <sub>female</sub>	OW	1283	$Age = (13.742 \times OW) - 2.669$	0.847	2.1858
Age	OL	2129	$Age = (1388 \times OL) - 15.709$	0.340	4.1324
Age	OB	2281	$Age = (2.119 \times OB) - 16.828$	0.318	4.1367
Age	OH	2289	$Age = (7.015 \times OH) - 14.143$	0.861	1.8758
Age <sub>male</sub>	OH	950	$Age = (6.237 \times OW) - 11.604$	0.852	1.5843
Age <sub>female</sub>	OH	1330	$Age = (7.465 \times OW) - 15.613$	0.874	1.9591

**Table 4.4**

Growth parameters derived from the von Bertalanffy growth function (VBGF) and population characteristics of *L. sebae* off the Kimberley coast of north-western Australia ( $n$  = sample size, FL is in mm, and age (t) is in years).

Parameters	Male	Female	Total
$n$	1001	1408	2384
$L_{\infty}$	627.79	482.62	524.77
K	0.1511	0.2710	0.2330
$t_0$	-0.5947	0.0650	0.0563
$r^2$	0.8044	0.8049	0.6179
$n$	1081	1516	2627
FL <sub>mean</sub>	508.5	450.5	472.4
FL <sub>min</sub>	211	183	183
FL <sub>max</sub>	728	584	728
$n$	977	1384	2386
$t_{\text{mean}}$	11.32	12.34	11.84
$t_{\text{min}}$	2	1	1
$t_{\text{max}}$	30	34	34

**Table 4.5**

Summary of total mortality (Z) estimates for *L. sebae* derived from catch curves based on ages determined from sectioned otoliths. Estimates of fishing mortality (F) are derived by subtraction since  $Z = F + M$  and are compared to estimates of optimum fishing mortality rates.

Year	Z	F	F <sub>opt</sub>	F <sub>limit</sub>
1997/98	0.321	0.199-0.217	0.052-0.061	0.069-0.082
1998/99	0.275	0.153-0.171	0.052-0.061	0.069-0.082

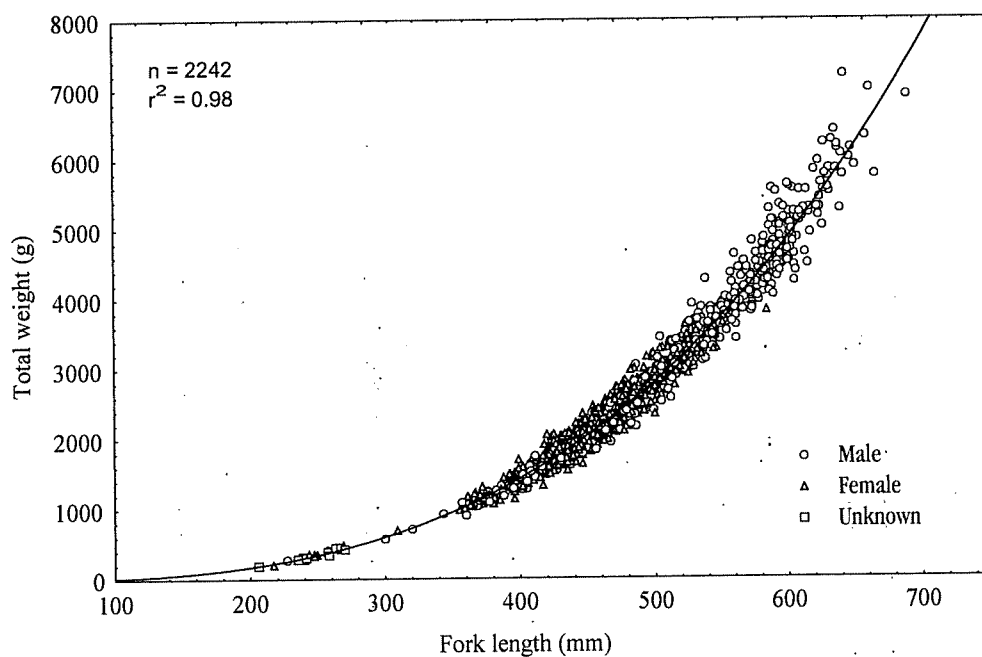


Figure 4.2: Relationship between fork length and total weight for *L. sebae* off the Kimberley coast of north-western Australia.

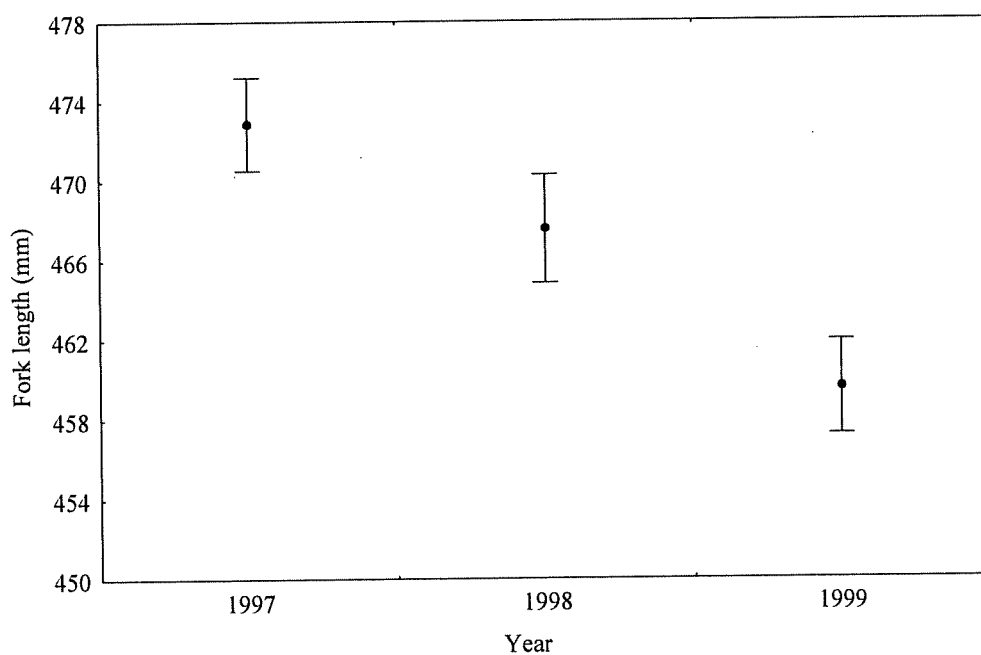


Figure 4.3: Temporal change in mean length ( $\pm$  SE) of *L. sebae* off the Kimberley coast of north-western Australia from 1997 to 1999.

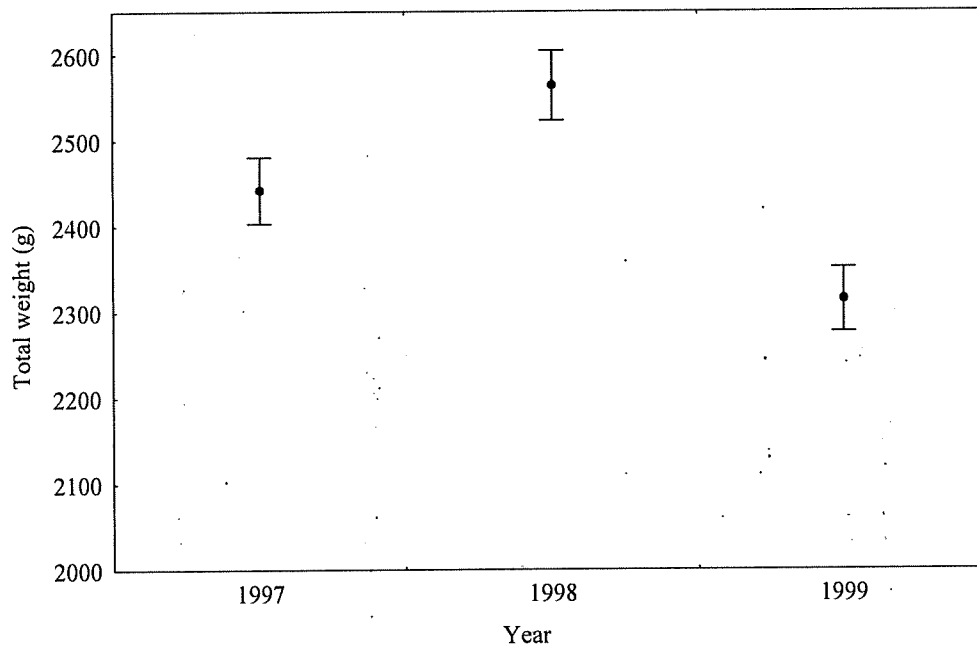


Figure 4.4: Temporal change in mean weight ( $\pm$  SE) of *L. sebae* off the Kimberley coast of north-western Australia from 1997 to 1999.

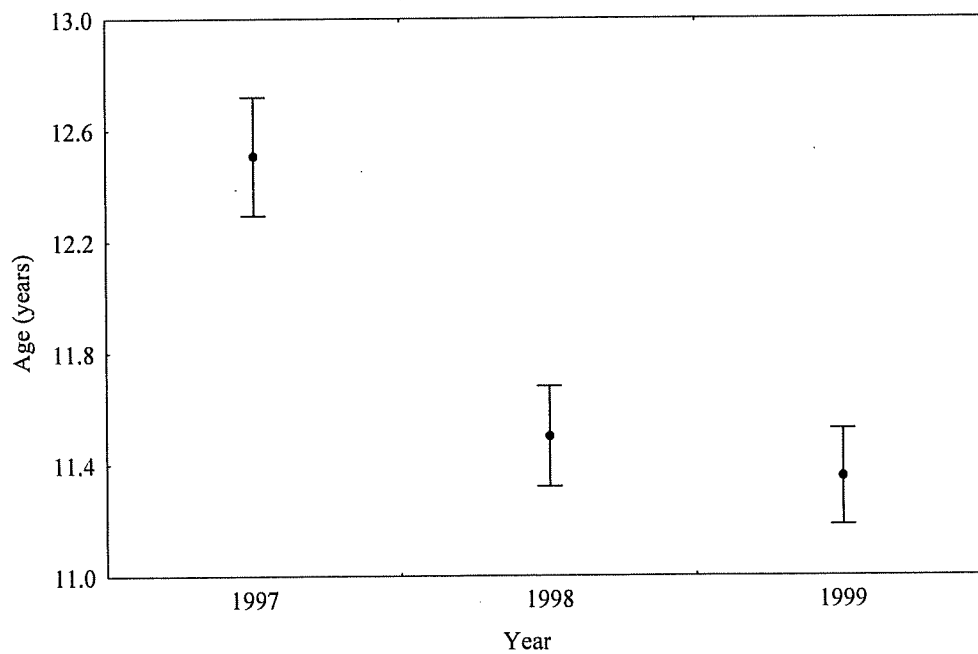


Figure 4.5: Temporal change in mean age ( $\pm$  SE) of *L. sebae* off the Kimberley coast of north-western Australia from 1997 to 1999.

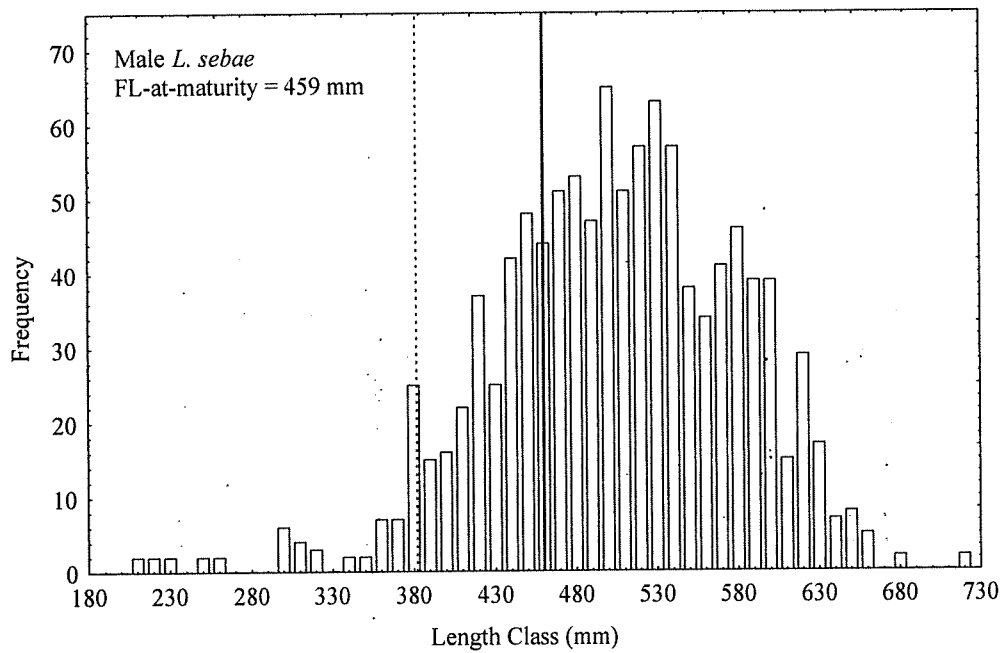


Figure 4.6: Length frequency distribution (10 mm length classes) of male *L. sebae* sampled for age determination in association with the size-at-maturity for male *L. sebae* (the minimum legal length for *L. sebae* is 410 mm TL, dashed line).

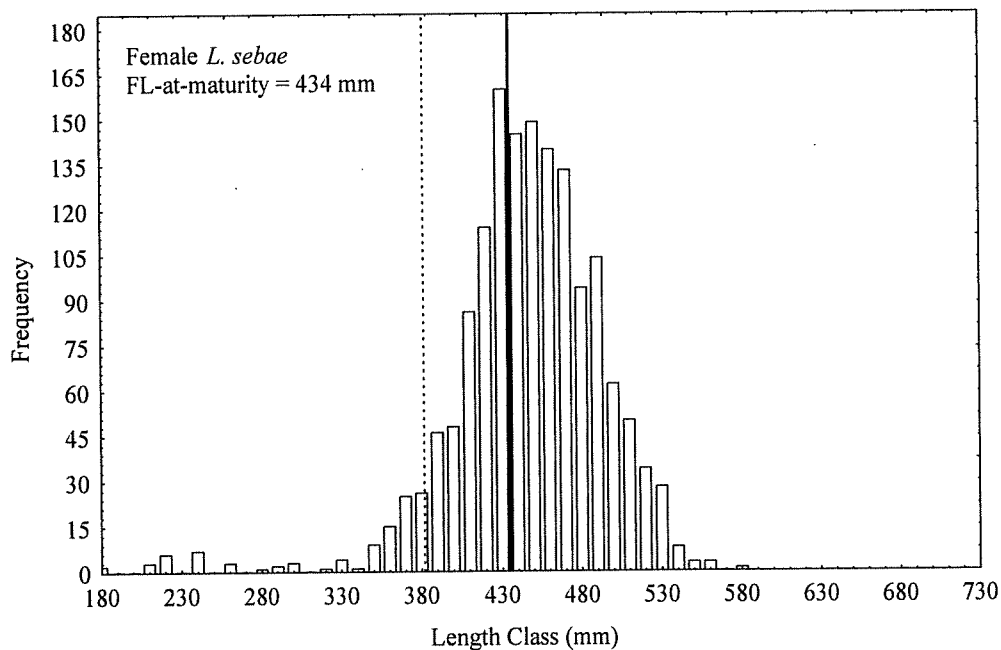


Figure 4.7: Length frequency distribution (10 mm length classes) of female *L. sebae* sampled for age determination in association with the size-at-maturity for female *L. sebae* (the minimum legal length for *L. sebae* is 410 mm TL, dashed line).

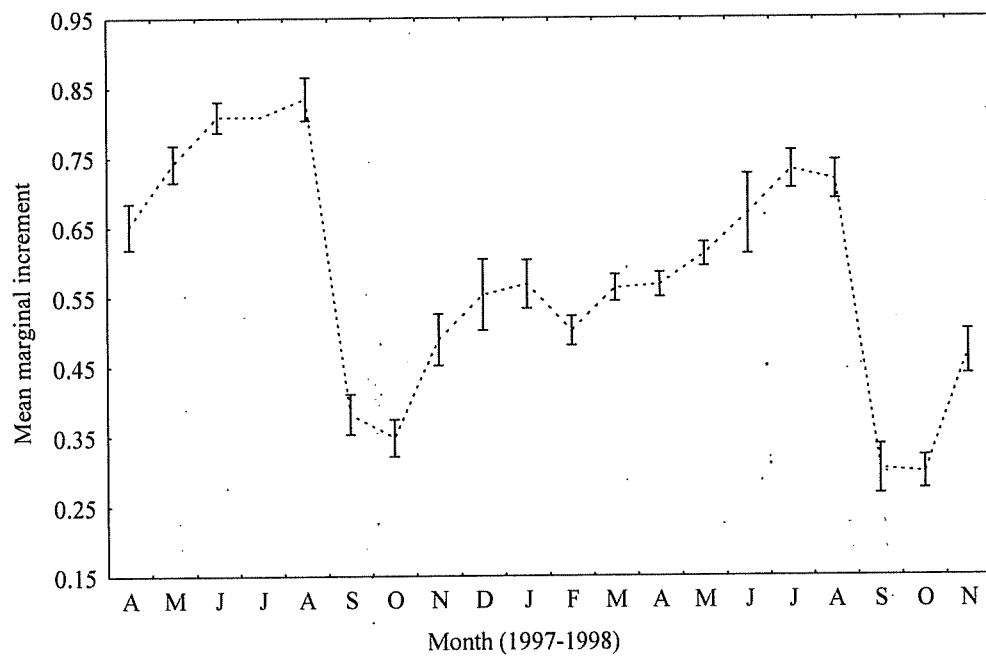


Figure 4.8: Mean monthly marginal increments for *L. sebae* from April 1997 to November 1998 ( $\pm$  SE).

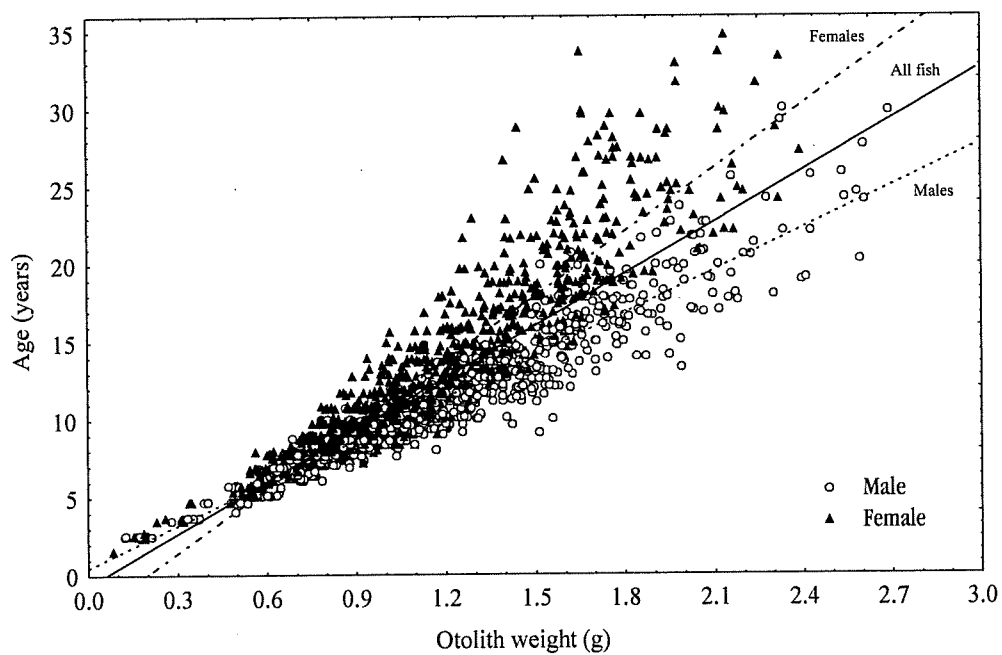


Figure 4.9: Relationship between otolith weight and age of *L. sebae* estimated from sectioned otoliths.

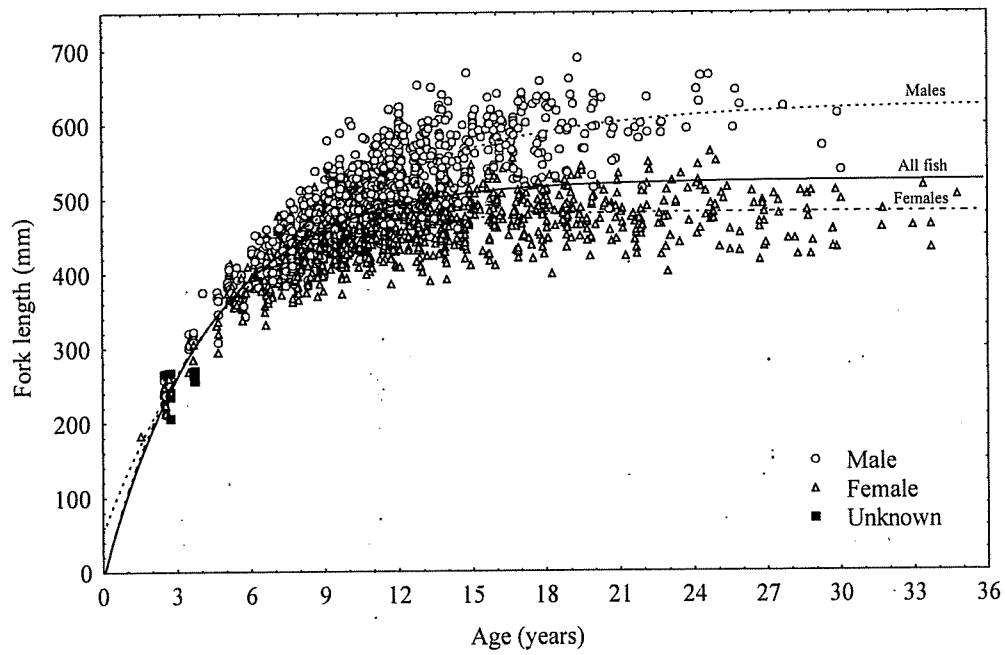


Figure 4.10: Length-at-age and von Bertalanffy growth curves for *L. sebae* off the Kimberley coast of north-western Australia.

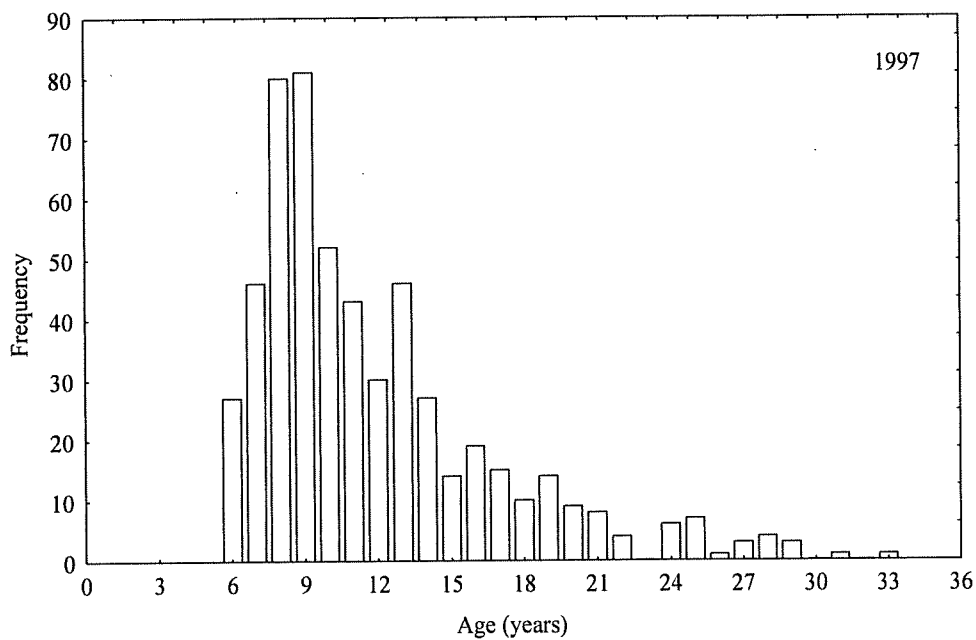


Figure 4.11: Age frequency distribution of *L. sebae* from the NDSF in 1997.

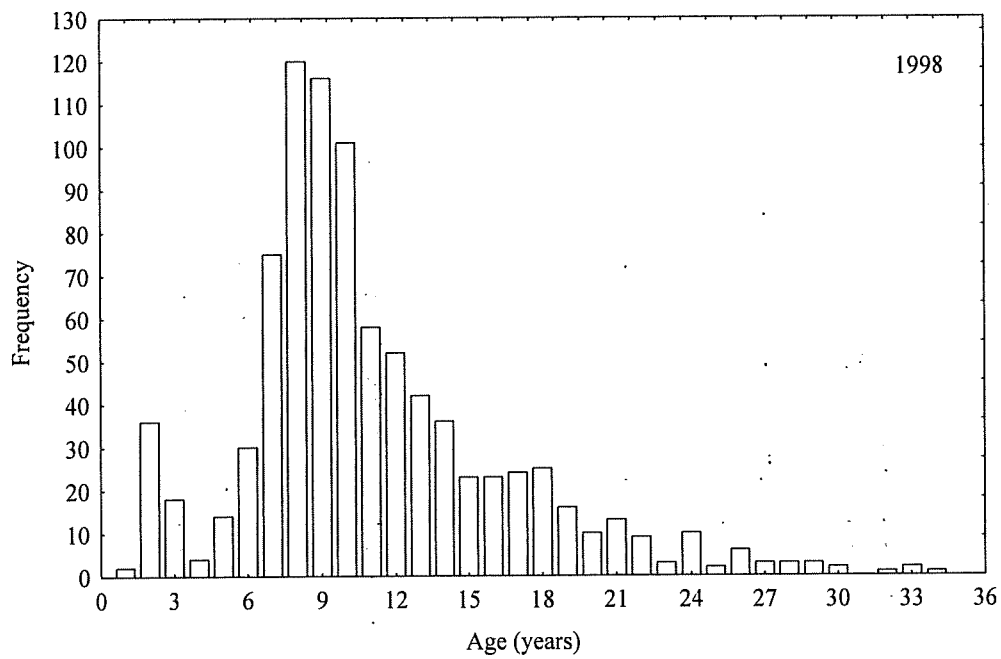


Figure 4.12: Age frequency distribution of *L. sebae* from the NDSF in 1998.

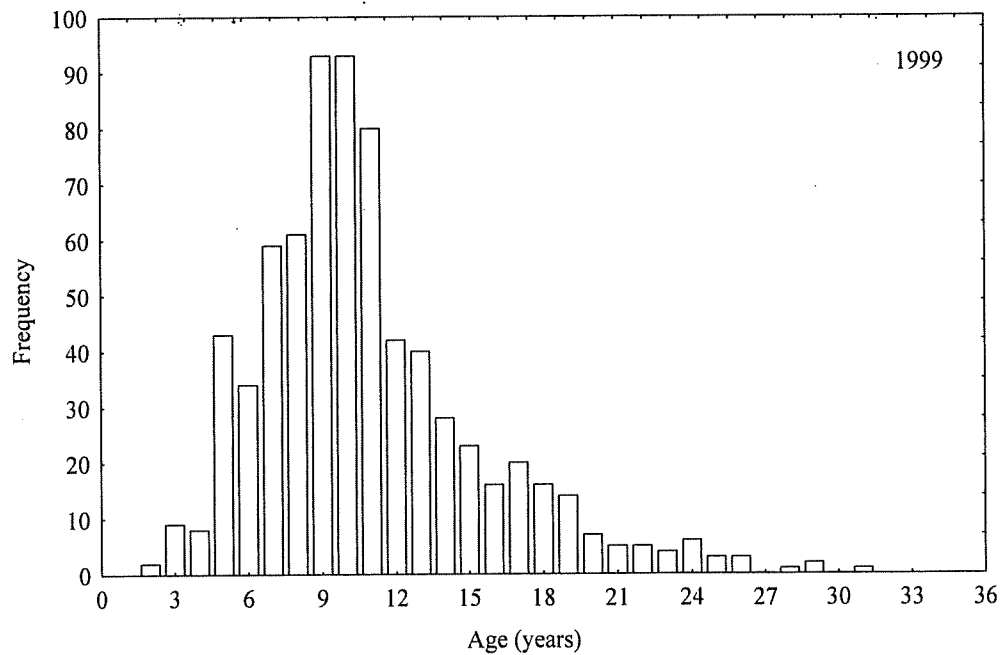


Figure 4.13: Age frequency distribution of *L. sebae* from the NDSF in 1999.

## 5. Reproductive biology of the red emperor snapper, *Lutjanus sebae*.

*Stephen J. Newman, Richard A. Steckis and Jerry Jenke*

The mean monthly GSIs for mature male *L. sebae* in the Kimberley region rose sharply from ca.  $< 0.07$  in the period from April to September to a major peak at 0.15 in October, then declining to 0.075 in December, before rising to minor peaks at ca. 0.1 in January and March, before declining to ca. 0.05 in April (Fig. 5.1). The GSI for male fish is extremely low, with the maximum male GSI representing ca. 5% of the corresponding maximum GSI recorded for female fish. The mean monthly GSIs for mature females was higher than 1.5 throughout the year (Fig. 5.1). The relatively high female GSI throughout the year indicates that they are in a state of reproductive readiness in all months.

Overall the mean monthly GSIs for mature females displayed trends, which paralleled those, exhibited by male fish (although values were considerably higher). The major peak in GSI for female fish occurred in October, with minor peaks present in January and March, identical to those reported for male fish. The similarity in the variation in gonadosomatic indices indicates that the significant reproductive period for *L. sebae* was October with opportunistic spawning periods in January and March (Fig. 5.1). Furthermore, in contrast to females, male *L. sebae* do not remain in a high state of reproductive readiness in the months outside the peak spawning months suggesting that they and not the females initiate the spawning process.

Females and males with gonad Stages II and III were present throughout the year. Stage IV ovaries and testes were also present throughout much of the year (Fig. 5.2). Stage V ovaries were present throughout the year, however, the proportion of Stage V ovaries peaked in October, with a smaller peak evident in March. Stage V testes were recorded only in October and March, with peak abundance in October. Stage VI ovaries were only recorded in February and March, while Stage VI testes were only recorded in October. Stage VII ovaries were present in low proportions throughout much of the year. Stage VII testes (spent condition) were present only from February to April with a marked increase in proportions in the April sampling period.

The proportion of Stage VIII testes was lowest in October in comparison to other months, while the only month in which Stage VIII ovaries were not recorded was October, indicating that the developmental activity within the ovary is at a maximum at this time (Fig. 5.2). October is also the month, which represents the peak in female and male GSI (Fig. 5.1). The increasing number of females with Stage VIII ovaries in November and the decline in the prevalence of Stage V ovaries in association with the marked increase in Stage VIII testes in November and the absence of Stage IV and V testes indicates that the peak spawning period was complete at this time. The clear trend in the monthly percentage contributions of the different stages of testicular development in *L. sebae* indicate, that there are two spawning periods, October (spring) and March (autumn), with the spring spawning period the more concentrated of the two. Furthermore, male development is clearly defined in the March and October spawning periods in comparison to females (Fig. 5.2), indicating that male fish initiate the spawning process.

Oocytes from ovaries of *L. sebae*  $< 200 \mu\text{m}$  in diameter were present in all months of the year, with several modes in the frequency distributions of oocytes for each month (Fig. 5.3). These oocytes represent an early stage in development, either chromatin nucleolar or perinucleolar oocytes. The distribution of larger oocytes ( $> 200 \mu\text{m}$  in diameter) was relatively similar throughout the year (Fig. 5.3), indicating a high state of reproductive readiness and a continuous progression of oocyte modes through the ovary. Oocytes larger than  $400 \mu\text{m}$  in diameter were relatively more abundant in the August to October and February to May periods in comparison to other months. Oocytes in the process of undergoing atresia were present in all months of the year.

The overall sex ratio of *L. sebae* was 1.5:1, female to male. This sex ratio was significantly different from 1:1 ( $\chi^2$  test,  $p < 0.01$ ). The proportion of each sex in the landed catch over each month in the study period was significantly different ( $\chi^2$  test,  $p < 0.01$ ). The proportion of each sex in the landed catch in each month was variable, with females always more abundant than males (Fig. 5.4). Females composed greater than 60% of the catch in the June-July and October-November period. Similar ratios of females to males were only recorded in the August-September period (Fig. 5.4). The

distribution of sexes by length interval (Fig. 5.5) revealed that the proportion of males increased significantly with increasing fish length ( $\chi^2$  test,  $p < 0.01$ ). Females comprised at least 70% of the landed catch up to 500 mm FL. From the 500 mm length class onwards the preponderance of males in the landed catch increased, with most fish greater than 560 mm FL recorded as males (Fig. 5.5). Females and males were only present in similar proportions in the 520 mm length interval. Females dominated the smaller length classes while males dominated the larger length classes (Fig. 5.5).

The seasonal PMI indicated that the number of mature fish in samples decreased from July to September ( $< 50\%$ ), was relatively constant between January and May ( $> 60\%$ ), with the largest proportion of mature fish present in the catch in October (Fig. 5.6). Mature fish are most abundant in the catch during the spawning period. The temporal trend in PMI was somewhat similar over the study period (Fig. 5.7). However, the number of immature fish present in the catch in 1999 was higher than that recorded in 1998 (Fig. 5.7).

The relationship between length and gonad weight was examined for females and males (Fig. 5.8). Gonad weight increased exponentially with increasing length of fish. However, a large amount of variation was present in gonad weight at a given length as fish mature. The length at maturity,  $L_{50}$  for *L. sebae* derived from the logistic model was 429 mm FL (461 mm TL) for females and 457 mm FL (491 mm TL) for males (Fig. 5.9). The high level of agreement between the observed data and the logistic model (Fig. 5.9) for *L. sebae* is an indication of the accuracy and robustness of the macroscopic staging system. The estimated age at maturity ( $A_{50}$ ) for females was 8.2 years, while the  $A_{50}$  for males was 8.0 years.

Table 5.1: Development stages of ovaries and testes of *Lutjanus sebae* based on macroscopic and histological examination of gonads (modified from West (1990) and Davis and West (1993)).

Stage	Macroscopic description	Histological description
I – Immature (Virgin)	Small thread-like gonads, ovaries brownish-grey to translucent and occupy one-third of the length of body cavity, testes are very small and threadlike	Chromatin nucleolar stage: very small oocytes, nucleus surrounded by a thin layer of dark-blue stained cytoplasm
II – Early developing (Maturing virgin)	Ovary translucent, grey-red, small capillaries present, ovary taugt and round, occupies 1/3 length of body cavity, oocytes not visible. Testes still small and threadlike but thicker in cross section, no milt present	Perinuclear stage: oocyte size increases slightly as dark blue-stained cytoplasm thickens, nucleoli appear at the periphery of nucleus
III – Developing	Ovary opaque-reddish with increased capillary development, occupies 1/2 the length of body cavity, small granular oocytes becoming visible. Testes lobed in formation, thicker, milt sometimes present	Cortical alveoli stage: appearance of cortical alveoli in pale-blue-stained cytoplasm, pink stained zona radiata distinguishable, oil-vesicles appearing, lampbrush chromosomes often visible In the nucleus
IV – Late developing (Maturing yolked)	Gonads occupy well over 1/2 the length of body cavity, ovaries have small granular oocytes visible, ovary taugt and round, ovary wall thin and transparent, many small capillary vessels evident. Testes increased in size, milt present	Yolk stage: marked increase in oocyte size, cytoplasm filled with pink-stained yolk granules, cortical alveoli and oil vesicles increase in size and number, degenerating postovulatory follicles visible if spawning has started
V – Ripe (Pre-spawning)	Gonads occupy well over 1/2 the length of body cavity, ovaries with many blood vessels present, large transparent (hydrating) oocytes visible among smaller opaque oocytes. Testes large and thick, milt flows when pressure is applied	Nuclear migration stage: migration of nucleus to periphery of oocyte, fusion of yolk granules into yolk plates, fusion of oil vesicles into the oil droplet, degenerating postovulatory follicles visible if spawning has started
VI – Running ripe (Spawning)	Ovaries large distending the body cavity, many large hydrated oocytes visible, oocytes easily expressed from ovaries with slight pressure. Testes large with free flowing milt	Hydration stage: further increase in size of oocytes, all yolk granules fused into a few plates
VII – Spent	Ovary reduced in size and flaccid, ovary wall thickened, greyish colour, some hydrated oocytes still present, no opaque eggs left in ovary, often purple-red in colour through haemorrhage. Testes contracted, flaccid, milt sometimes present	Postovulatory follicles clearly visible, no yolked oocytes remain, some atretic oocytes present, structure of oocytes generally loose, hydrated oocytes may be present in lumen
VIII – Resting	Ovary reduced in size and empty. Ovary not taugt or round. Testes small, milt not present.	Stage II & III oocytes dominate, no trace of postovulatory follicles left, advanced atresia of remaining yolked oocytes, large empty spaces present in lumen

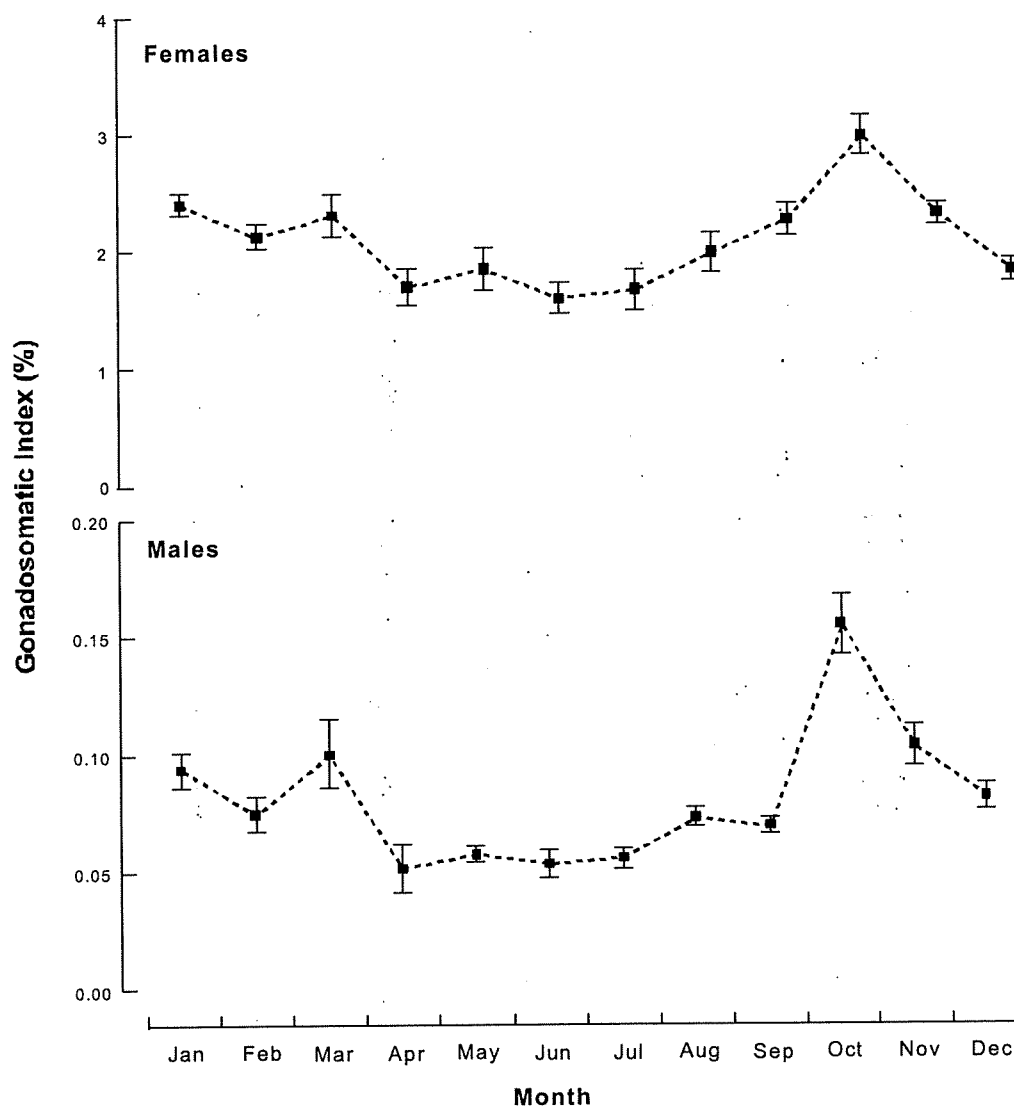


Figure 5.1. Seasonal changes in mean monthly gonadosomatic indices ( $\pm$  SE) for female and male *Lutjanus sebae* in the Kimberley region of north-western Australia for gonad stages IV–VIII.

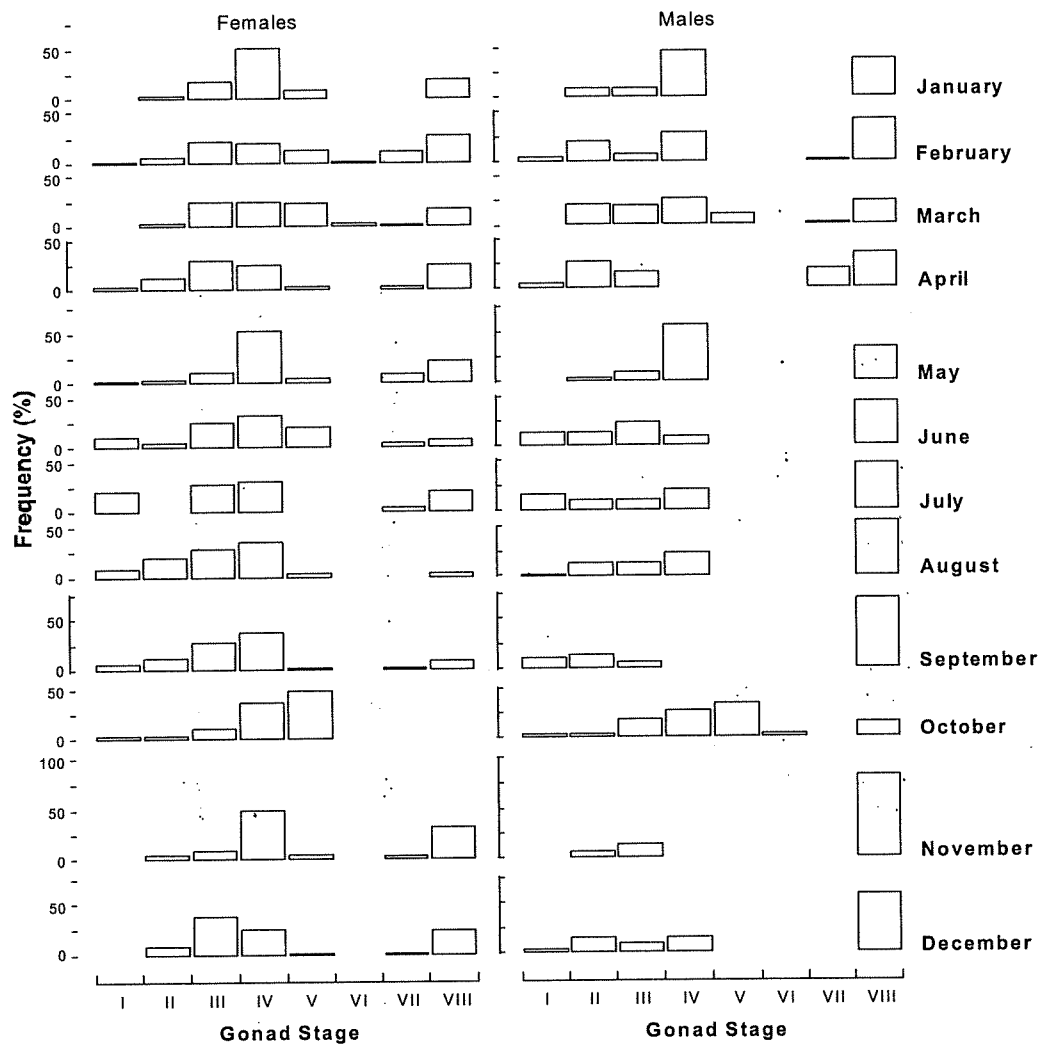


Figure 5.2. Monthly percentage contributions of different stages in gonadal development in female and male *Lutjanus sebae* in the Kimberley region of north-western Australia.

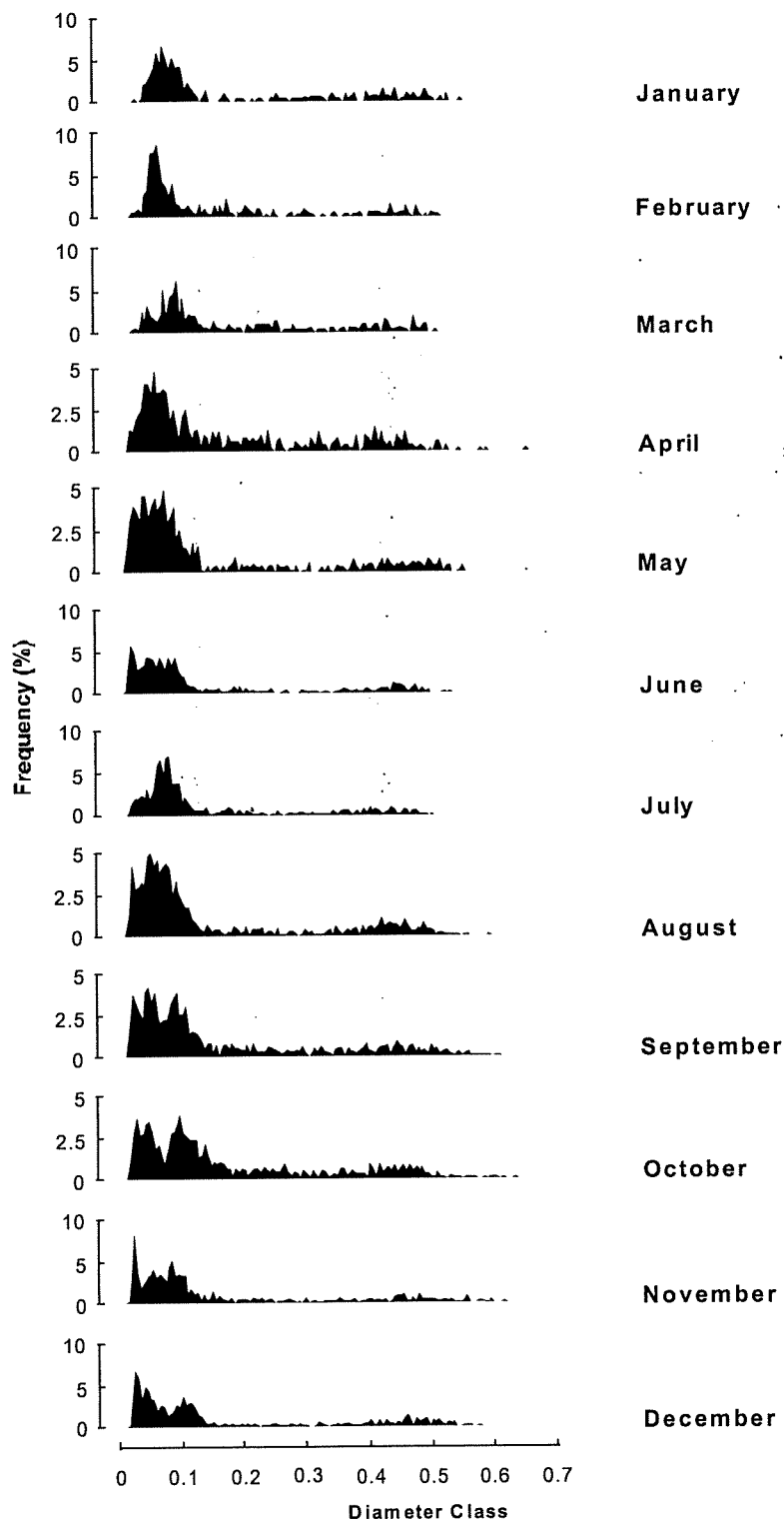


Figure 5.3. Monthly size frequency distributions of oocyte diameters of *Lutjanus sebae*, measured from histological sections of ovaries.

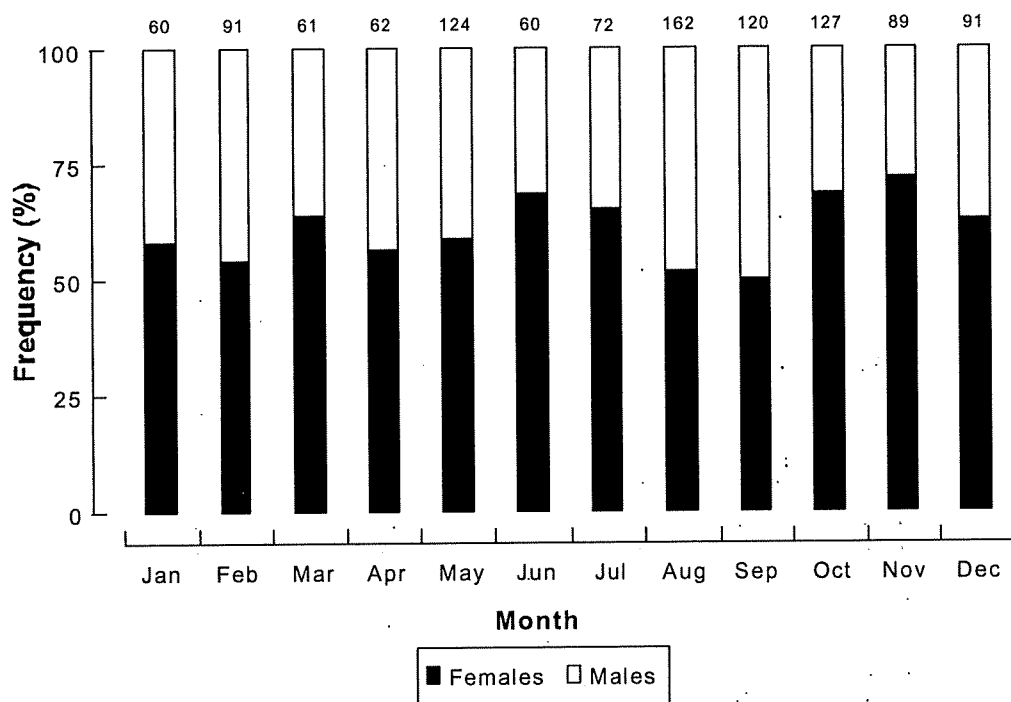


Figure 5.4. Sex ratio of female and male *Lutjanus sebae* in each month in the Kimberley region of north-western Australia (sample sizes are shown above each bar).

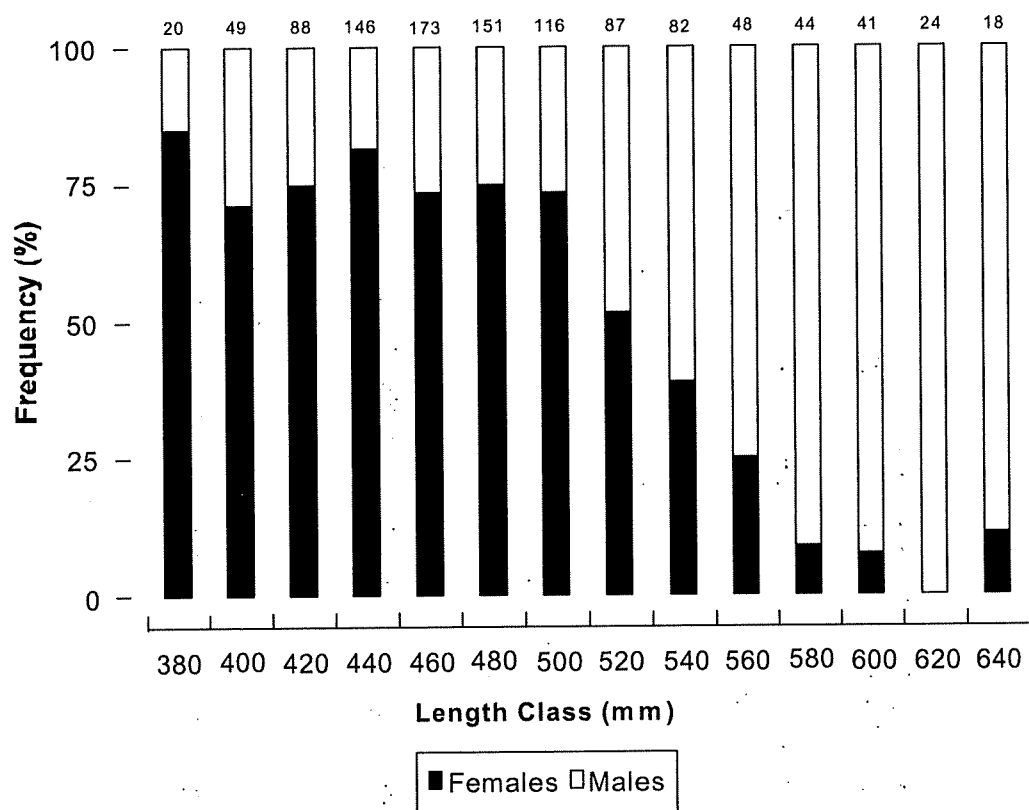


Figure 5.5. Sex ratio of female and male *Lutjanus sebae* in the Kimberley region of north-western Australia by 20 mm length classes (sample sizes are shown above each bar).

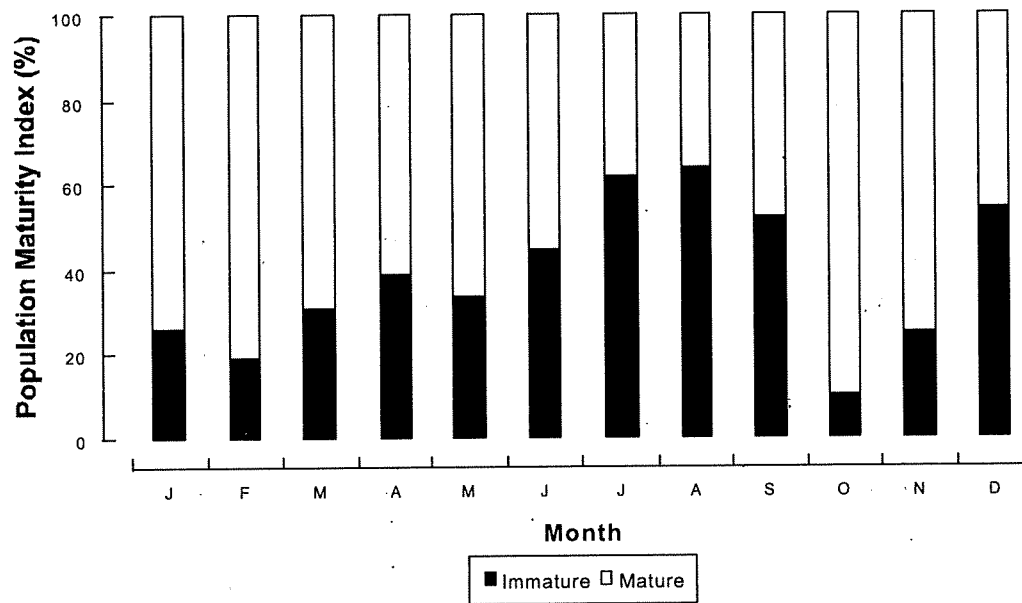


Figure 5.6: Seasonal change in the monthly population maturity index for *Lutjanus sebae* in the Kimberley region of north-western Australia.

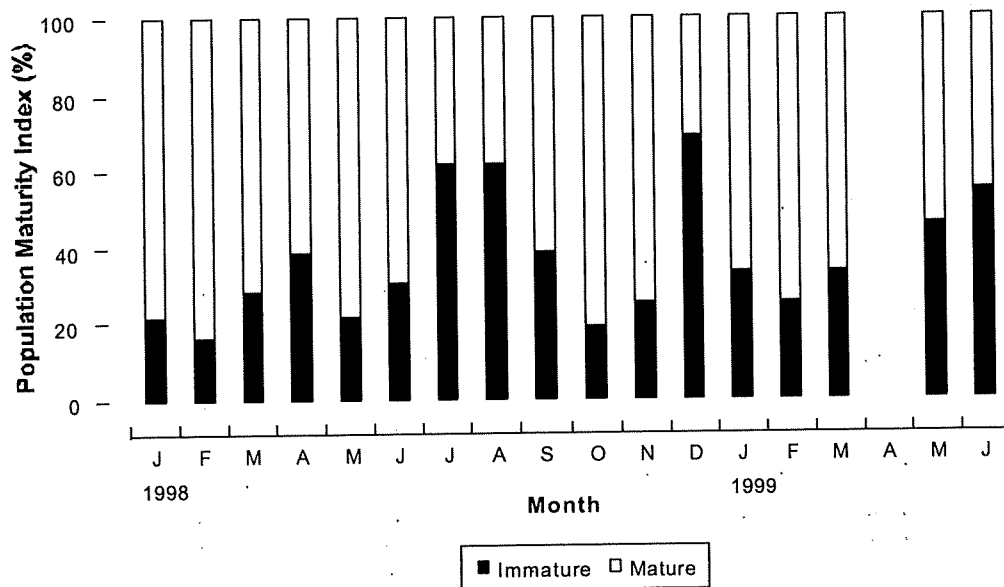


Figure 5.7. Temporal change in the monthly population maturity index for *Lutjanus sebae* in the Kimberley region of north-western Australia over the duration of the study period.

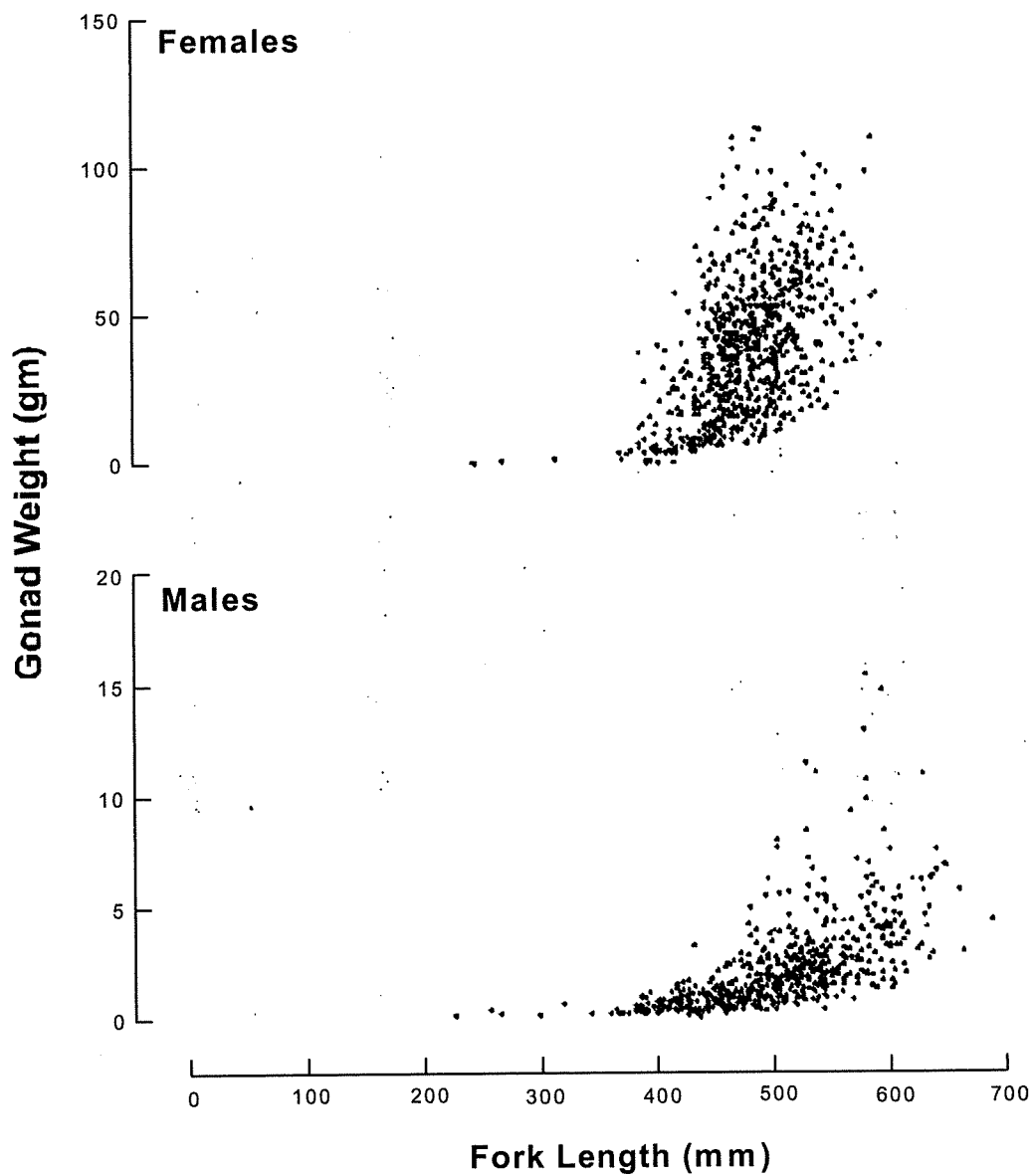


Figure 5.8. The relationship between fork length and gonad weight for female and male *Lutjanus sebae* in the Kimberley region of north-western Australia.

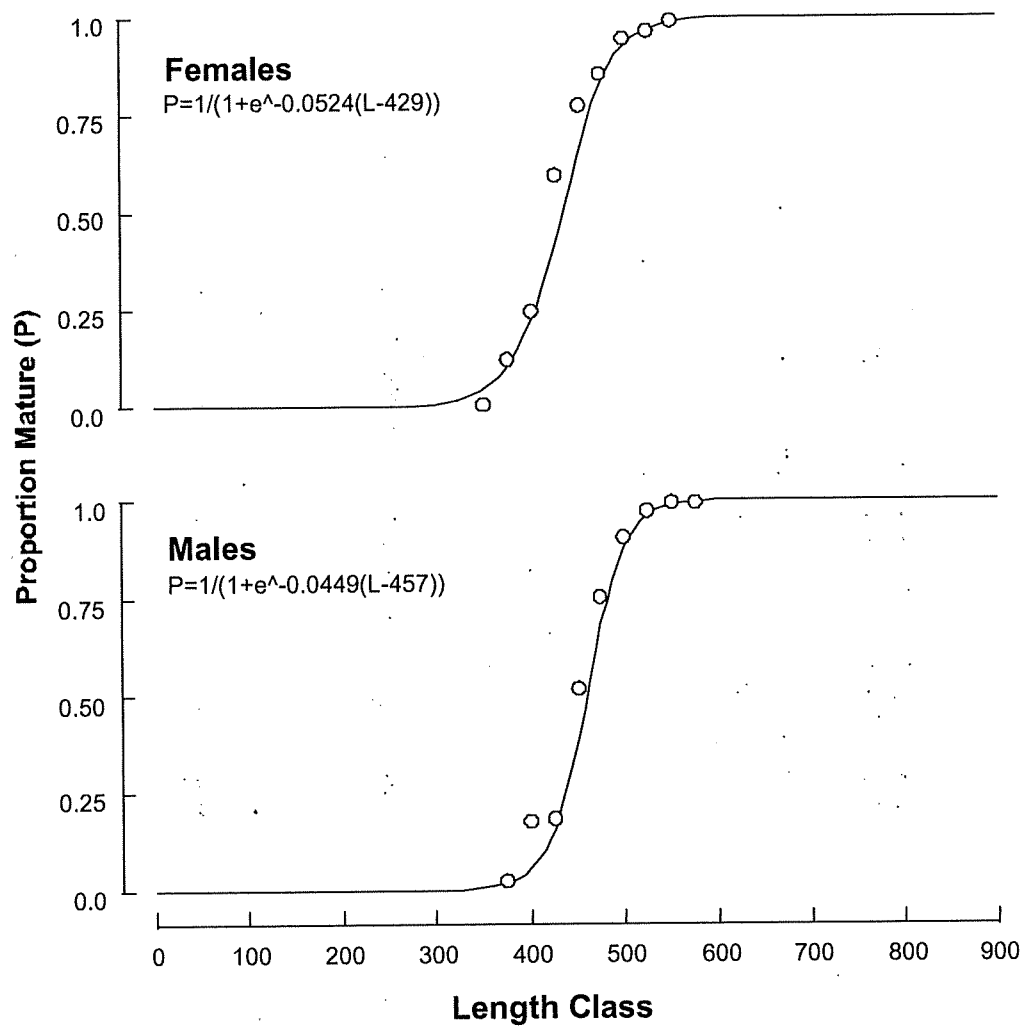


Figure 5.9. Length at maturity relationship showing the proportion of mature female and male *Lutjanus sebae* from the Kimberley region of north-western Australia. A logistic curve is fitted to the data for each sex. Size classes are in 20 mm intervals.

## 7. Yield per recruit and eggs per recruit models.

*Stephen J. Newman*

Yield per recruit (YPR) models evaluate the fate of a cohort or year class of fish once it has recruited to the fishery. The YPR model assumes a steady state stock structure, that is, the total yield in any one year from all age classes is the same as that from a single cohort over its entire life span. YPR models may include age-dependent vulnerability. YPR calculates, for the whole cohort over time, gains in biomass by growth and losses in biomass due to mortality. Therefore it is possible to affect the amount of yield you can obtain from a cohort by controlling the age at first capture of the fish and  $F$ .

The object of this study was to calculate the age at first capture that maximizes yield in biomass from the cohort. All cohorts in the population are assumed to have the same growth and mortality rates, regardless of cohort size. Furthermore, many yield per recruit analyses conclude that maximum YPR is achieved at a length of first capture that is similar to length at first reproduction. This occurs because somatic growth slows as energy requirements are directed towards reproductive activity. Therefore, length at maximum YPR is often similar to length at first reproduction (eg. Newman et al. 2000a).

Manipulation of the age at first capture for fishery management purposes is dependent upon the selectivity of the fishing gear used by fishers. If manipulation of fishing gear is possible then by setting a high age at first capture, fish have time to grow before capture thus reducing the potential for growth overfishing. If fishing mortality is set too high or if the age at first capture is below the length at first reproduction (or when breeding commences), the fishery is at risk of recruitment overfishing. Eggs per recruit analyses (EPR) allow evaluation of yield and egg production in order to seek a balance between the attempt to maximize yield with the need to ensure that sufficient reproduction occurs to guard against recruitment overfishing.

A YPR analysis was undertaken for *P. multidentis* using the growth parameters of the VBGF, weight-length relationship (TW-FL) and the estimate of  $M$  determined from the age and growth study. The YPR model indicated that maximum yields per juvenile

fish recruiting to the population were in the range from 500 to 600 grams, for ages at first capture from 4 to 8 years (Fig. 6.1). The optimum age at first capture varies according to the level of fishing mortality to which the population is subjected. Under high levels of fishing mortality yield is increased if fish do not become vulnerable to fishing until they are older than 7 years of age. At all levels of fishing mortality, greater yields are possible if the age at first capture can be delayed until at least 5 years of age.

Fishers in the NDSF should be aware that harvesting *P. multidentis* at or above 557 mm total length (477 mm FL) or age 6+ will result in an increased yield to the fishery. However, given the high mortality associated with the capture of *P. multidentis* resulting from the effects of embolism, it is not prudent to introduce a minimum legal length for this species as any released fish have an extremely low chance of survival. Fishers should be encouraged to move to new areas if they begin to capture large numbers of *P. multidentis* less than 557 mm TL.

An EPR analysis was undertaken for *P. multidentis* using the growth parameters of the VBGF, weight-length relationship (TW-FL), the estimate of M determined from the age and growth study and the fecundity relationship of Kikkawa (1984) for *P. filamentosus*, as we were not able to obtain ripe gonads for fecundity work in this study. Unlike the YPR analysis, EPR relationships provide no optimum age, which maximises egg production. Essentially the longer fish have before they become vulnerable to capture, the greater the egg production (Fig. 6.2).

Egg production should not be allowed to fall below 30% of the unfished egg production ( $F_{30} = 0.14$ ). Egg production is increased if levels of fishing mortality are approximately 40% of the unfished egg production ( $F_{40} = 0.10$ ). Egg production is increased if the age at first capture can be increased at all levels of fishing effort. However, egg production is much reduced for any ages at first capture below 8 years of age. Given that at least 4 age classes are harvested in the NDSF before *P. multidentis* reaches sexual maturity indicates that *P. multidentis* is very vulnerable to over-exploitation.

A YPR analysis was undertaken for *L. sebae* using the growth parameters of the VBGF, weight-length relationship (TW-FL) and the estimate of M determined from the age and growth study. The YPR model indicated that maximum yields per juvenile fish

recruiting to the population were in the range from 600 to 700 grams, for ages at first capture from 5 to 8 years (Fig. 6.3). The optimum age at first capture varies according to the level of fishing mortality to which the population is subjected. Under high levels of fishing mortality yield is increased if fish do not become vulnerable to fishing until they are older than 7 years of age. At all levels of fishing mortality, greater yields are possible if the age at first capture can be delayed until at least 6 years of age.

Fishers in the NDSF should be aware that harvesting *L. sebae* at or above 492 mm total length (459 mm FL) will result in an increased yield to the fishery. The current minimum legal length for *L. sebae* is 410 mm total length (ca. 382 mm FL), is below the size at maturity (492 mm TL for males, 468 mm TL for females) for this species. Yield per recruit analysis indicates that the maximum yield for fishers is obtained at ages of first capture from 5 to 8 years or correspondingly sizes at first capture from 450 to 500 mm TL. An increase in the minimum legal length of *L. sebae* in the Kimberley region of Western Australia to 500 mm total length is recommended (if it can be suitably enforced). This corresponds to ca. 460 mm FL, which is above the length at maturity for both male and female *L. sebae* and within the optimum range for yield per recruit.

An EPR analysis was undertaken for *L. sebae* using the growth parameters of the VBGF, weight-length relationship (TW-FL), the estimate of M determined from the age and growth study and the annual fecundity relationship derived from Collins et al. (1996) for *L. campechanus*, as we were not able to obtain ripe gonads for fecundity work in this study. Unlike the YPR analysis, EPR relationships provide no optimum age, which maximises egg production. Essentially the longer fish have before they become vulnerable to capture, the greater the egg production (Fig. 6.4).

Egg production should not be allowed to fall below 30% of the unfished egg production ( $F_{30} = 0.12$ ). Egg production is increased if levels of fishing mortality are approximately 40% of the unfished egg production ( $F_{40} = 0.09$ ). Egg production is increased if the age at first capture can be increased at all levels of fishing effort. However, egg production is much reduced for any ages at first capture below 7 years of age.

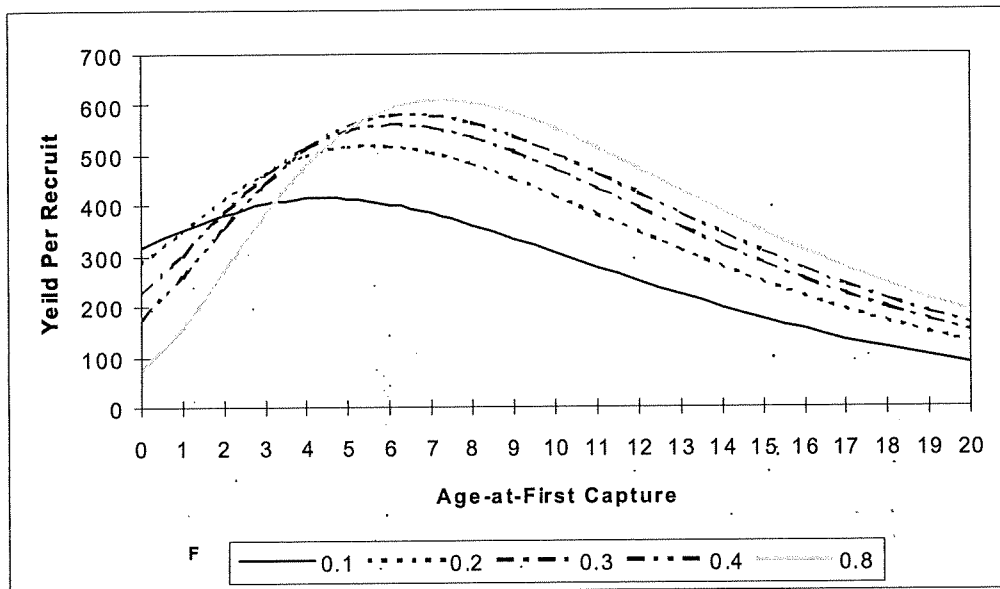


Figure 6.1: The effect of age-at-first capture on the yield per recruit of *Pristipomoides multidentis* at various levels of fishing mortality F.

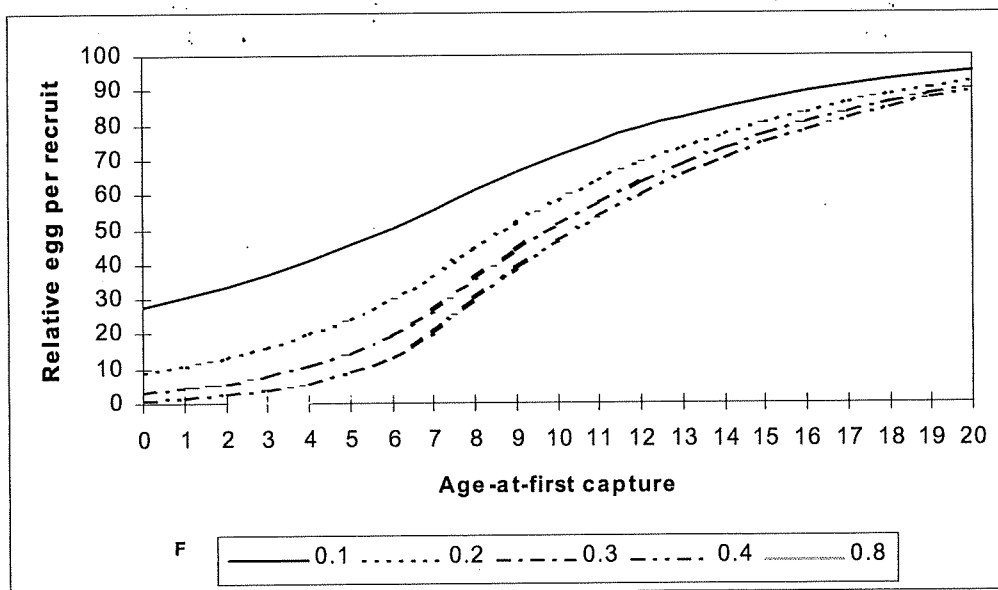


Figure 6.2: The effect of age-at-first capture on the relative eggs per recruit of *Pristipomoides multidentis* at various levels of fishing mortality F.

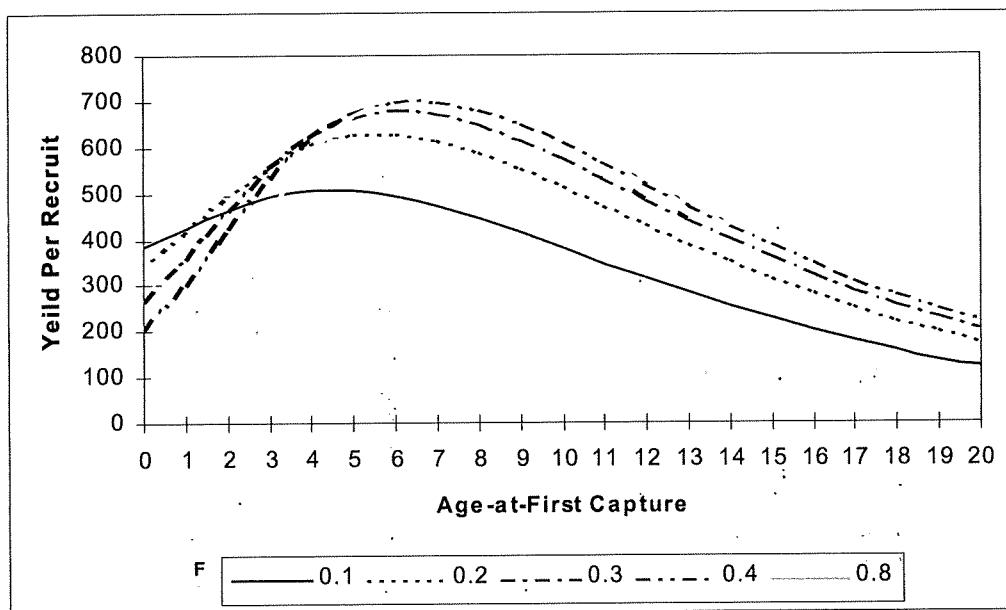


Figure 6.3: The effect of age-at-first capture on the yield per recruit of *Lutjanus sebae* at various levels of fishing mortality F.

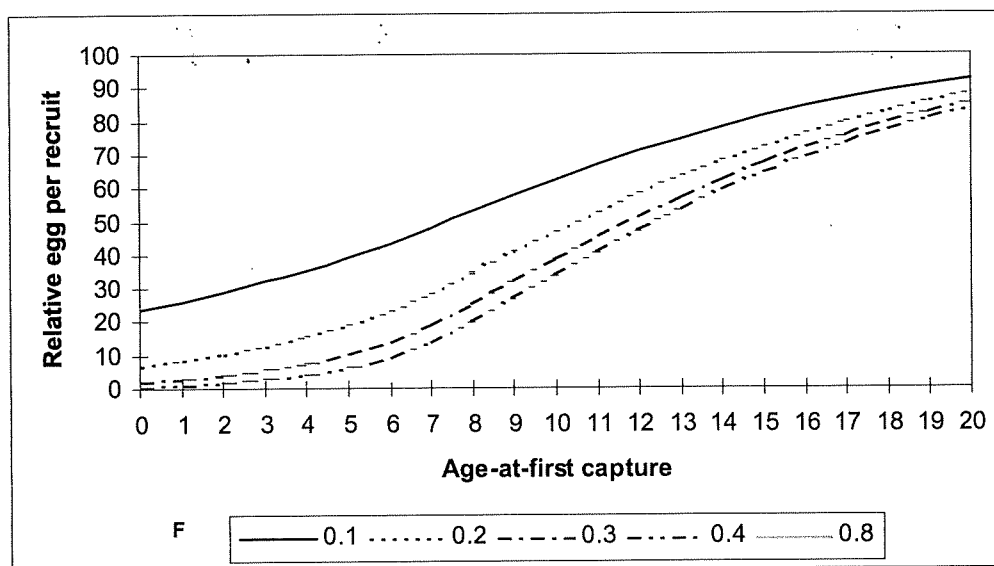


Figure 6.4: The effect of age-at-first capture on the relative eggs per recruit of *Lutjanus sebae* at various levels of fishing mortality F.

## 7. Selectivity of fish traps.

*Stephen J. Newman and Peta C. Williamson*

Escape gaps in fish traps in the NDSF were examined in 1998 and 1999. The escape gaps consist of two types; vertical 15×5 cm escape gaps and square 10×10 cm escape gaps. The vertical escape gaps were positioned either side of the rear door to each trap, while the square escape gaps were positioned at the top of each trap. The vertical 15×5 cm escape gaps were designed to facilitate the escape of small red emperor, *Lutjanus sebae*, a laterally compressed species. These escape gaps were positioned on the bottom side of the trap as observations revealed that once inside the trap, *L. sebae* swam predominantly around the bottom of the trap. The 10×10 cm escape gaps were designed to facilitate the escape of small goldband snapper, *Pristipomoides multidens*, a rounded fusiform species. These escape gaps were positioned at the top of the trap as observations revealed that once inside, *P. multidens* swam predominantly around the top of the trap. Treatments consisting of a control trap (no escape gaps), a trap with 2 escape gaps of each type, and a trap with 6 escape gaps of each type were fished systematically with 3 replicates of each treatment. The effects of escape gaps on the number and size range of the captured fish was examined.

Fish traps were fished in two locations within the fishery, in the northern area (in the vicinity of Heywood Shoal) and in the southern area (in the Broome region). Traps were fished throughout the day and at night in the same manner as used by the fishing industry. Replication was incorporated at all levels of the treatment effects. Traps were deployed randomly in each location to ensure independence and to avoid systematic errors.

The trap design used was the fishing industry standard. Each trap was baited with ca. 1 kg of pilchards (*Sardinops sagax*) for each set. The catch of each trap was identified to species and measured to the nearest millimetre. Sampling was carried out during the day with approx 2 trap sets. Traps set during the day had soak times (ie. the time the trap was in the water) of between 2 and 4 h. Traps were also set overnight with night set traps having a soak time of between 12 and 14 h. Catch per unit effort (CPUE) data for day and night set traps was standardised by soak time ( $\text{kg h}^{-1}$ ).

CPUE data from the fish traps for each of the treatments was analysed by parametric analysis of variance (ANOVA). Multiple comparison of means (with  $\alpha = 0.05$ ) were conducted using Tukey's Honestly Significant Difference (HSD) method. Three factor ANOVAs were carried out on the CPUE data for all fish caught and the two key species, *P. multidentis* and *L. sebae*. The three factors in the analysis were location, diel sampling period and escape gap treatment. Each factor was treated as fixed and orthogonal in the analysis.

Examination of the raw data revealed that the catch rates of many species in traps were characterised by a number of extremely high catches and numerous zero catches, thus the cell variances tended to be functions of the cell means (the larger the mean the larger the variance). This heterogeneity was a consistent feature of the trapping data and not an error of observation. To alleviate this problem the 3 replicate traps in each set were pooled. Pooled data were then transformed to  $\log_e (x + 0.1)$  to improve normality and homogeneity of variances. Since the known effect of this level of heterogeneity is to slightly increase the chance of a Type I error (Snedecor and Cochran, 1989), the analyses of variance were conducted with the more conservative significance level of  $\alpha = 0.01$ .

The length frequency of *P. multidentis* and *L. sebae* in each escape gap treatment are shown in Figures 7.1 and 7.2. Figure 7.1 shows an increasing size at capture of *P. multidentis* in relation to the number of escape gaps. Development of a logistic selectivity model indicates that the length of first capture for *P. multidentis* appears to increase with increasing number of treatments (Fig. 7.5). However, the data available in the 6 escape gap treatment are too few to make any sound conclusions. For example, the increased number of escape gaps may have actually increased escapement of *P. multidentis* of all sizes. In contrast, Figure 7.2 shows that escape gaps have no influence on the size frequency distribution of *L. sebae*.

Results from the three factor ANOVAs were carried out on the CPUE data for all fish caught and the two key species, *P. multidentis* and *L. sebae* are summarised in Table 7.1. The catch rate of all the fish caught was significantly different among escape gap treatments, with significantly more fish caught in control traps (Tukey HSD: Control > [2 = 6]). There was also a significant location  $\times$  treatment interaction. The

control trap catch rate in the Broome area was significantly higher than all other treatments. The Broome offshore area is an area where other lutjanid species are an important component of the trap catch (see Section 1).

The catch rates of each species were not significantly different between escape gap treatments. However, significant diel differences were found for all the fish caught, *P. multidentis* and to a lesser extent *L. sebae* (Fig. 7.3 and 7.4), reflecting both a strong diurnal catch rate which is in part attributable to the greater of trap sets undertaken during the day.

In summary, the use of escape gaps significantly altered the catch rates of all fish but not the two key species in the fish traps within the locations sampled in the NDSF. There is no evidence to suggest that the use of escape gaps facilitates the escapement of small immature *L. sebae* (< 450 mm). In contrast, the use of escape gaps for *P. multidentis* suggests that they may provide a mechanism for the release of small, immature fish (< 460 mm FL). This aspect of the study needs to be investigated further to determine whether it has general applicability throughout the fishery. However, there may be a trade-off in the number of other species landed. Results to date indicate that while the escape gaps may limit the capture of immature goldband snapper, they also preclude the capture of a number of smaller species, which are also economically important to the fishers of the NDSF.

**Table 7.1**

Summaries of three factor analyses of variance of CPUE data for all fish caught, *P. multidentis*, and *L. sebae*.

Source of Variation	d.f.	Total fish			<i>P. multidentis</i>			<i>L. sebae</i>		
		F-ratio	MS	F	p	MS	F	p	MS	F
Location	1, 140	0.09	0.15	0.70	0.02	0.24	0.63	1.38	7.56	0.007
Diel	1, 140	46.4	76.3	0.000	0.87	13.09	0.0004	0.89	4.89	0.029
Treatment	2, 140	7.24	11.9	0.000	0.02	0.31	0.74	0.00	0.01	0.99
Location × Diel	1, 140	2.09	3.43	0.07	0.02	0.32	0.57	0.17	0.93	0.34
Location × Treatment	2, 140	3.52	5.80	0.004	0.07	1.10	0.33	0.01	0.06	0.94
Diel × Treatment	2, 140	0.06	0.09	0.91	0.01	0.17	0.84	0.02	0.14	0.87
L × D × T	2, 140	0.22	0.35	0.70	0.07	1.00	0.37	0.02	0.10	0.90
Residual		0.61	---	---	0.07	---	---	0.18	---	---

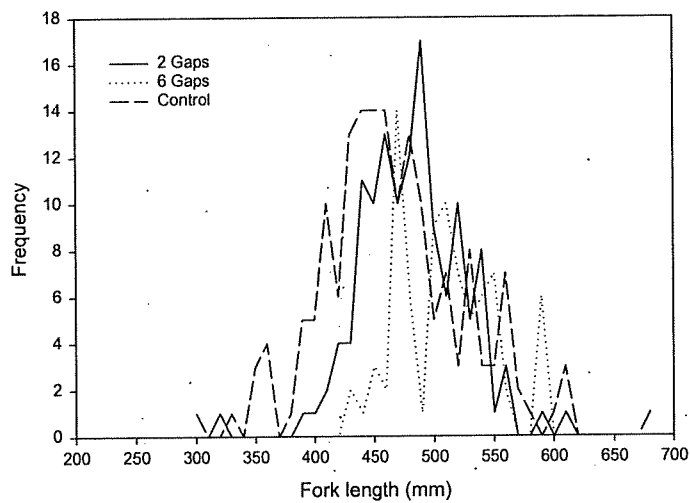


Figure 7.1: Length frequency of *P. multidentis* by 10 mm length classes for each of the escape gap treatments.

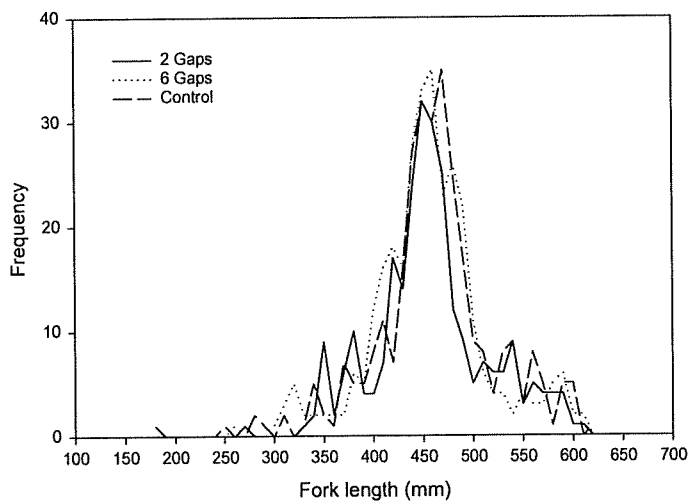


Figure 7.2: Length frequency of *L. sebae* by 10 mm length classes for each of the escape gap treatments.

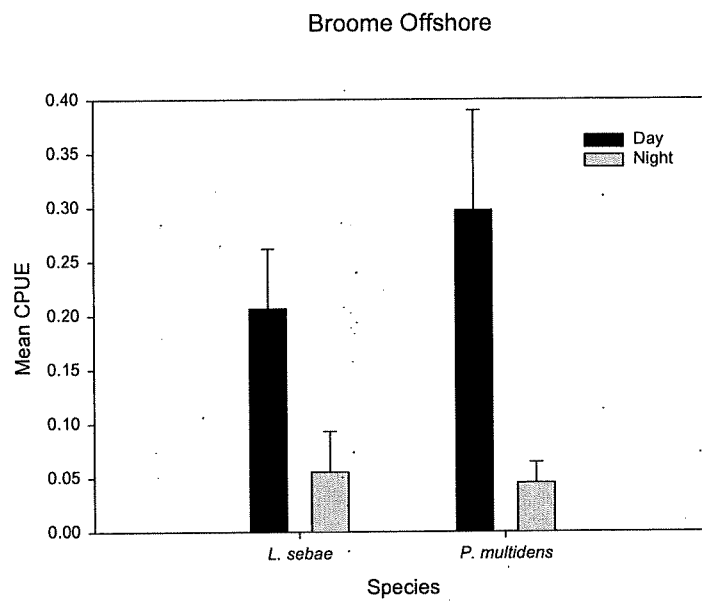


Figure 7.3: Diel catch rates of each of the key species in the Broome region of the NDSF.

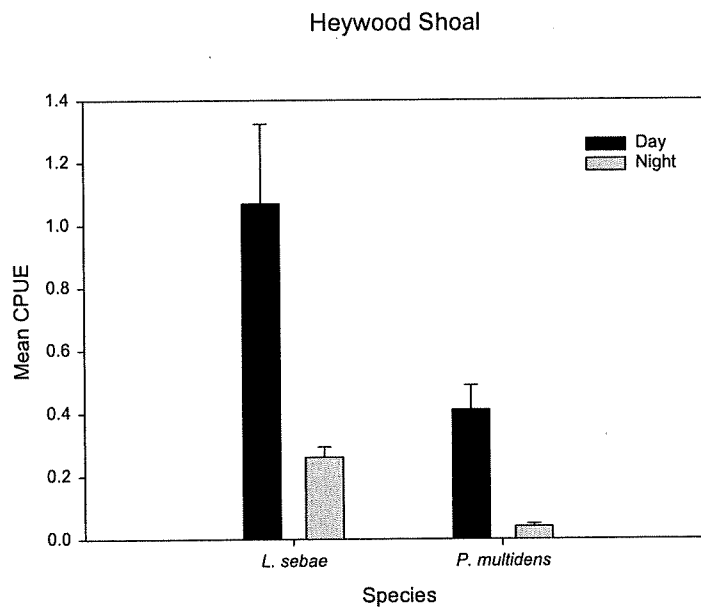


Figure 7.4: Diel catch rates of each of the key species in the Heywood Shoal region of the NDSF.

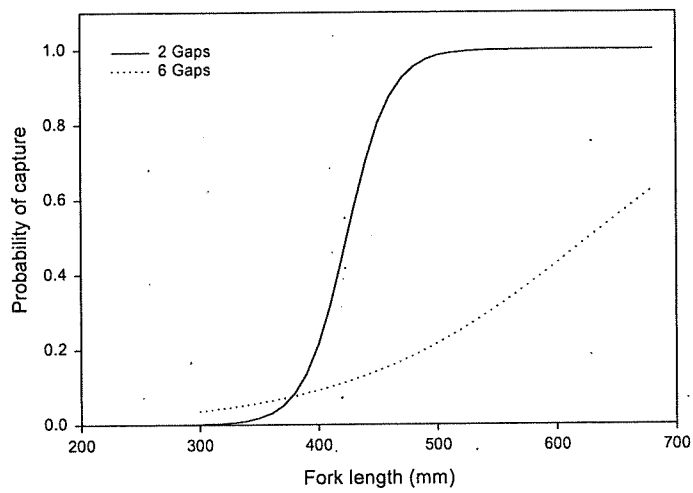


Figure 7.5: Logistic model of selectivity of each of the escape gap treatments for *P. multidentis* in reference to the control.

## Discussion

The optimum fishing mortality rate of long-lived species such as *P. multidentis* and *L. sebae* is low and is considered to be less than the natural loss rate or natural mortality rate. Recent work by Patterson (1992) and Walters (in press) indicates that the optimum fishing mortality rate is in the range of 0.5 to 0.67 times the natural mortality rate. Therefore, it is important that a large standing stock of these fish is conserved as part of the management plan for the demersal fish resources of the NDSF.

The fishery management plan for the NDSF incorporates single-species management approaches by attempting to optimise the exploitation of the most desirable species. The two most desirable species in the NDSF are *P. multidentis* and *L. sebae* (comprising over 70% of the total catch in 1999). The NDSF management plan utilises an individual transferable effort (ITE) system to control harvest rates of the key species. The basis for adopting management controls and hence limiting harvest rates is to ensure the continued sustainable exploitation of the demersal fish resources of the NDSF. Limiting harvest rates to levels at or below accepted international reference points attempts to ensure adequate egg production (preservation of spawning stock biomass) and maintenance of recruitment.

The results of this study indicate that the exploitation levels of the two key species are presently considered to be above optimum levels. Estimates of  $F_{opt}$  and the results of YPR and EPR analyses indicate that the optimum fishing mortality rate for the key species in the NDSF is low. The estimates of  $F$  derived from age based catch curves for each of the key species in the NDSF indicates that harvest rates are currently above optimum levels.

The long life span, relatively slow growth, low rates of natural mortality, large size and age at maturity in association with the low estimate of  $F_{opt}$  indicates that the NDSF populations of *P. multidentis* and *L. sebae* cannot sustain high harvest rates. In addition, the ability of fishers in the NDSF to harvest both species at small sizes and several age classes below the age-at-maturity of 8 years places them at risk of over-exploitation. Care must be taken to ensure the ratio of mature to immature fish in the catch is not too low. The level of exploitation of both these species in the NDSF needs

to be carefully monitored. Furthermore, the degree of survivorship of fish below the minimum legal size that are released needs to be investigated and considered in future assessments.

Monitoring of the age structure of the *P. multidentis* and *L. sebae* populations in the NDSF is likely to be a much more sensitive indicator of the effects of exploitation than monitoring of catch and effort data in isolation. This is due to the likelihood that catch rate data is not a good indicator of stock abundance, as the catch rate may well be affected by hyperstability, where high, stable CPUE may persist long after declines in overall population abundance have occurred. Both *P. multidentis* and *L. sebae* are targeted in aggregations over hard bottom areas that can be easily located on an ongoing basis by fishers using global navigation systems and high intensity depth sounders. Although the number of these aggregations may well decrease with persistent fishing pressure, catch rates experienced on the remaining individual aggregations are likely to remain relatively high and not reflect the overall decline in abundance of the stock.

The individual transferable effort allocation system and estimation of a sustainable target catch in the NDSF is still dependent to a large extent on the catch and effort data provided on the statutory monthly returns of fishers. The Kimberley region in north-western Australia is remote from major cities and hence the cost of conducting independent research in this region is very high. As such there is a critical reliance on fishers to provide accurate data regarding their catch details and the effort expended to land that catch. However, the lack of support by fishers with the voluntary logbook program has meant that there are limited data available for a spatial assessment of the demersal fish stocks of the NDSF. More robust stock assessments can only be undertaken once fishers agree to provide detailed daily catch and effort data via the voluntary logbook program.

Management of multi-species demersal fisheries resources is a complex issue. It is important to obtain catch information on a species-specific basis. Despite their high cost fishery independent surveys may be required on an ongoing basis to accurately assess and monitor the demersal fish stocks of the NDSF in the absence of adequate fishery dependent data.

The spawning behaviour of *P. multidentis* and *L. sebae* are quite different. In *P. multidentis* the size of the testes in the breeding season is much larger, greater than 25% of the corresponding ovary mass. Therefore, due to the large relative size of the testes we conclude that *P. multidentis* forms multiple male-multiple female spawning groups during the spawning season, with males trying to spawn with as many females as is practicable (sperm is not limited). In contrast, the size of the testes of *L. sebae* in the breeding season is very low (ca. 5% of the ovary mass), suggesting competition for sperm (sperm limitation). The testes of *L. sebae* are not large enough to produce the sperm output required for a multiple male-multiple female spawning system such as that evident for *P. multidentis*. Therefore, we conclude that *L. sebae* are pair spawners, producing only enough sperm to ensure fertilisation. The significant differential growth evident between sexes, with males larger than females suggests that males may be behaviourally dominant during the spawning season. Males may initiate sex and prevent competing males from spawning with their female partner.

Pair spawners such as *L. sebae* are very susceptible to overfishing. Fishing activity may disrupt the breeding system by selectively removing large behaviourally dominant spawning males (the female to male sex ratio of *L. sebae* is 1.5:1). This can result in sperm limitation or reduced spawning opportunities for females. Either or both of these factors reduce reproductive success.

Furthermore, *P. multidentis* and *L. sebae* are contrasting species in terms of their resilience to capture and handling stress. The capture of *P. multidentis* from depths of 60 metres or greater results in a high mortality of fish from physoclistous over-expansion injuries and hence there is a low probability of survival of any fish returned to the sea. In contrast, *L. sebae* rarely suffers from embolism injuries and therefore is more likely to survive release after capture. The high mortality rate associated with the release of *P. multidentis* indicates that size limits are not an effective management tool for this species. This poses a problem for fishery managers. The apparent ability of the escape gaps to reduce the capture of *P. multidentis* smaller than the size at first reproduction however needs further investigation, based on the initial work undertaken. In contrast, manipulations of the size at first capture through regulation of escape gaps on fishing gear appears limited for *L. sebae*.

Given the low production potential of the key demersal fish species in the NDSF, harvest strategies of low frequency or low intensity are also suggested for the sustainable exploitation of these fish stocks in the wider Indo-Pacific region. The demersal fish resources in the NDSF is currently being managed with an innovative total allowable effort / individually transferable effort unit system, however the highly mobile, efficient and wide ranging capacity of the NDSF fleet may require more complex management arrangements to maintain future breeding stock levels.

Yield and egg per recruit models indicate that yield to fishers can be increased if the age at first capture can be delayed several years. However, as a consequence of the apparent low survival rate for released (tagged) fish in the fishing depths of the NDSF fleet, the traditional use of legal minimum sizes to increase survival to spawning sizes is not a practical option. Inclusion of targeted spatial or temporal closures within the effort management framework is however likely to be a useful mechanism to maintain spawning stock biomass and protect against recruitment overfishing.

### **Acknowledgements**

We gratefully acknowledge financial support from the Fisheries Research and Development Corporation and logistical support from Department of Fisheries, Government of Western Australia.

The core project team consisted of Dr. S. Newman, Mr. R. Steckis, Mr. I. Dunk and Mr. J. Jenke. Mr. B. Rome, Mr. A. Kitchingman, Ms. P. Williamson and Ms. G. Nowara provided additional project support. Mr. R. Steckis was primarily responsible for the maintenance of the databases used for this project, logbook development and collection, supervision of data entry, database validation and the processing and analysis of gonad tissues. Mr. I. Dunk was primarily responsible for development of ageing protocols, age validation, otolith reading and interpretation in conjunction with the principal investigator. Mr. Jerry Jenke was responsible for sample processing, industry liaison, otolith sectioning, sampling aboard industry vessels and general logistical support throughout all phases of the project. Ms. P. Williamson significantly assisted with the analysis of the trap selectivity data.

Discussions with Dr. M. Mackie, Dr. Y. Cheng, Dr. N. Hall, and Dr. J. Penn greatly improved this final report. The project team wish to thank the fishers of the Northern Demersal Scalefish Fishery for the provision of catch samples and the fish wholesalers of Perth and Broome, in particular Attadale Seafoods Pty. Ltd., Kailis Bros., New West Foods (W.A.) Pty. Ltd., Festival Fish Wholesalers and Fortescue Seafoods of Broome for access to the landed catch of fishers from the NDSF.

### **Benefits**

The primary beneficiaries of this project will be the commercial fishers of the NDSF. However, the demographic parameters derived for *L. sebae* have application to the management of this important recreational fish species. The direct benefit to fishers and the wider community will be the sustainability of the demersal fish resources of the NDSF.

### **Further Development**

Otolith weight may provide a cost effective and rapid method of generating age structure information. The utility of generating otolith weight-age keys for stock assessment purposes needs to be evaluated. For example, it may be possible to use otolith weight-age keys for a number of years (eg. 3 years) before there is a need for re-validation of the otolith weight-age key. Ongoing development of the age-structured population dynamics models for *P. multidens* and *L. sebae* for stock assessment purposes is also required. Assessment of larger escape gaps may also be beneficial.

The current effort management model in the NDSF and the associated decision rules need to be reviewed and re-evaluated in light of the results gathered from this project. The most important task in this review process is to determine an appropriate target total allowable effort (TAE) for the fishery.

The information provided in this report will be presented to both industry and fishery managers for their consideration.

## Conclusions

The optimum fishing mortality rate for *P. multidentis* and *L. sebae* based on estimates of the natural loss rate (natural mortality rate) appears low. This work provides the basis for the development of a detailed age-structured model of the NDSF populations of *P. multidentis* and *L. sebae*. The age structured stock assessment model being developed combines both age-structure data over a number of years with the history of catch removals from the area of the fishery. The NDSF populations of *L. sebae* and *P. multidentis* may be particularly vulnerable to over-exploitation given there is a mismatch between the age-at-first capture and the age-at-maturity. The optimal harvest rate is most sensitive to the level of vulnerability (age-at-recruitment to the fishery), in relation to the size-at-maturity.

The results of this report indicate a need for ongoing, but improved protection of the spawning stock biomass of each of the key target species. The methods available to provide this protection of the spawning stock biomass of each of the target species include targeted spatial closures, closed seasons, effort reductions or a combination of these methods. It should be noted that population recovery times for long-lived species of this type can be considerable.

The relatively stable  $Z$ 's (total mortality rates) from the catch curves reflect long-term average mortality rates. The impact of the domestic fishery is relatively recent, and as such has only fully impacted the ascendance of the young age classes (up to 8+) in the population. In a fishery where gear controls are of limited effect in regulating the size/age at first capture, traditional management practices such as the introduction of legal minimum sizes are not a practical option. More innovative management strategies are required in order to safeguard against recruitment overfishing. Inclusion of targeted spatial or temporal closures within the effort management framework is likely to provide a useful mechanism to safeguard against recruitment overfishing. The results from this project will provide the basis for a detailed age-structured stock assessment of the *P. multidentis* and *L. sebae* populations in the NDSF and thus determine whether the spawning stock biomass these fishes has been reduced to a level that may be of concern

to fishery managers (i.e. are the stocks of the two key target species currently fished above optimum levels).

## References

- Beamish, R.J. and Fournier, D.A. 1981. A method for comparing the precision of a set of age determinations. *Can. J. Fish. Aquat. Sci.* 38 (8): 982-983.
- Beverton, R.J.H. and Holt, S.J. 1957. On the dynamics of exploited fish populations. *Fish. Invest. Minist. Agric. Fish. Food (G.B.), Ser. 2 (19): 533p.*
- Brouard, F., Grandperrin, R. Kulbicki, M. and Rivaton, J. 1984. Note on observations of daily rings on otoliths of deepwater snappers. *ICLARM Translations No. 3: 8p.*
- Cerrato, R.M., 1990. Interpretable statistical tests for growth comparisons using parameters in the von Bertalanffy equation. *Can. J. Fish. Aquat. Sci.* 47 (7): 1416-1426.
- Collins, L.A., Johnson, A.G. and Keim, C.P. 1996. Spawning and annual fecundity of the red snapper (*Lutjanus campechanus*) from the northeastern Gulf of Mexico, pp. 174-188. In Arreguin-Sanchez, F., Munro, J.L., Balgos, M.C. and Pauly, D. (Eds.). 1996. *Biology, fisheries and culture of tropical groupers and snappers. ICLARM Conf. Proc. 48: 449p.*
- Davis, T.L.O. and West, G.J. 1992. Growth and mortality of *Lutjanus vittus* (Quoy and Gaimard) from the North West Shelf of Australia. *Fish. Bull. (US)* 90 (2): 395-404.
- Edwards, R.C.C. 1985. Growth rates of Lutjanidae (snappers) in tropical Australian waters. *J. Fish. Biol.* 26: 1-4.
- Gulland, J.A., 1970. The fish resources of the ocean. *FAO Fish. Tech. Pap.* 97: 425p.
- Hart, A.M. and Russ, G.R. 1996. Response of herbivorous fish to crown of thorns starfish *Acanthaster planci* outbreaks. III. Age, growth, mortality and maturity indices of *Acanthurus nigrofuscus*. *Mar. Ecol. Prog. Ser.* 136: 25-35.
- Hoenig, J.M. 1983. Empirical use of longevity data to estimate mortality rates. *Fishery Bulletin (U.S.)* 82 (1): 898-902.
- Kikkawa, B.S. 1984. Maturation, spawning, and fecundity of Opakapaka, *Pristipomoides filamentosus*, in the northwestern Hawaiian Islands, pp. 149-160. In Grigg, R.W. and Tanoue, K.Y. (Eds.). *Proceedings of the Second Symposium on Resource Investigations in the Northwestern Hawaiian Islands. Vol. 2. University of Hawaii Sea Grant College Program, Honolulu, Hawaii.*
- Laevastu, T. 1965. Fascicule 9. Section 4. Research on fish stocks. 51p. *Manual of methods in fisheries biology. FAO Manuals in Fisheries Science No. 1, FAO, Rome.*

Loubens, G., 1980. Biologie de quelques especes de poissons du lagon Neo-Caledonian. III. Croissance. Cahiers de l'Indo-Pacifique 2: 101-153.

Myers, R.A. and Mertz, G. 1998. The limits of exploitation: a precautionary approach. Ecol. Appl. 8 (Suppl. 1): S165-S169.

Newman, S.J., Williams, D.McB. and Russ, G.R. 1996. Age validation, growth and mortality rates of the tropical snappers (Pisces: Lutjanidae), *Lutjanus adetii* (Castelnau, 1873) and *L. quinquelineatus* (Bloch, 1790) from the central Great Barrier Reef, Australia. Marine and Freshwater Research 47 (4): 575-584.

Newman, S.J., Cappo, M. and Williams, D.McB. 2000a. Age, growth, mortality rates and corresponding yield estimates using otoliths of the tropical red snappers, *Lutjanus erythropterus*, *L. malabaricus* and *L. sebae*, from the central Great Barrier Reef. Fisheries Research 48 (1): 1-14.

Newman, S.J., Cappo, M. and Williams, D.McB. 2000b. Age, growth and mortality of the stripey, *Lutjanus carponotatus* (Richardson) and the brown-stripe snapper, *L. vitta* (Quoy and Gaimard) from the central Great Barrier Reef, Australia. Fisheries Research 48 (3): 263-275.

Nowara, G.B. and Newman, S.J. 1996. The Kimberley Demersal Scalefish Fishery: Extent and nature of the resource and the ability of a trap fishery to exploit it - Part 1: A history of fishing activities in the region. Final Report to the Fisheries Research and Development Corporation (FRDC) on Project No. 94/026. 104p.

Patterson, K. 1992. Fisheries for small pelagic species: an empirical approach to management targets. Reviews in Fish Biology and Fisheries 2 (4): 321-338.

Pearson, D.E. 1996. Timing of hyaline-zone formation as related to sex, location, and year of capture in otoliths of widow rockfish, *Sebastes entomelas*. Fish. Bull. 94 (1): 190-197.

Polovina, J.J. and Ralston, S. (Eds.) 1987. Tropical snappers and groupers : biology and fisheries management. Westview Press, Boulder, Colorado. 659p.

Richards, A.H. 1987. Aspects of the biology of some deepwater bottomfish in Papua New Guinea with special reference to *Pristipomoides multidens* (Day). Fisheries Research and Surveys Branch Report No. 87-01: 31p. Department of Primary Industry, Port Moresby, Papua New Guinea.

Ricker, W.E. 1975. Computation and interpretation of biological statistics of fish populations. Bull. Fish. Res. Board Can. 191: 382p.

Snedecor, G.W., and Cochran, W.G. 1989. Statistical Methods. Eighth Edition. Iowa State University Press, Ames, Iowa. 503p.

Stergiou, K.I. 1999. Intraspecific variations in size- and age-at-maturity for red bandfish, *Cepola macrophthalma*. *Env. Biol. Fishes* 54: 151-160.

Walters, C.J. in press. Stock assessment needs for sustainable fisheries management. *Bull. Mar. Sci.*

West, G. 1990. Methods of assessing ovarian development in fishes: a review. *Aust. J. Mar. Freshwater Res.* 41: 199-222.

### **Publications**

Newman, S.J. 1999. Red emperor, goldband snapper in Kimberley tagging program. **Western Fisheries**, Winter 1999, pp. 32-33.

**Appendix 1: Intellectual Property**

Nil.

**Appendix 2: Staff**

Dr. S. Newman  
Mr. R. Steckis  
Mr. I. Dunk  
Mr. J. Jenke  
Mr. B. Rome  
Mr. A. Kitchingman  
Ms. G. Nowarra

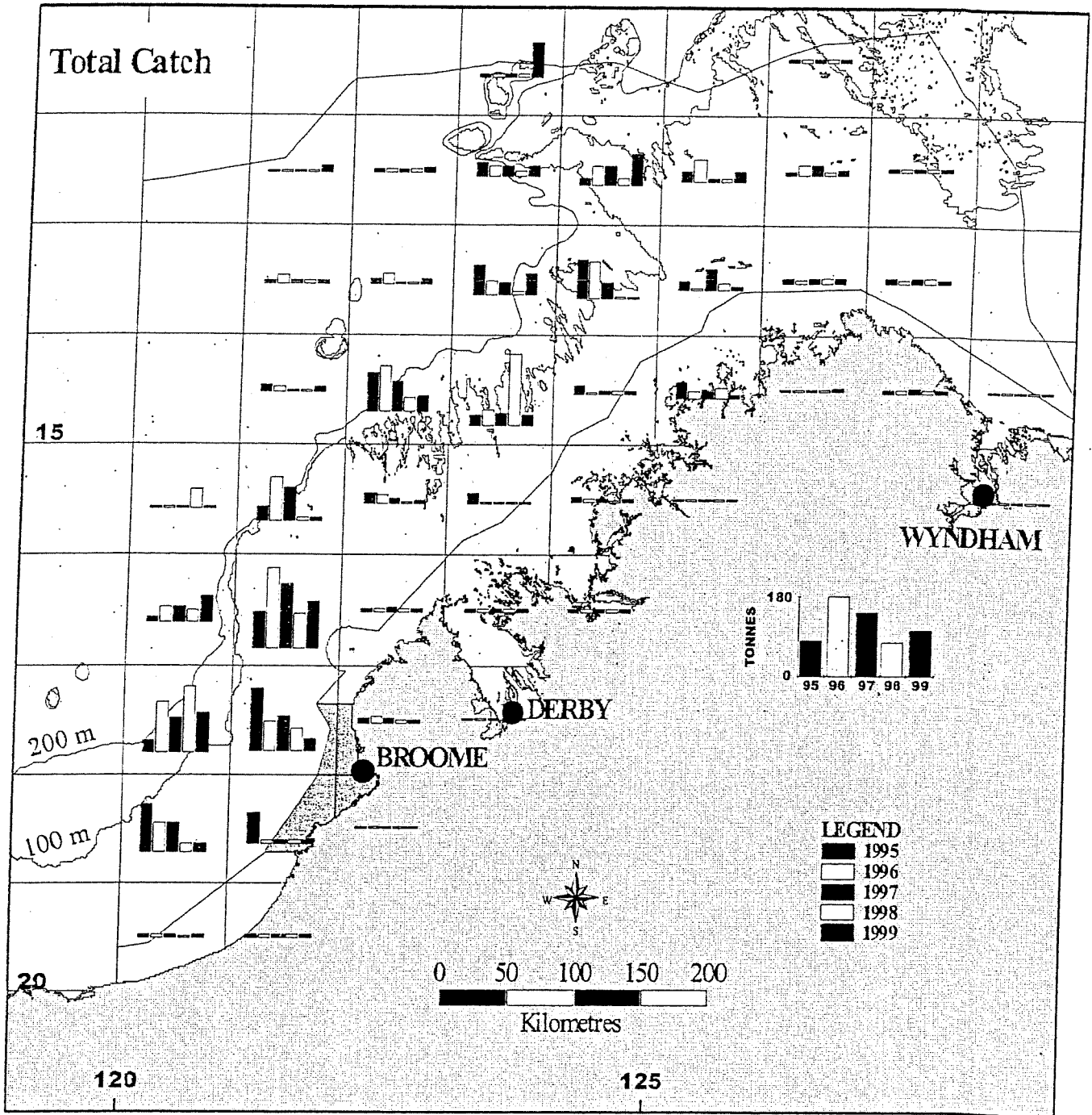


Figure A1. Spatial distribution of the catch of all species landed by both trap and line fishing vessels in the NDSF from 1995-1999.

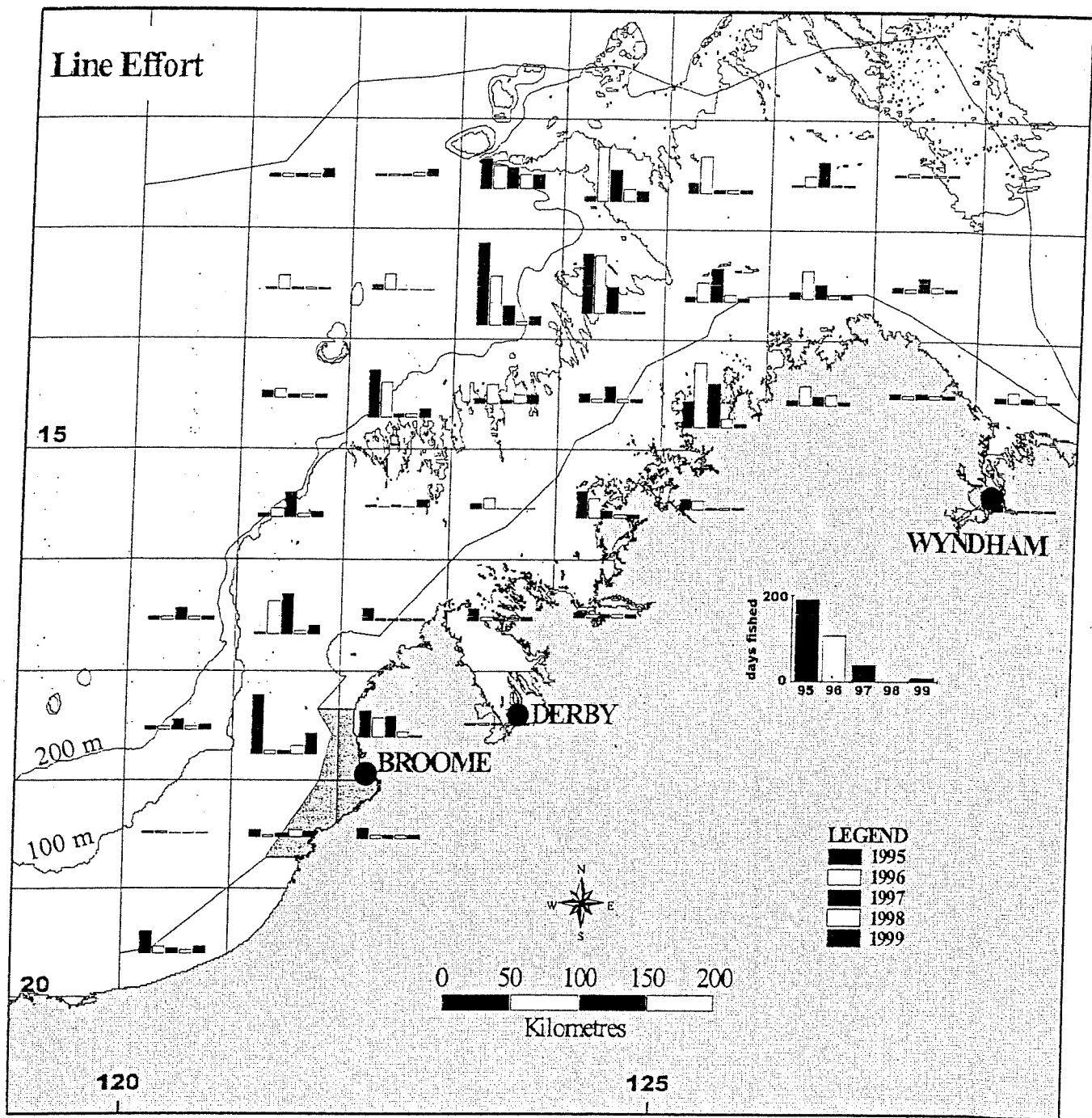


Figure A2. Spatial distribution of the effort expended by line fishing vessels in the NDSF from 1995-1999.

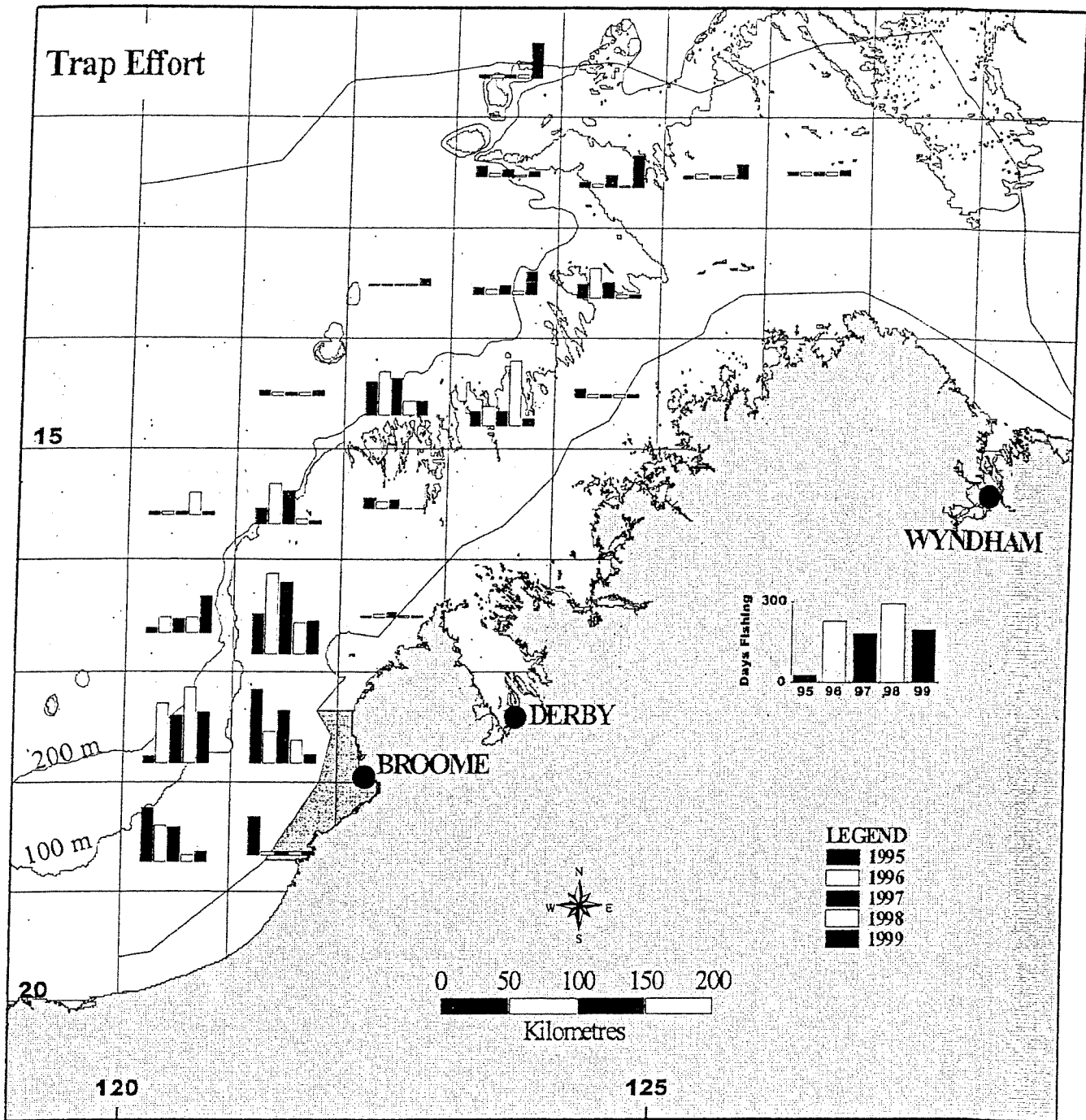


Figure A3. Spatial distribution of the effort expended by trap fishing vessels in the NDSF from 1995-1999.

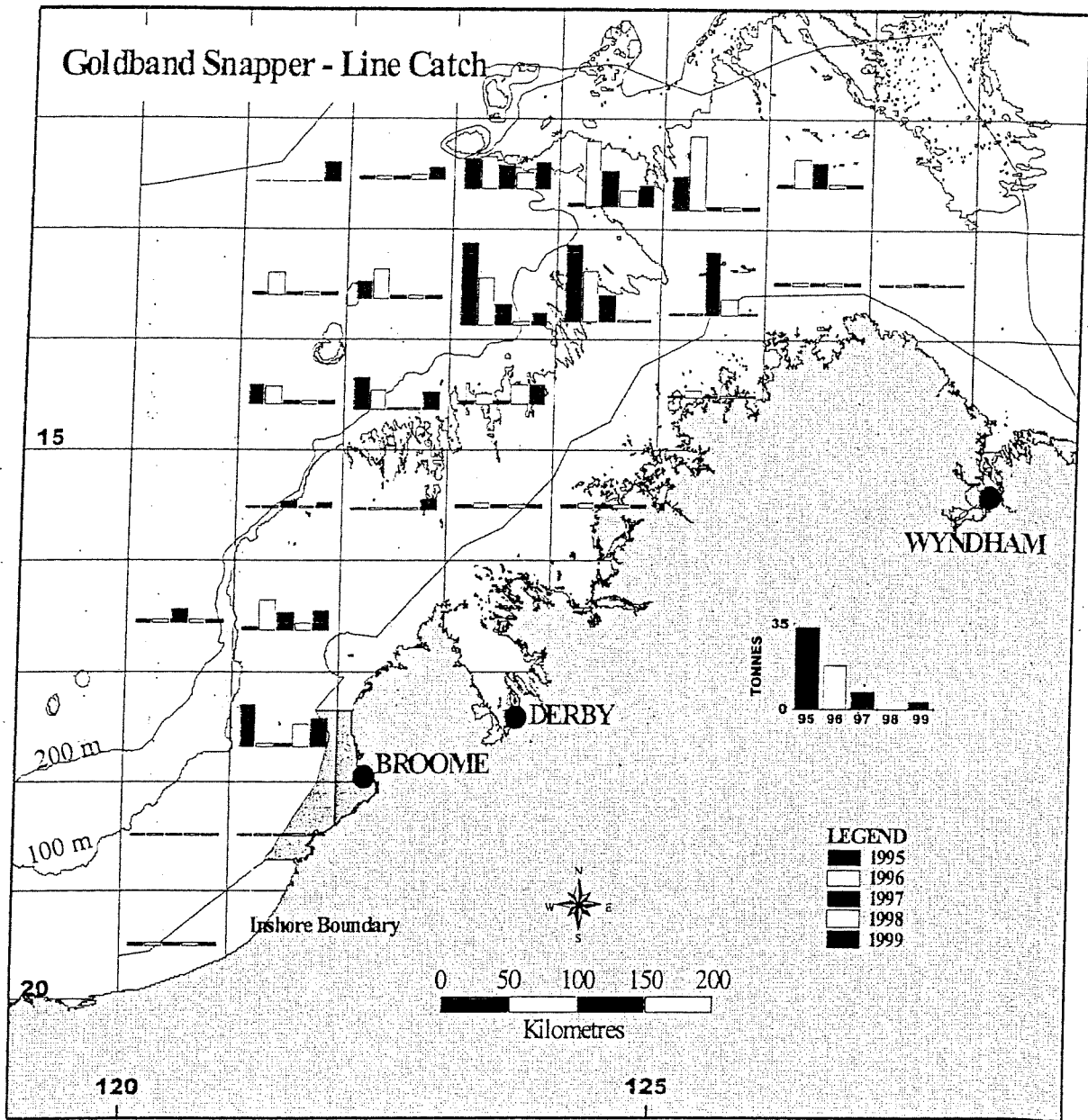


Figure A4. Spatial distribution of the catch of goldband snapper landed by line fishing vessels in the NDSF from 1995-1999.

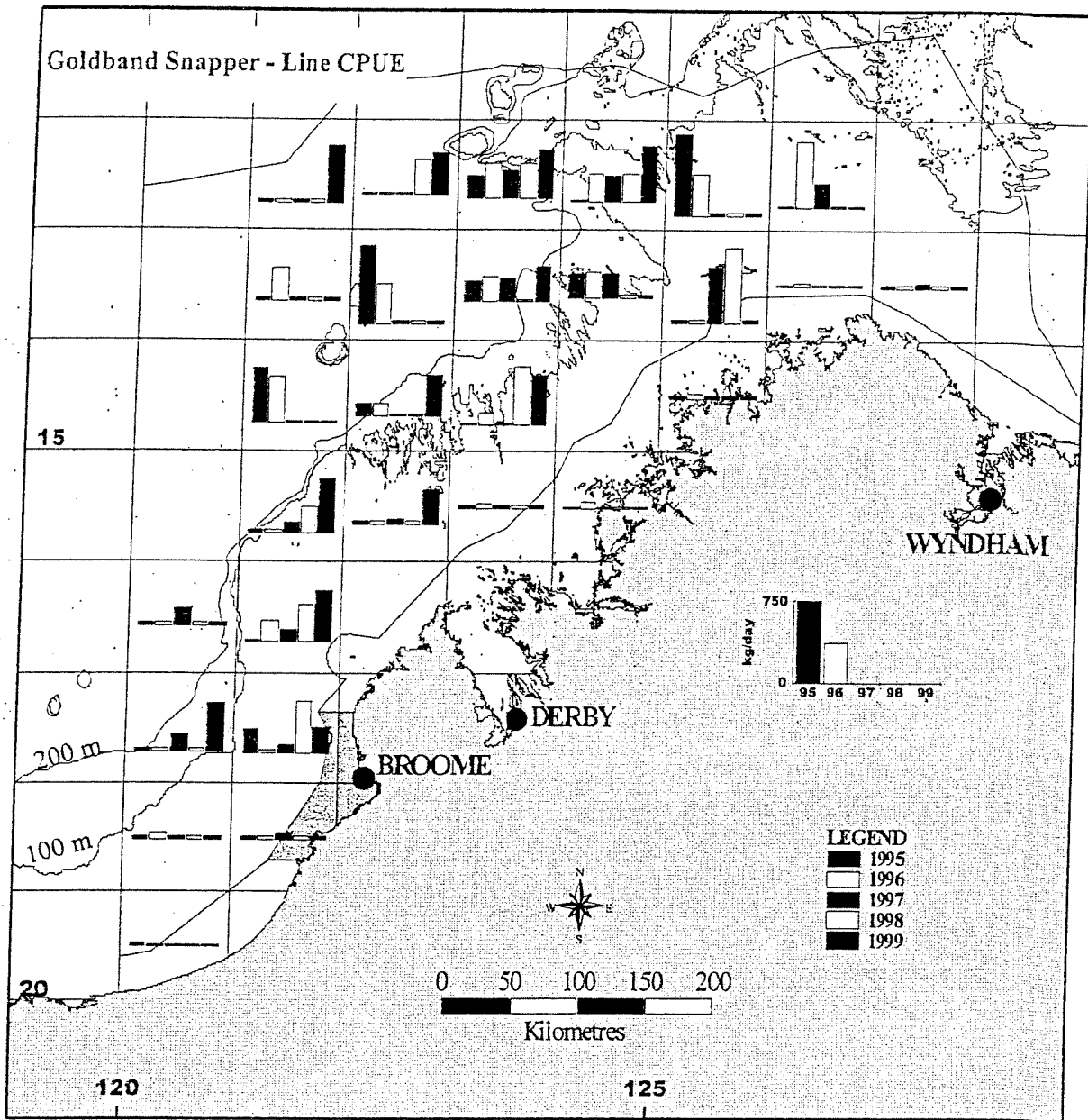


Figure A5. Spatial distribution of the CPUE of goldband snapper landed by line fishing vessels in the NDSF from 1995-1999.

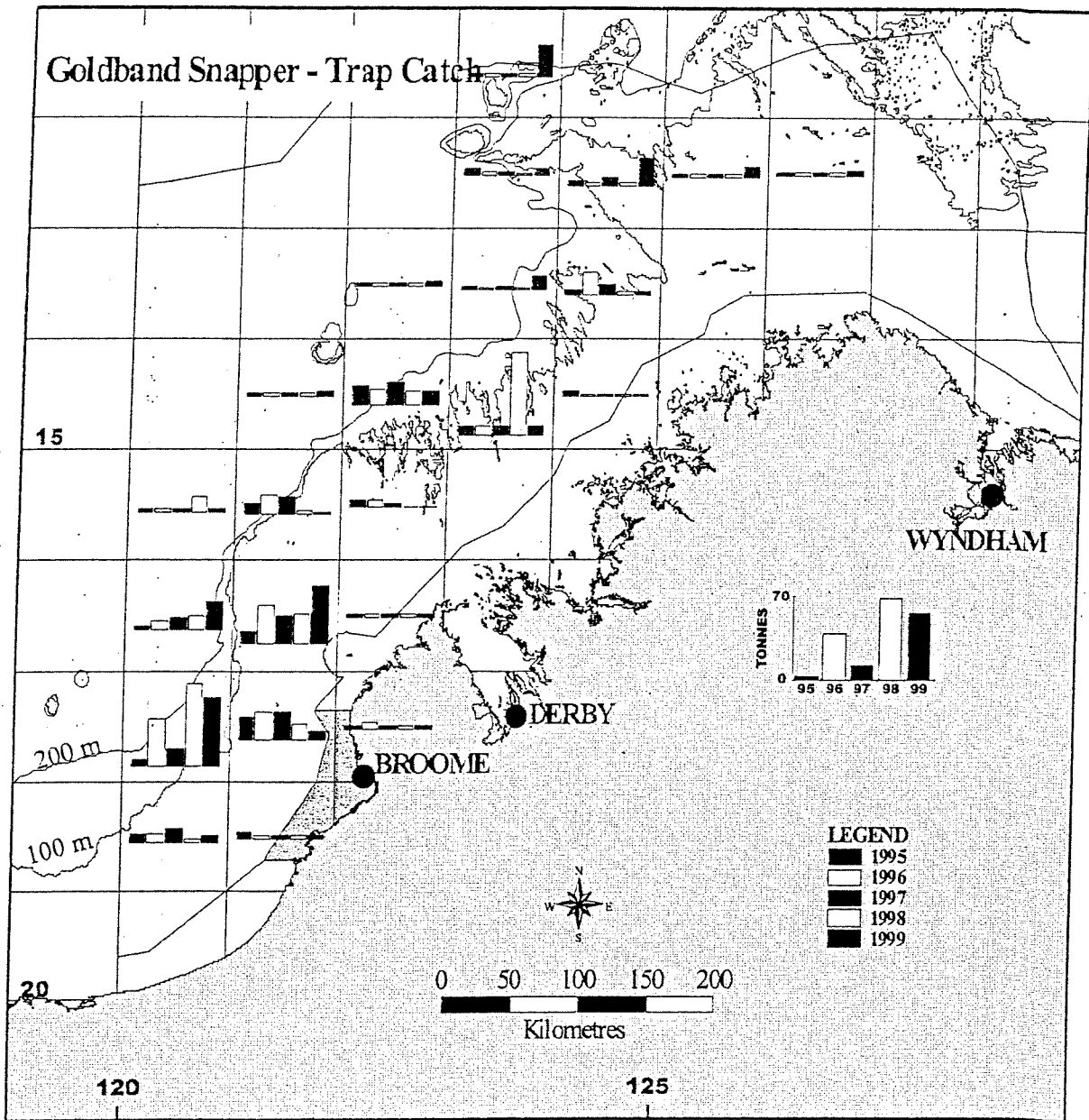


Figure A6. Spatial distribution of the catch of goldband snapper landed by trap vessels in the NDSF from 1995-1999.

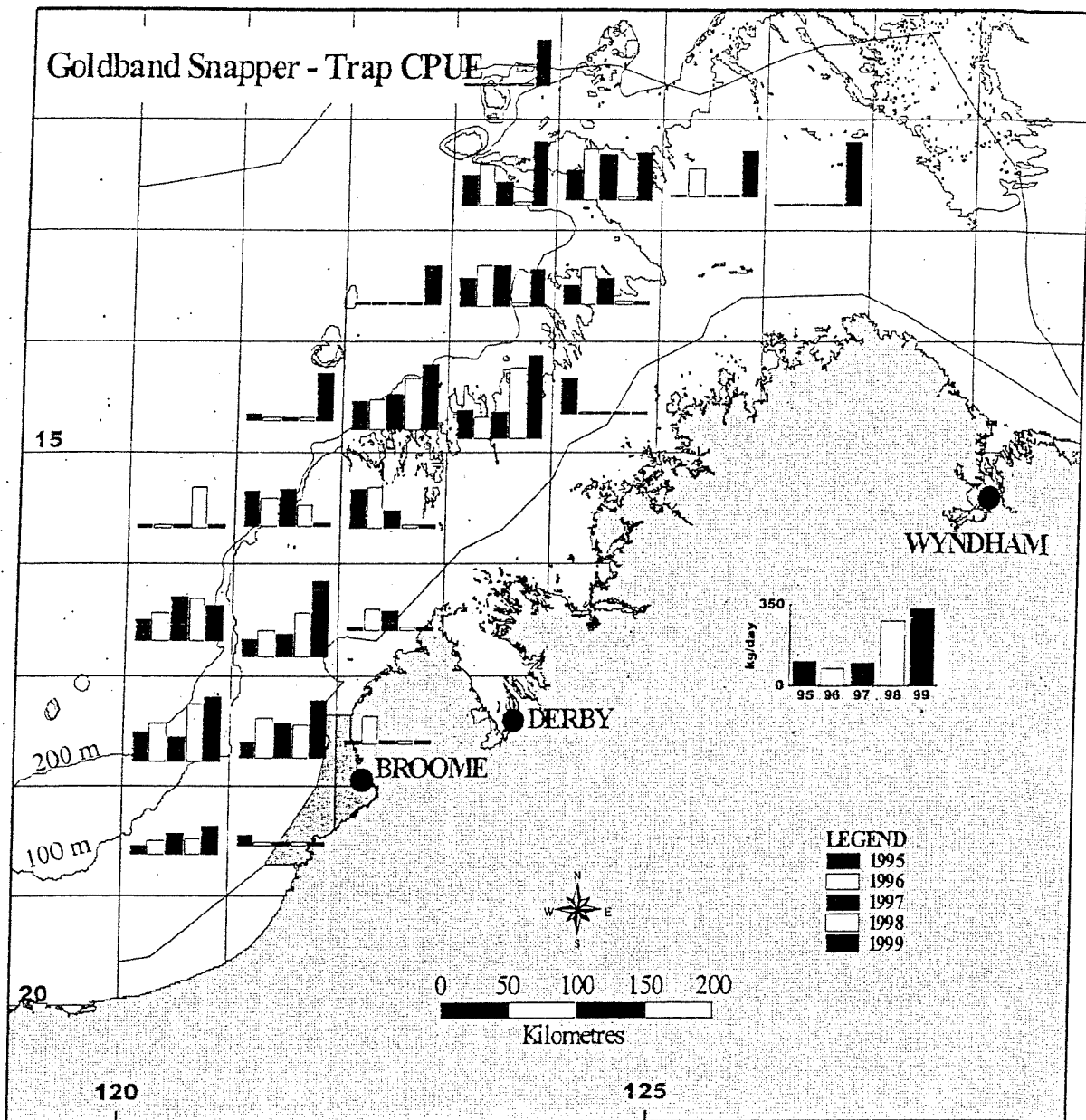


Figure A7. Spatial distribution of the CPUE of goldband snapper landed by trap vessels in the NDSF from 1995-1999.

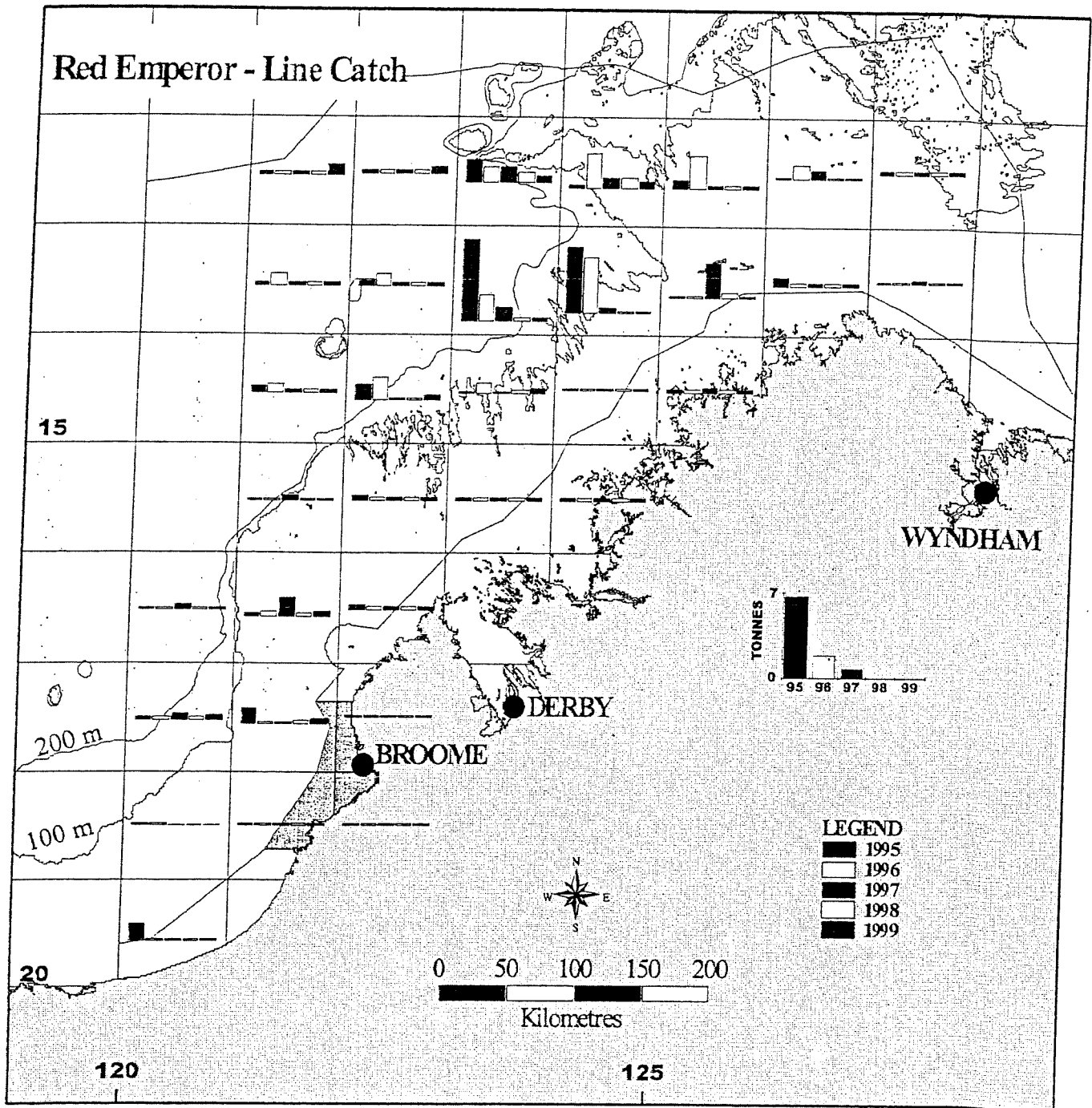


Figure A8. Spatial distribution of the catch of red emperor landed by line fishing vessels in the NDSF from 1995-1999.

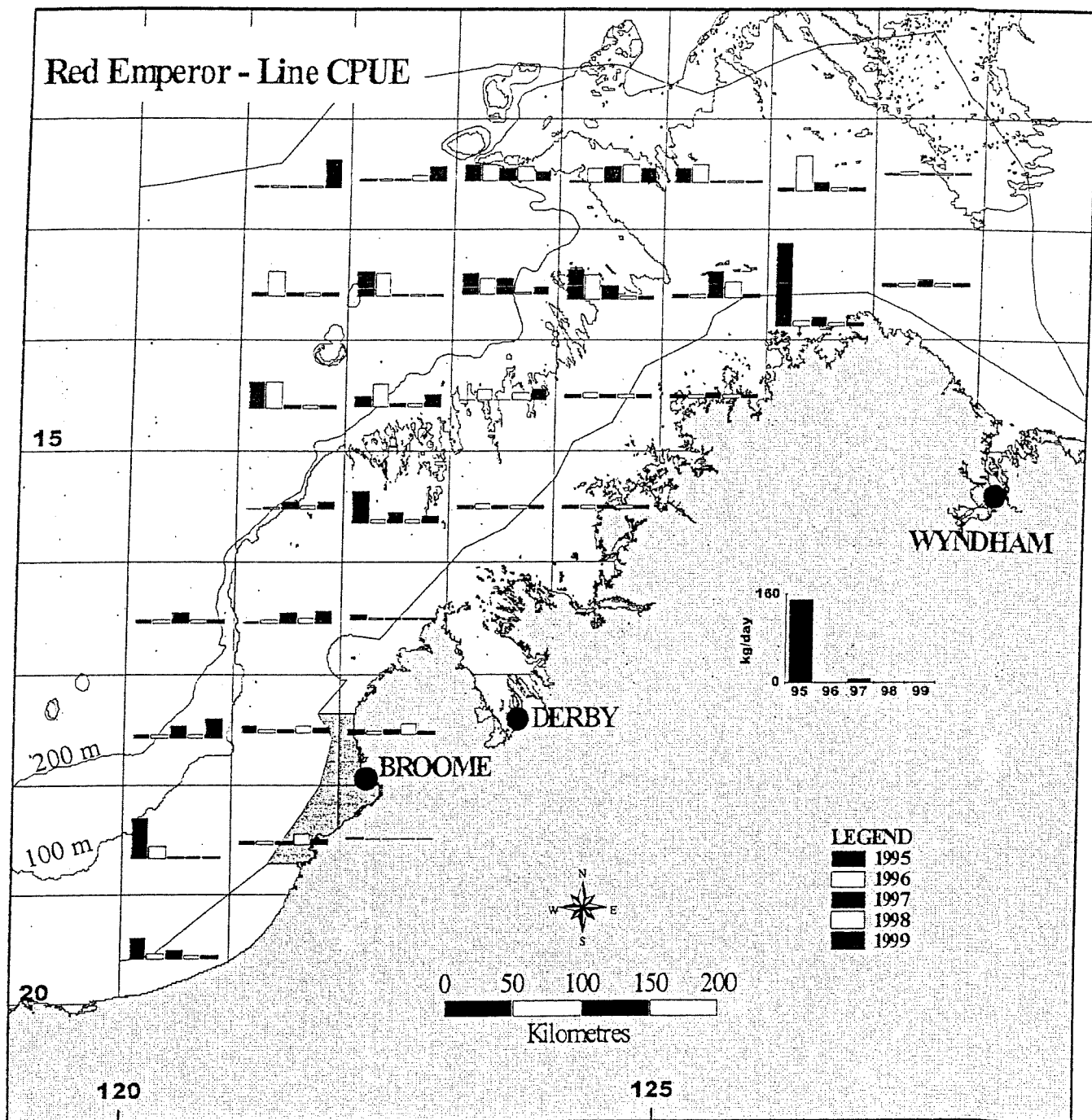


Figure A9. Spatial distribution of the CPUE of red emperor landed by line fishing vessels in the NDSF from 1995-1999.

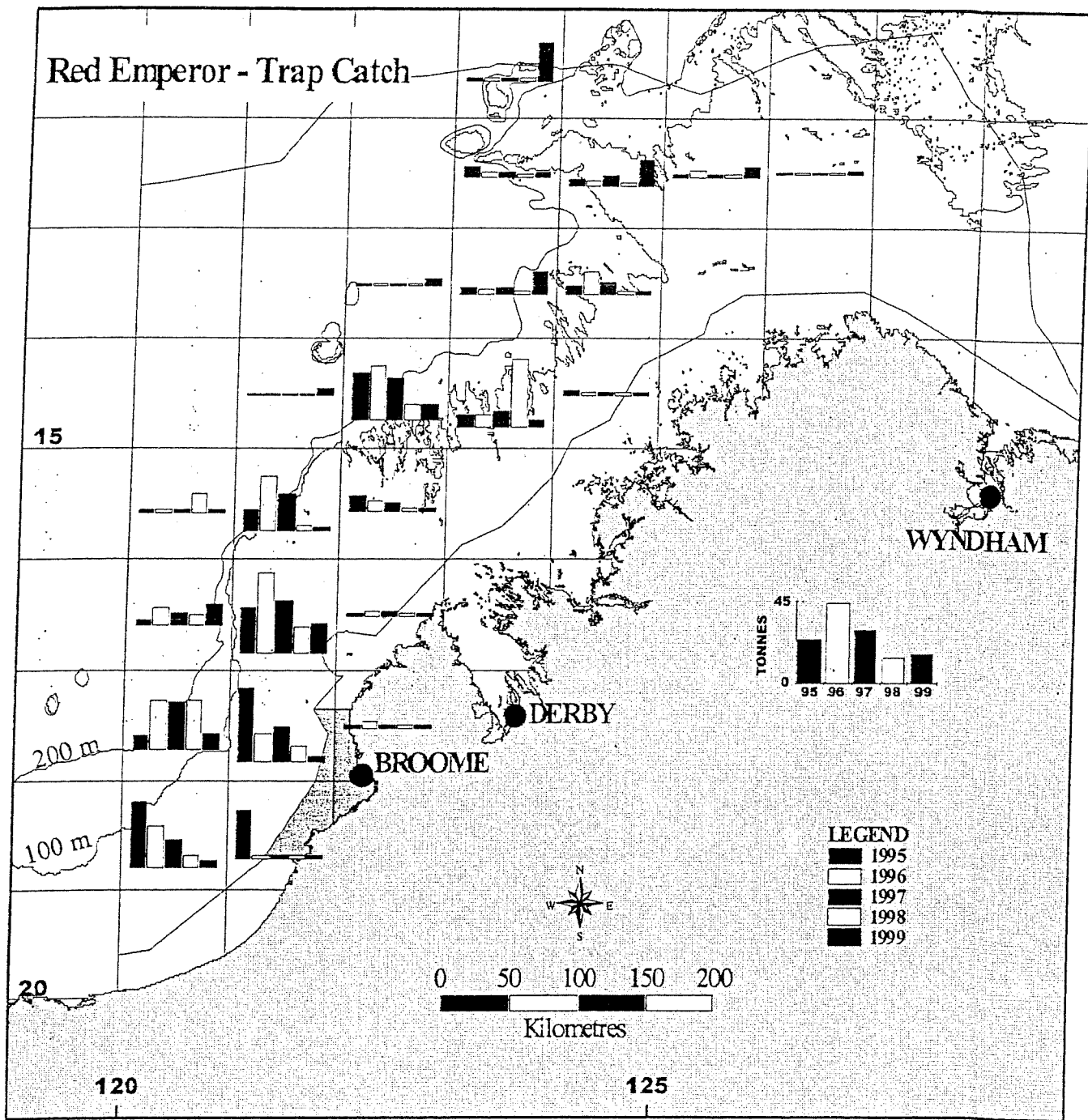


Figure A10. Spatial distribution of the catch of red emperor landed by trap fishing vessels in the NDSF from 1995-1999.

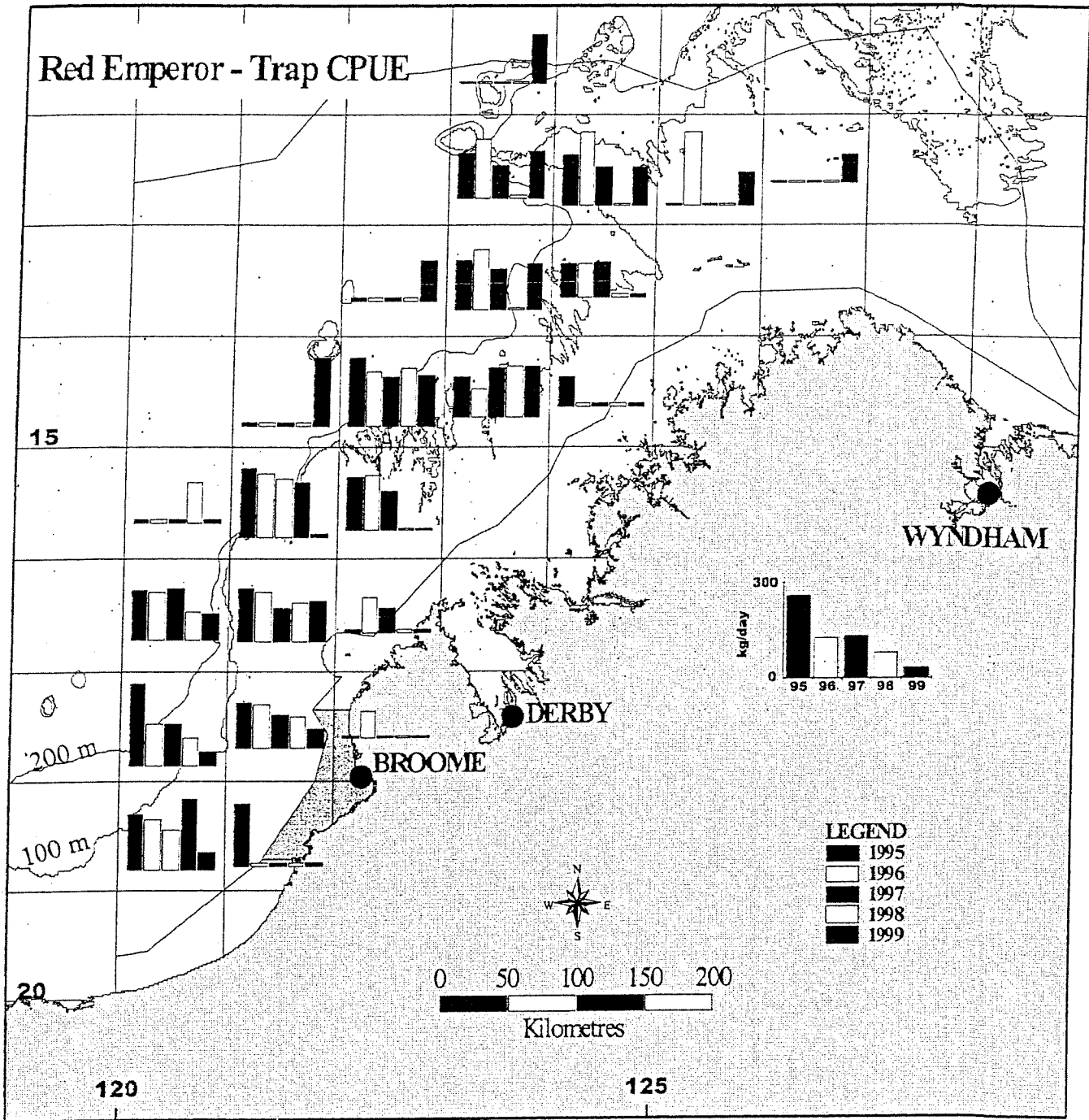


Figure A11. Spatial distribution of the CPUE of red emperor landed by trap fishing vessels in the NDSF from 1995-1999.

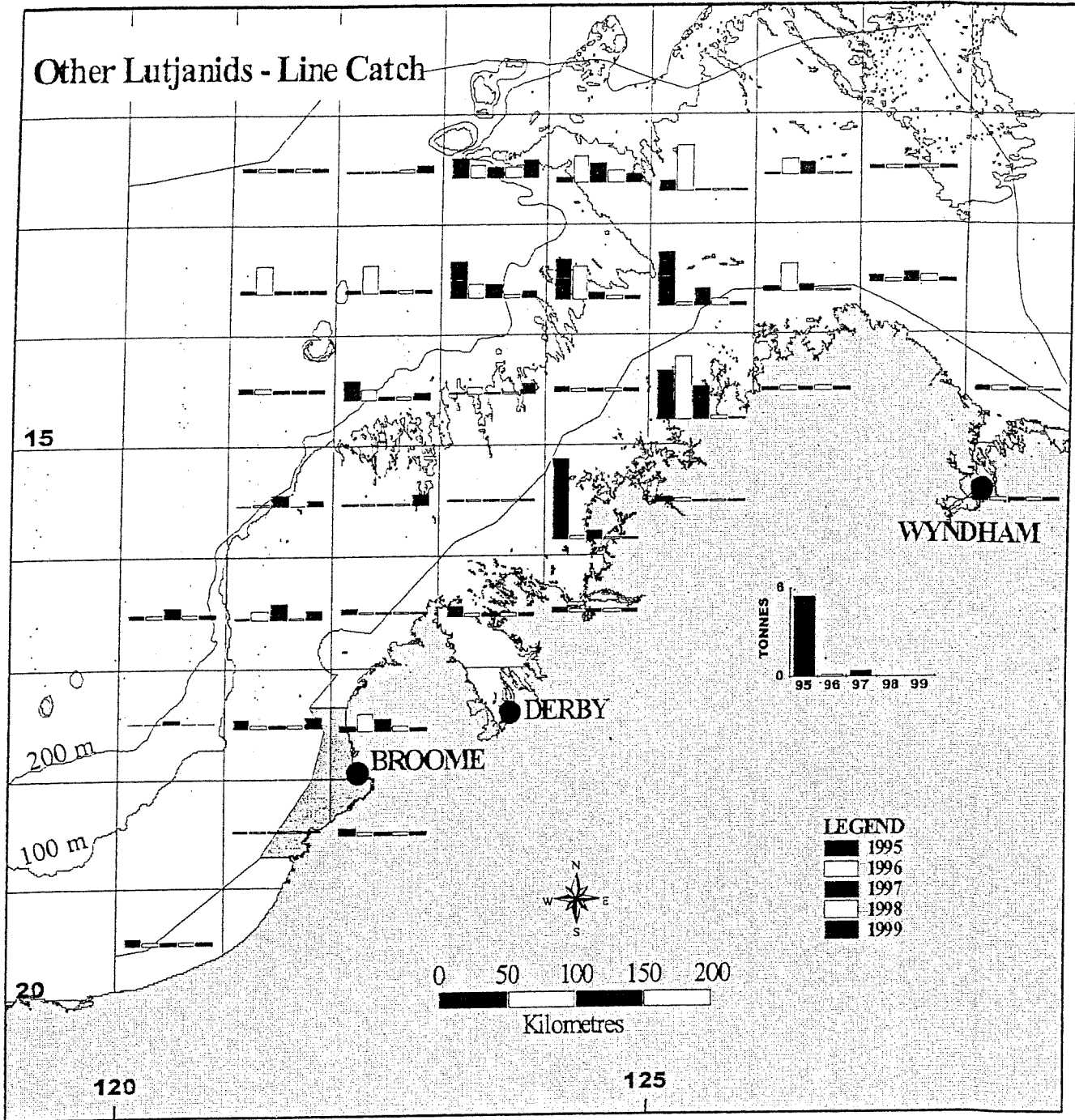


Figure A12. Spatial distribution of the catch of Lutjanids other than goldband snapper and red emperor landed by line fishing vessels in the NDSF from 1995-1999.

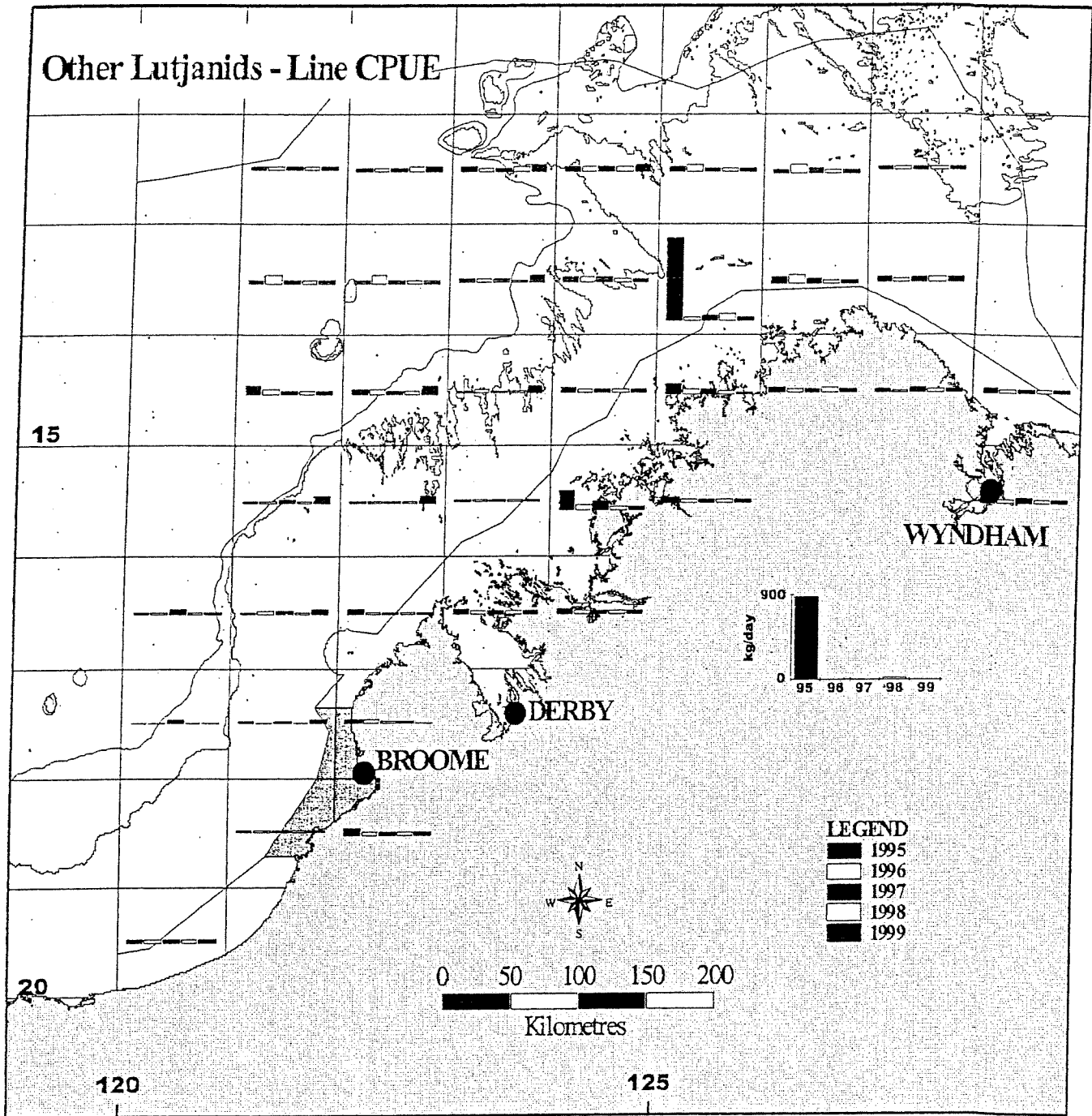


Figure A13. Spatial distribution of the CPUE of Lutjanids other than goldband snapper and red emperor landed by line fishing vessels in the NDSF from 1995-1999.

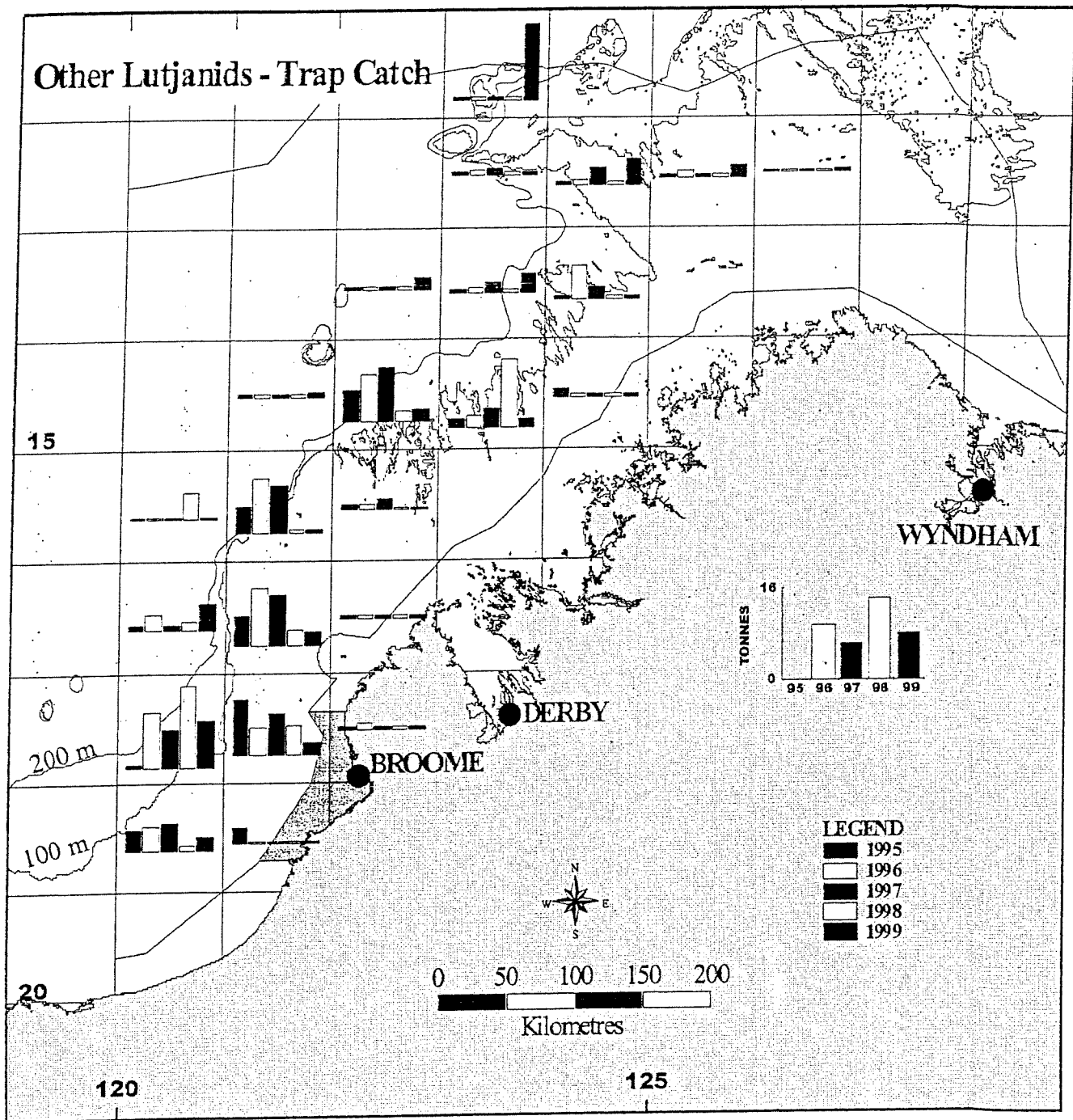


Figure A14. Spatial distribution of the catch of Lutjanids other than goldband snapper and red emperor landed by trap fishing vessels in the NDSF from 1995-1999.

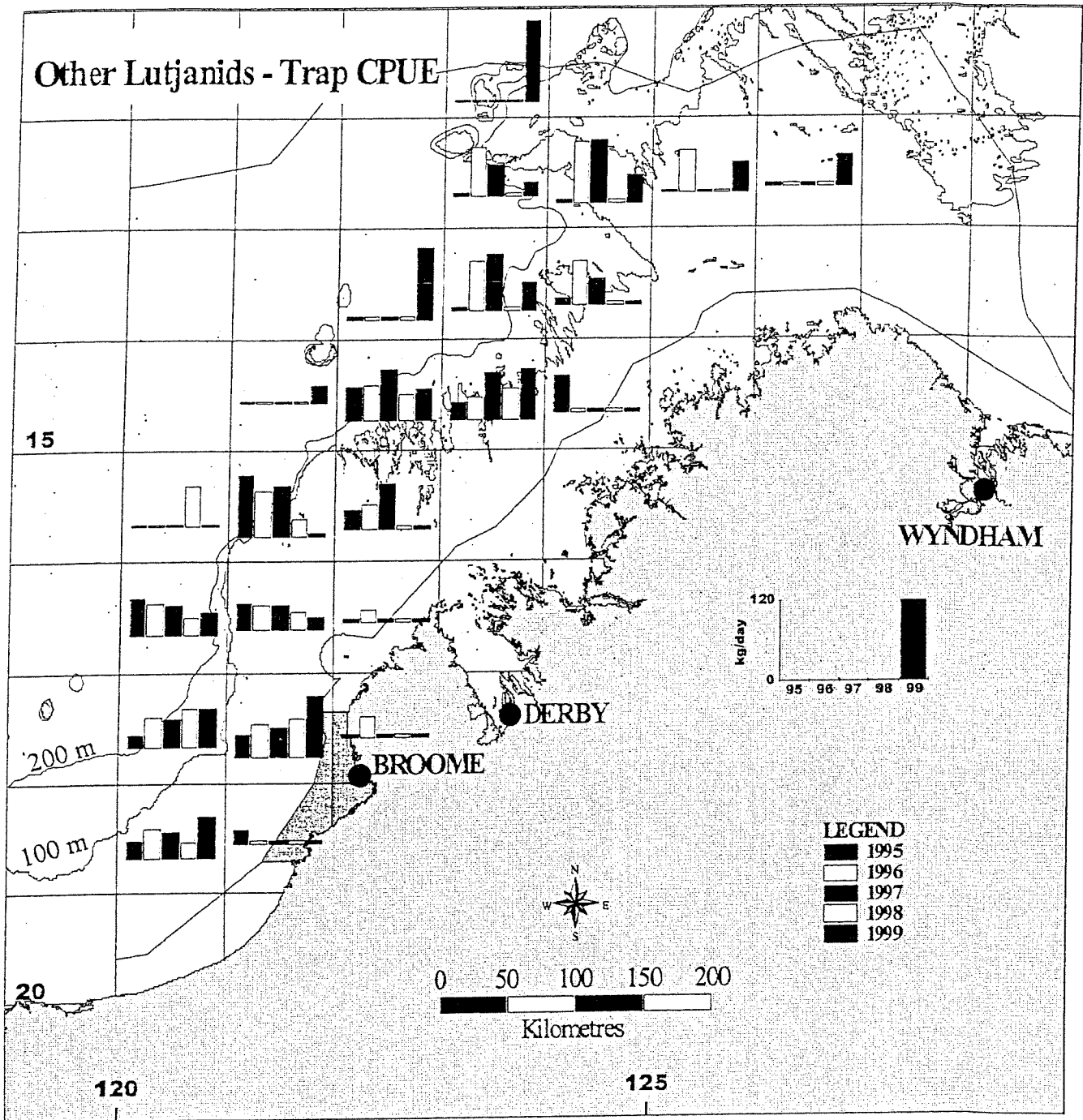


Figure A15. Spatial distribution of the CPUE of Lutjanids other than goldband snapper and red emperor landed by trap fishing vessels in the NDSF from 1995-1999.

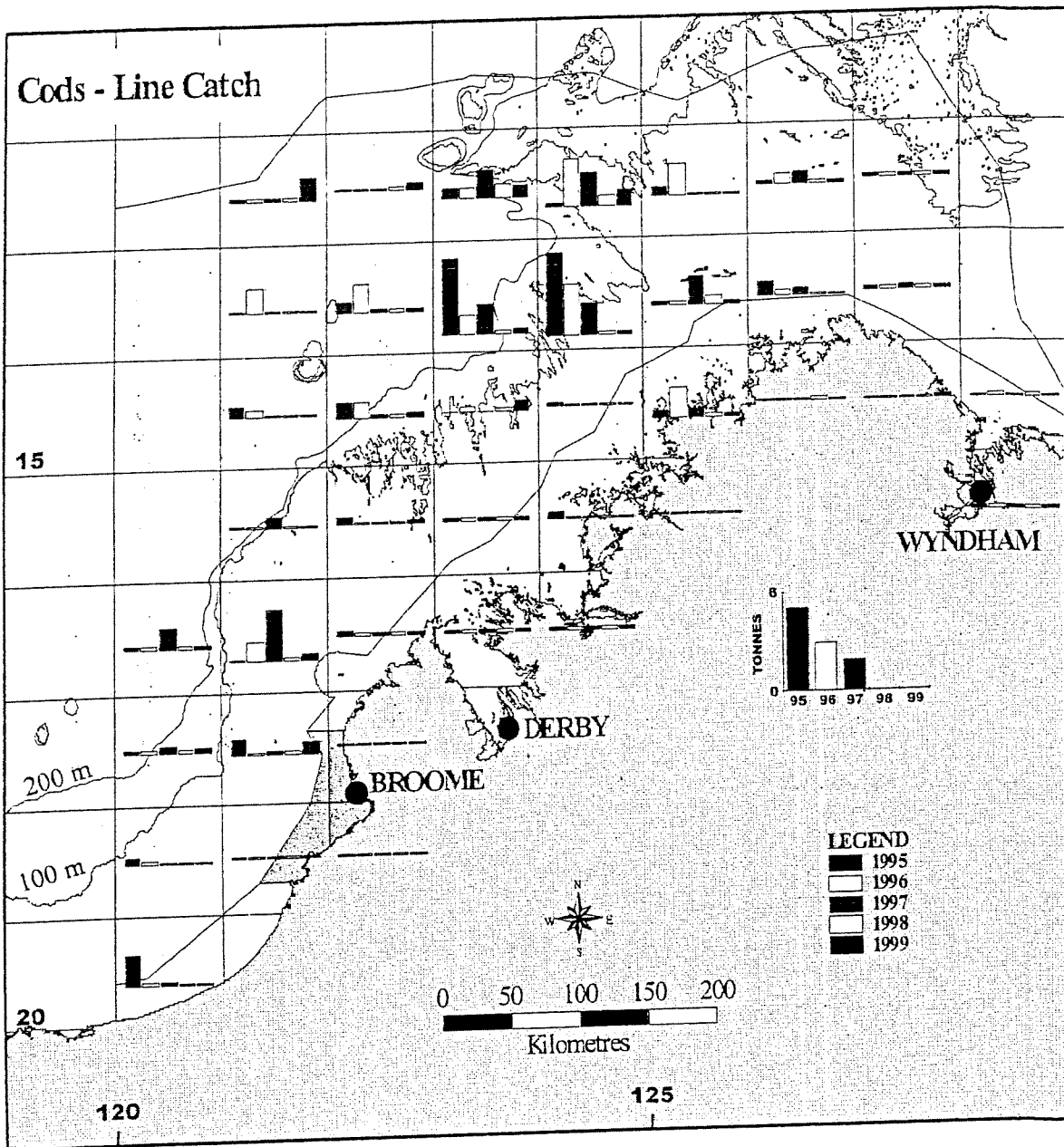


Figure A16. Spatial distribution of the catch of cods landed by the line fishing vessels in the NDSF from 1995-1999.

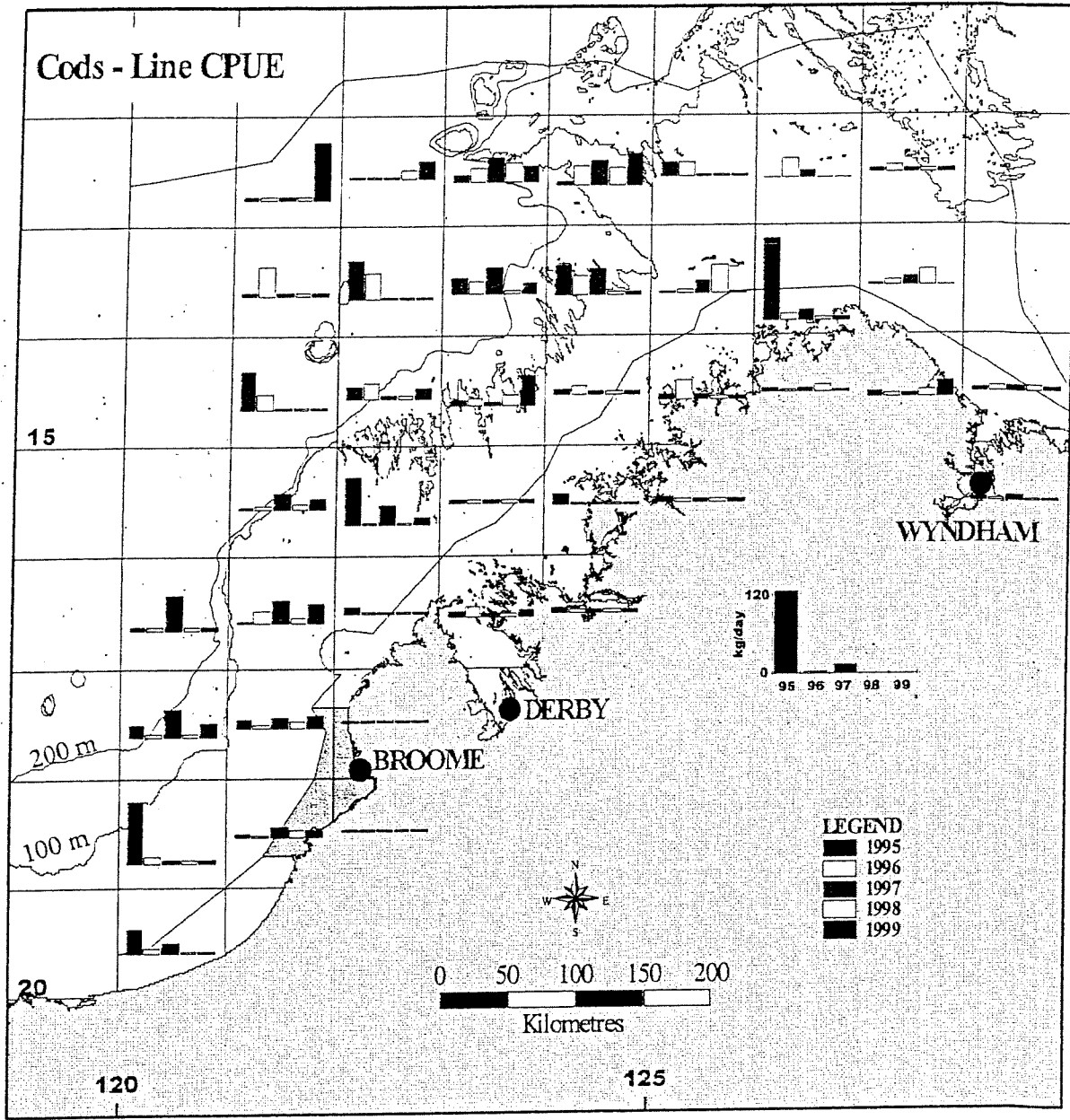


Figure A17. Spatial distribution of the CPUE of cods landed by line fishing vessels in the NDSF from 1995-1999.

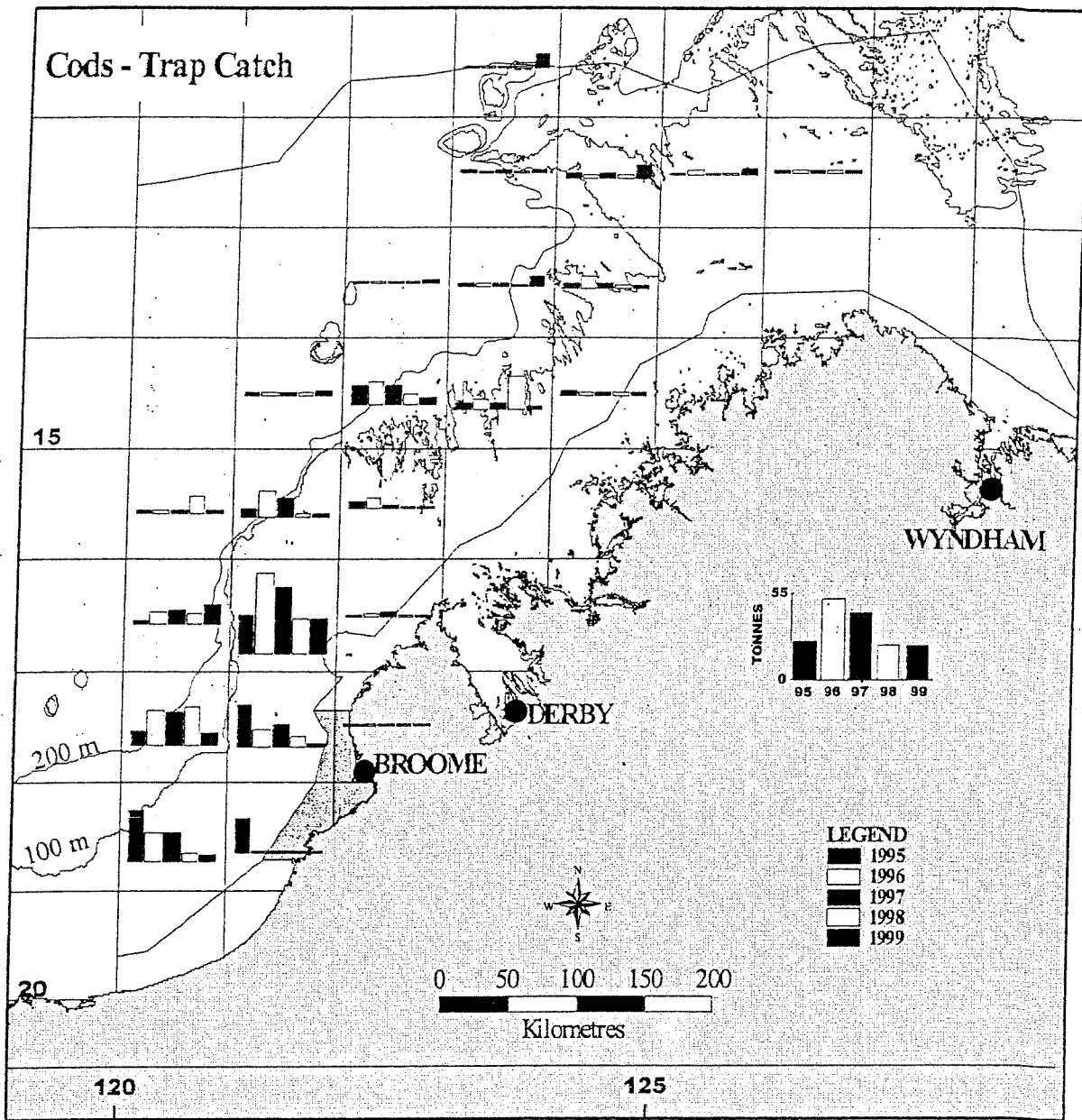


Figure A18. Spatial distribution of the catch of cods landed by trap fishing vessels in the NDSF from 1995-1999.

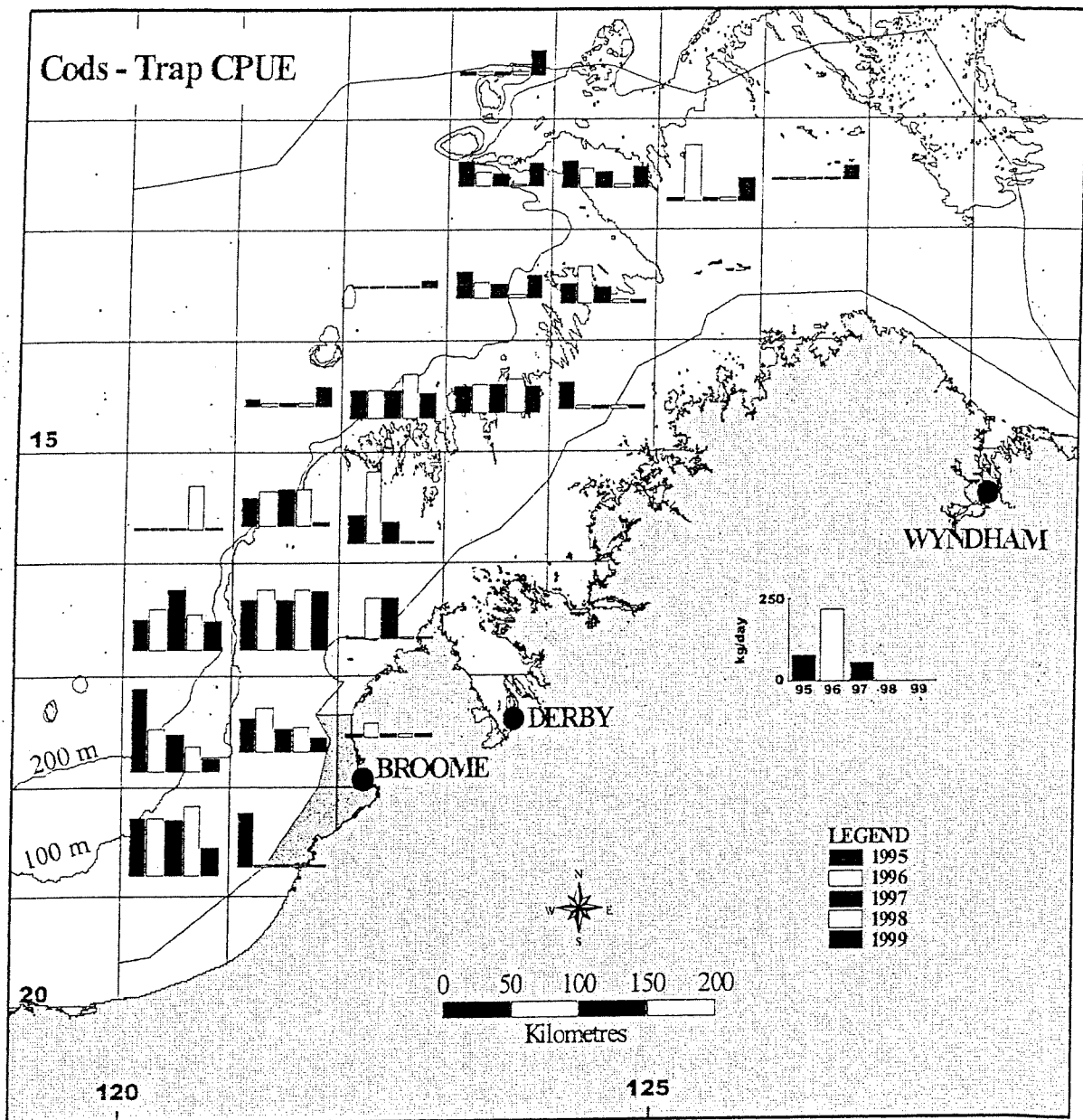


Figure A19. Spatial distribution of the CPUE of cods landed by trap fishing vessels in the NDSF from 1995-1999.